CORTICO-MUSCLE ENCODING:
EVOKING PRINCIPLES OF CORTICO-MUSCLE CONNECTIVITY WITH RL-ICMS

By

GUSTAF M. VAN ACKER III

Submitted to the graduate degree program in Molecular and Integrative Physiology
and the Graduate Faculty of the University of Kansas in partial
fulfillment of the requirements for the degree of
Doctor of Philosophy.

_____

Paul D. Cheney, Ph.D., Chairman

_____

Steven M. Barlow, Ph.D.

_____

Thomas J. Imig, Ph.D.

_____

Randolph J. Nudo, Ph.D.

_____

John A. Stanford, Ph.D.

Dissertation defended: August 12th, 2011

The Dissertation Committee for Gustaf M. Van Acker III
certifies that this is the approved version of the following dissertation:

CORTICO-MUSCLE ENCODING:
EVOKING PRINCIPLES OF CORTICO-MUSCLE CONNECTIVITY
WITH RL-ICMS

Paul D. Cheney, Ph.D., Chairman

Steven M. Barlow, Ph.D.

Thomas J. Imig, Ph.D.

Randolph J. Nudo, Ph.D.

John A. Stanford, Ph.D.

Date Approved: August 12th, 2011

ABSTRACT

The specific aims of this study focus on three interrelated issues utilizing long-duration intracortical microstimulation (RL-ICMS) to elicit the organization and function of the rhesus macaque primary motor cortex (M1). The first focus concerns the timing between cortical activity and corresponding muscle activity, of which previous studies have revealed a broad range depending upon the research methods. Our findings suggest that the latency of cortico-muscle transmission observed (11.5 ± 5.6 ms) approaches the stimulus-triggered average (StTA)-derived minimum conduction time (9.6 ± 2.1 ms). We conclude that, during active movement, the best estimate of the delay between cortical cell firing and muscle activity is the physical conduction time from cortex to muscle.

Secondly we investigated the relationship between RL-ICMS parameters applied to M1 and resulting muscle activation and evoked movement. We applied stimulation as combinations of frequency, amplitude and duration while concurrently recording EMG activity of 24 forelimb muscles and stimulus-evoked kinematics using a Vicon motion capture system. Our results suggest optimal parameters for evoking forelimb movements and stable spatial end-points are 70 - 130 Hz, 70 - 130 µA and 750 - 1000 ms, with median successful parameters of 110 Hz and 110 µA and a mean spatial end-point stabilization time of 479.0 ± 178.9 ms. Establishing stimulation parameters that yield consistent stimulus-evoked end-points forms the basis for comprehensive mapping of movement space represented in M1.

The third study objective was to acquire a comprehensive M1 representation map of RL-ICMS-evoked forelimb movement end-points. This study expands upon previous

RL-ICMS studies by producing a systematic and comprehensive stimulus-evoked spatial end-point map of M1. The results reveal that stable end-points generated by stimulating adjacent M1 cortical sites tended to be spatially contiguous in the monkey's work space, yielding a cortical map of end-point positions in which the monkey's three-dimensional work space was represented on the two-dimensional M1 cortical surface. While there were distinct cortical topographical differences between monkeys, there were also clear similarities such as hand-to-mouth postures elicited from sites neighboring the M1 face representation. These results reveal an extensive movement reportoire that can be elicited by applying RL-ICMS to M1.

To my wife, J. Eva Selfridge, with whom this road less traveled

has been a wonderful adventure.

ACKNOWLEDGEMENTS

I am deeply grateful to my advisor, Paul D. Cheney, for being a tremendous mentor and a paragon of a scientist by which I hope to guide my future career, and for his patient and passionate effort to impart as much of his vast knowledge and experience I could absorb. To my committee I am also deeply indebted; due to the scientific suggestions and guidance of Randolph J. Nudo, John A. Stanford, Thomas J. Imig, and Steven M. Barlow, my graduate experience has been outstanding.

My colleague and collaborator Sommer L. Amundsen, with whom much of the data in this dissertation was co-collected, was a tremendous asset both for her engineering and programming expertise as well as her sensibility and sense of humor. Sommer's advisor, Carl W. Luchies, provided invaluable help with data analysis as well as in trouble shooting our motion capture system, proving to be very patient during the year it took to raise to functional status.

The data herein exists only with the help of my colleagues William G. Messamore, Heather M. Hudson, Darcy M. Griffin, and Hongyu Y. Zhang. For technical assistance throughout I would like to thank Ian Edwards for his remarkable machining and electronic expertise; Anthony Kovac for his clinical anesthesiology guidance; Nathan Culley and Judith Larson for their outstanding veterinary care; and Allan Schmitt, Bill Brooks and Phil Lee for their MRI expertise. I would also like to thank Timothy Fields and Joseph Bast for their determined effort in helping me and all their MD/PhD students succeed in this amazing program at KUMC. Shari Standiferd and Jennifer Fajardo provided helpful administrative assistance.

I would like to thank my family, each member of whom has been amazing and supportive, and has guided who I have become today. Specifically, I would like to thank my parents Jana and Jeff Lord and Gustaf and Denise Van Acker, who have provided immeasurable guidance and love, and Brad and Lynn Selfridge, who have supported me tremendously throughout my training at KUMC.

Above all, I would like to thank my wife, J. Eva Selfridge, who has been my colleague and partner for each step of training and life since starting the MD/PhD program. She has been the perfect study partner, a great problem solver and, most importantly, my foundation.

TABLE OF CONTENTS

LIST OF TABLES

CHAPTER II

LIST OF FIGURES

CHAPTER II

CHAPTER III

CHAPTER IV

ABBREVIATIONS AND DEFINITIONS

CM cell:	*Corticomotoneuronal cell*. Cell body resides in lamina V of the motor cortex and axon has monosynaptic connectivity with motoneurons in the spinal cord.
EPSP/IPSP:	*Excitatory/Inhibitory postsynaptic potential*. Transient depolarization of the postsynaptic membrane resulting in excitation or inhibition of the postsynaptic cell.
ICMS:	*Intracortical microstimulation*. Electrical stimulation of the cortex using a microelectrode suitable for single cell recording.
M1:	*Primary motor cortex*. Located in the precentral gyrus; involved in late stage encoding of motor commands.
PDC:	*Proximal-distal co-facilitation.* Refers to stimulus- or spike-triggered averaging (StTA or SpTA, respectively) muscle representation-derived map areas that yield poststimulus or postspike effects (PStE or PSpE, respectively) in both distal and proximal muscles.
PStE/PSpE:	*Poststimulus/Postspike effect.* A transient increase (facilitation) or decrease (suppression) in target muscle EMG activity observed with a stimulus- or spike-triggered average, respectively.
PStF/PSpF:	*Poststimulus/Postspike facilitation.* A transient increase in target muscle EMG activity observed with a stimulus- or spike-triggered average, respectively.
PStS/PSpS:	*Poststimulus/Postspike suppression*. A transient decrease in target muscle EMG activity observed with a stimulus- or spike-triggered average, respectively.
RL-ICMS:	*Repetitive long-duration intracortical microstimulation*. Stimulation parameters are typically≥500 ms duration and 100-400 Hz.
RS-ICMS:	*Repetitive short-duration intracortical microstimulation*. Stimulation parameters are typically 10 pulses at 330 Hz.
SpTA:	*Spike-triggered average*. A method of correlating *CM cell activity* with EMG activity. Averages reveal transient facilitation (PSpF)

and suppression (PSpS) events that are mediated by underlying EPSPs and IPSPs.

StTA: *Stimulus-triggered average of EMG activity*. A method of correlating applied *electrical stimulus* pulses in M1 (that activate local CM cells) with EMG activity. Averages reveal transient facilitation (PStF) and suppression (PStS) events that are mediated by underlying EPSPs and IPSPs.

CHAPTER I:

INTRODUCTION

“If we knew what it was we were doing, it would not be called research, would it?”

- Albert Einstein

The importance of understanding mechanisms behind cortical control of movement

A question often arises within contemporary biomedical research when addressing research questions and findings. "How is the research clinically relevant?" However this question, seemingly harmless and relevant as it may be, is loaded. More directly, the question proposes that if the research hypothesis under investigation, or the subsequent research findings, doesn't yield results that can be directly applied to improve patient care, why is it important? To answer this tricky question we must refer to the basic tenet that knowledge and understanding of the system in question is, in itself, important.

Research groups investigating the mechanisms and structure underlying cortical encoding of voluntary movement often begin with one of two interrelated modes of approach. The first approach is explorative in nature, the goal being to increase our understanding of how this complex system operates on a fundamental level. This involves making use of contemporary technology to build upon existing knowledge, often resulting in greater investigative resolution directly attributable to available technology. This approach falls into the category of what we refer to as basic science, and is a method by which science has been conducted for millennia. In essence, it is an approach of discovery that attempts to make sense of our complex world. Approaching biomedical research involving cortical encoding of movement in this manner of scientific discovery is similar in some respects to the contemporary research fields of theoretical astrophysics and quantum mechanics: knowledge gained may yield little in the way of immediate

practical application, yet gives us greater understanding of our place in the universe and provides the framework for our second approach.

This second approach is to advance, from our present understanding, practical modalities to increase the effectiveness of current therapeutic applications or to develop better therapies within the clinical setting. Analogous lines of research would be those that result in directly applicable products, such as the development of highly efficient energy sources which reduce our carbon footprint and need for fossil fuels, or to increase treatment efficacy with the development of therapeutic drugs.

The study of cortical encoding of motor control, indeed study within most of biomedical research, exists on the front lines of this dichotomy between exploration and application. Each increase in understanding of a system brings with it the hope and expectation that the knowledge gained will have direct impact on the quality of our lives. However, thought must come before action; exploration and understanding must precede appropriation and application. Yet while one should come before the other, action is often preferred whether or not adequate thought has preceded it.

In some instances, biomedical research findings are directly applicable to human endeavors; however, leaps from discovery to application typically take years or decades of study to yield such results. Often research discoveries reveal yet more questions about the system in question. This often boils down to a singular issue: we are still learning about both healthy and pathological aspects of the human body, and biomedical investigation into the system is in some respects still in its infancy, bordering on exploration of the unknown.

We have learned a tremendous amount over the past two centuries in terms of structure and connectivity that are involved in the planning and execution of voluntary movement, both in

healthy and pathological systems. As a consequence, the logical next step is to apply this knowledge to the treatment of pathological cases such as Parkinson's Disease and spinal cord injury, as well as to improve the quality and longevity of life in those that are healthy. Yet while we see in front of us the horizon of opportunity for improving our lives with the knowledge we've gained, there remains much to learn. Our effectiveness in developing adequate treatment is wholly dependent upon the depth of our understanding.

It is important to keep in mind when approaching any scientific endeavor the importance of discovery and understanding. Historically, science is based upon a search for understanding, and only from this vast history of basic research do we now sit upon the precipice of applying this knowledge for potential gain.

A brief history of electrophysiological approaches to studying encoding of motor control

Our present understanding of how the brain synthesizes conscious cortical commands to produce voluntary movement is the product of centuries of research conducted using a multitude of scientific techniques. These techniques include but are not limited to histological methods, medical imaging techniques, tracer studies and electrophysiological approaches. Each method has been dependent upon the contemporary technology to allow exploration of the brain's structure and function. For example, the use of histology to study the nervous system at the cellular level came about only after the invention of various iterations of the microscope and cellular staining techniques. The development of the first microscope, in turn, was reliant upon prior discovery of visual magnification utilizing convex and concave lenses in series.

Similarly, the first application of electrophysiology to study the nervous system was dependent upon the discovery of electricity, and subsequently the finding that neuronal conduction is mediated by flow of electricity. Understanding that functionality of the brain is, to some degree, localized at particular loci in the brain was an advance aided in part by the use of electrophysiology. Studies conducted as early as the 1860s by Hughlings Jackson revealed, upon observing patterns of muscle activation during muscle convulsions, that functional motor output must be localized within the brain. Subsequently, the first experimentally determined brain motor map was introduced when, in 1870, Fritsch and Hitzig first discovered the electrical excitability of cortex in the dog (Fritsch and Hitzig, 1870). Ferrier furthered motor mapping when, in 1875, he produced the first motor map of the primate brain using electrical stimulation (Ferrier, 1875).

Meanwhile, investigation of the human motor system remained difficult due to the invasiveness of electrophysiological methods. By the beginning of the 20th century, however, surgeons that had access to intact human nervous systems began to localize motor and sensory areas during the course of surgery by applying electrical stimulation to neural tissue. In 1937, Penfield and Boldrey produced the first experimentally-derived motor map of the human brain by stimulating motor areas in epileptic patients (Penfield and Boldrey, 1937). This work was later elaborated upon in a publication by Penfield and Herbert Jasper entitled *Epilepsy and the Functional Anatomy of the Human Brain* (Penfield and Jasper, 1954), and contains the primary motor cortex (M1) *homunculus* that is still referenced today. Following Penfield and Boldrey's work, Woolsey produced a detailed map of the monkey motor cortex which included the monkey version of the homunculus, or *simunculus* (Woolsey et al., 1952).

Such work was revolutionary regarding our understanding of the brain's encoding of motor control. The techniques used, however, relied upon stimulation of the cortex with

concurrent observation of overt effect. In 1958, Jasper, utilizing the tungsten microelectrode techniques suitable for single unit recordings developed by David Hubel (Hubel, 1957), made the first recordings from cortical neurons in an awake monkey during behavior. Later, in 1964, Edward Evarts used Jasper's technique to investigate the properties of neurons in awake monkeys during voluntary movement (Evarts, 1964). Paul Cheney and Eberhard Fetz, in 1980, developed a method of correlating the activity of recorded corticomotoneuronal (CM) cells with concurrent activity of target muscles in a technique called spike-triggered averaging (SpTA) (Cheney and Fetz, 1980). From among the many cell types in the cortex, this method enabled the identification of cells with a direct output linkage to motoneurons. The advent of recording cellular electrical potentials directly associated with volitional movement has added a valuable layer of understanding in the cortical control of movement.

Directly following the trend toward recording cellular activity as the primary means for investigating motor output, a renewed interest in mapping utilizing stimulation occurred due to the development of applying microstimulation to the cortex using equipment developed for single unit recording. While early stimulation techniques relied upon cortical surface stimulation that activated relatively large areas of the cortex, intracortical microstimulation would lead to a higher resolution of cortical mapping. In 1967 Hiroshi Asanuma utilized microelectrodes, previously developed and suitable for single unit recordings, to apply intracortical microstimulation (ICMS) from which detailed mapping of cortical motor output was produced (Asanuma and Sakata, 1967). This was followed by another increase in resolution of mapping by Cheney and Fetz when, in 1985, they introduced stimulus triggered averaging (StTA) as a method for functional motor mapping (Cheney and Fetz, 1985). StTA was used later by Michael Park to produce a detailed muscle map of forelimb representation in the monkey M1 (Park et al.,

2000). Thus stimulation techniques developed over the past century have become increasingly refined to produce higher resolution maps of the motor cortex.

Recently, in 2002, Michael Graziano used a modified version of ICMS to investigate cortico-motor output. This adaptation, called repetitive long-duration ICMS (RL-ICMS), applies ICMS for durations that approach those of natural movements (Graziano et al., 2002). This intriguing method seems at present to be a potentially enlightening union between coarse stimulation techniques developed a century earlier and more recent techniques that have allowed for increasingly refined mapping. Questions remain as to what this method ultimately reveals as well as the underlying mechanisms. This leads us to the subject of the present dissertation.

Specific aim 1: to assess the timing of cortico-muscle transmission during active movement

This study will be addressed in detail in Chapter II. As with each aim mentioned in this thesis, the study expands upon the research and methods described previously in the brief history of electrophysiology. The synaptic connectivity between M1 and motoneurons has been studied extensively with a variety of methods (Porter and Lemon, 1993, Morrow and Miller, 2003, Rathelot and Strick, 2006, Townsend et al., 2006, Schieber and Rivlis, 2007, Rathelot and Strick, 2009). Using SpTA and StTA of electromyographic (EMG) activity, previous studies have shown that the mean time delay between CM cell firing and the onset of facilitation of distal forelimb muscle activity ranges from 6.7 – 9.8 ms, depending on the forearm muscle group tested (Cheney and Fetz, 1980, Lemon et al., 1986, McKiernan et al., 1998, Park et al., 2004). These delays are consistent with the estimated conduction time from cerebral cortex to forelimb muscle (Humphrey and Corrie, 1978, Cheney and Fetz, 1985, Baker and Lemon, 1998).

In contrast, numerous studies have reported much longer delays of 60-122 ms between the onset of cortical cell firing and the onset of EMG activity and natural movement (Evarts, 1972, Cheney and Fetz, 1980, Porter and Lemon, 1993). In addition, delays of 40 – 50 ms have been used to produce optimal correlations between EMG activity and M1 neurons (Morrow and Miller, 2003, Townsend et al., 2006). These delays, coupled with the time delay of 60-122 ms observed between the onset of cortical activity and EMG activity, have been used as a rationale for phase shifting the timing between cortical cell activity and muscle activity in studies of cortical encoding of EMG activity (Morrow and Miller, 2003, Townsend et al., 2006, Schieber and Rivlis, 2007).

Various hypotheses have been suggested to account for the timing discrepancies observed in these studies compared to the minimum conduction time over the corticospinal pathway measured with SpTA and StTA. One hypothesis is that plateau potentials, caused by persistent inward currents in the dendrites of motoneurons, may delay the transmission of incoming signals (Morrow and Miller, 2003). These plateau potentials may utilize slow L-type Ca^{2+} channels and act as low-pass filters that amplify and substantially delay the incoming signals.

Another hypothesis is that motoneurons may require integration of signals from both direct corticospinal pathways and indirect, multi-synaptic pathways (Schieber and Rivlis, 2007). Requiring input from multi-synaptic pathways could increase the delay from cortical activity to EMG activity, although it would require a very indirect route to account for the large discrepancy in latency between the minimum conduction time and the cortical cell to muscle onset time measured during active movement.

Yet another possibility is that the disparity could be due to the time required for motoneurons to achieve firing threshold, which requires summation of converging excitatory

postsynaptic potentials (EPSPs) from corticospinal and other inputs. This action could pose a significant delay during the initiation of movement; however, contrary to the first two hypotheses, discrepancies due to this mechanism should disappear or become minimal once motoneurons are actively firing.

While each of these hypotheses is plausible, the actual cause for the timing discrepancy remains unclear. In the present study, we investigated the delay between cortical activity and EMG activity during active movement while the motoneurons were at or above firing threshold. We applied time-varying modulations of corticospinal output to motoneurons by applying frequency-modulated stimulus trains to individual M1 cortical sites on a background of active movement-related EMG activity. This procedure yielded corresponding modulations of EMG activity whose timing could be measured relative to the applied stimulus train modulations. The latency results obtained could then be used to examine whether or not the large delays seen in other studies could be largely attributable to the time required to bring motoneurons to firing threshold during initiation of movement. We conclude that, during active movement, the best estimate of the delay between cortical cell firing and muscle activity is the physical conduction time from cortex to muscle.

Specific Aim 2: to determine the optimal stimulus parameters for M1 RL-ICMS-evoked translocation and subsequent stabilization of the forelimb

The goal of this study was to investigate the relationship between stimulus parameters applied to M1 and the resulting muscle activation and evoked movement. Cortico-motor connectivity between neurons in M1 and muscles has been mapped previously using various

forms of electrophysiological methods, tracer studies, and histological approaches (Penfield and Boldrey, 1937, Woolsey et al., 1952, Cheney and Fetz, 1985, Donoghue et al., 1992, Rathelot and Strick, 2006). While early clinical electrophysiological approaches utilized surface stimulation of the cortex to evoke grossly observable responses, the introduction of ICMS permitted refined mapping of cortical output to muscles (Porter and Lemon, 1993, Morrow and Miller, 2003, Rathelot and Strick, 2006, Townsend et al., 2006, Schieber and Rivlis, 2007, Rathelot and Strick, 2009). Short trains of high frequency ICMS (RS-ICMS) have been used to evoke twitch-like responses for cortical mapping and other purposes, while the development of spike- and stimulus-triggered averaging have allowed for an increased resolution in cortico-motor mapping (Asanuma et al., 1976, Strick and Preston, 1978, McKiernan et al., 1998, Park et al., 2004). More recently research groups have modified this method of ICMS by applying ICMS trains with durations (500 ms) that more closely match the timescale of natural movements (Graziano et al., 2002, Graziano et al., 2005, Ethier et al., 2006). RL-ICMS produced natural-appearing movements of activated limbs characterized by having a common spatial end-point for a particular cortical site stimulated regardless of the starting position of the limb.

In the current study, our aim was to determine the optimal RL-ICMS parameters that would yield forelimb translocation with subsequent stabilization at spatial end-points when applied to M1. We applied stimulation to M1 as combinations of frequency (30 - 400 Hz), current (30 - 200 µA) and duration (0.5 - 2 s) while concurrently recording the EMG output to 24 forelimb muscles as well as the stimulus-evoked limb kinematics using a Vicon motion capture system. Establishing stimulation parameters applied to M1 that yield consistent movements to stable spatial end-points forms the basis for a systematic and complete mapping of forelimb movement representations elicited from the primary motor cortex. Our results suggest a

relatively narrow range of stimulus parameters that were both effective and safe for forelimb translocation with subsequent stabilization at a spatial end-point.

Specific Aim 3: to obtain a comprehensive spatial end-point map elicited from the cortical forelimb representation using RL-ICMS

The goal of this study was to acquire a complete RL-ICMS-evoked spatial end-point map of the forelimb M1 cortex in the macaque monkey. The present study expands upon previous findings (Graziano et al., 2002, Ethier et al., 2006) by producing a systematic and comprehensive RL-ICMS-evoked spatial end-point map of M1 utilizing a subset of stimulus parameters, typically 100-120 Hz, 100-120 µA and 1 second duration, determined previously as part of this dissertation (Chapter III) to be optimal for eliciting forelimb movements with stable spatial end-points. Concurrently, we recorded the EMG activity of 24 forelimb muscles as well as movement kinematics and end-point positions of the wrist using a Vicon motion capture system. Forelimb muscle representation in M1 was derived for each monkey from effects in stimulus-triggered averages (StTA) of EMG activity (Park et al, 2001). From the data we produced two-dimensional topographical cortical maps representing the elicited forelimb movements in three-dimensional space. In addition, we generated maps illustrating the extent of the monkey's work space that was represented by stimulus-evoked movement end-points. These results reveal an extensive movement reportoire that can be elicited by applying RL-ICMS to M1.

The results discussed in the following chapters add to our understanding of how RL-ICMS applied to the motor cortex affects motor output, and contributes to our basic

understanding of cortical encoding of limb movements. Additionally, the results could aid in future advancement of neuroprosthetic devices.

CHAPTER II:

TIMING OF CORTICO-MUSCLE TRANSMISSION DURING ACTIVE MOVEMENT

ABSTRACT

Corticomotoneuronal (CM) cells in primary motor cortex (M1) have monosynaptic connections with motoneurons in the ventral horn of the spinal cord. Using methods such as spike- and stimulus-triggered averaging (SpTA and StTA, respectively) of EMG activity, previous studies have shown that the time delay between CM cell firing and facilitation of forelimb muscle activity ranges from 6.7 – 9.8 ms depending on the muscle group tested. This is consistent with the estimated conduction time through the pathway from cerebral cortex to muscle. In contrast, numerous studies have reported delays of 60-122 ms between the onset of cortical cell firing and the onset of natural movement. Although various hypotheses have been suggested, the reason for this disparity remains unclear. To further investigate this issue, we simulated conditions of rapid active movement by applying frequency-modulated stimulus trains to M1 cortical sites in a rhesus macaque performing an active movement task. This yielded corresponding modulations of EMG activity whose latency could be measured relative to the stimulus train modulations. The precise delay between reference points in the frequency-modulated stimulus train and the corresponding modulation in distal forelimb muscle activity varied somewhat with stimulus parameters; however, the mean latency for all parameters was 11.5 ± 5.6 ms, approaching StTA-derived latencies measured at the same cortical sites (9.6 ± 2.1 ms). We conclude that, during active movement, the best estimate of the delay between modulated M1 cortical output and its impact on muscle activity is the physical conduction time from cortex to muscle.

INTRODUCTION

The synaptic connectivity between the primary motor cortex (M1) and motoneurons has been studied extensively (Porter and Lemon, 1993, Morrow and Miller, 2003, Rathelot and Strick, 2006, Townsend et al., 2006, Schieber and Rivlis, 2007, Rathelot and Strick, 2009). Using methods such as spike triggered averaging (SpTA) and stimulus triggered averaging (StTA) of EMG activity, previous studies have shown that the mean time delay between CM cell firing and the onset of facilitation of distal forelimb muscle activity ranges from 6.7 – 9.8 ms, depending on the forearm muscle group tested (Cheney and Fetz, 1980, Lemon et al., 1986, McKiernan et al., 1998, Park et al., 2004). These delays are consistent with the estimated conduction time from cerebral cortex to forelimb muscle (Humphrey and Corrie, 1978, Cheney and Fetz, 1985, Baker and Lemon, 1998).

In contrast, numerous studies have reported mean delays of 60-122 ms between the onset of cortical cell firing and the onset of natural movement (Evarts, 1972, Cheney and Fetz, 1980, Porter and Lemon, 1993). In addition, delays of 40 – 50 ms have been used to produce optimal correlations between EMG activity and M1 neurons (Morrow and Miller, 2003, Townsend et al., 2006). These delays, coupled with the time delay of 60-122 ms observed between the onset of cortical activity and EMG activity, have been used as a rationale for phase shifting the timing between cortical cell activity and muscle activity in studies of cortical encoding of EMG activity (Morrow and Miller, 2003, Townsend et al., 2006, Schieber and Rivlis, 2007).

Various hypotheses have been suggested to account for the timing discrepancies observed in these studies compared to the minimum conduction time over the corticospinal pathway measured with SpTA and StTA. One hypothesis is that plateau potentials, caused by persistent inward currents in the dendrites of motoneurons, may delay the transmission of incoming signals (Morrow and Miller, 2003). These plateau potentials may utilize slow L-type Ca2+ channels and act as low-pass filters that amplify and substantially delay the incoming signals.

Another hypothesis is that motoneurons may require integration of signals from both direct corticospinal pathways and indirect, multi-synaptic pathways (Schieber and Rivlis, 2007). Requiring input from multi-synaptic pathways could increase the delay from cortical activity to EMG activity, although it would require a very indirect route to account for the large latency discrepancy between the minimum conduction time and the cortical cell to muscle onset time measured during active movement.

Yet another possibility is that the disparity could be due to the time required for motoneurons to achieve firing threshold, which requires summation of converging excitatory postsynaptic potentials (EPSPs) from corticospinal and other inputs. This action could pose a significant delay during the initiation of movement; however contrary to the first two hypotheses, discrepancies due to this mechanism should disappear or become minimal once motoneurons are actively firing.

While each of these hypotheses is plausible, the actual cause for the timing discrepancy remains unclear. In the current study, we investigated the delay between cortical activity and EMG activity during active movement, while the motoneurons were at or above firing threshold. We generated time-varying modulations of corticospinal

output to motoneurons by applying frequency-modulated stimulus trains to individual M1 cortical sites on a background of active movement-related EMG activity. This procedure yielded corresponding modulations of EMG activity whose latency could be measured relative to modulations in the applied stimulus train. The latency results obtained could then be used to examine whether or not the large delays seen in other studies could be attributable largely to the time required to bring motoneurons to firing threshold during initiation of movement.

The overall mean latency observed in this study (11.5 ± 5.6 ms) was only 1.9 ms longer than the minimum conduction time through the cortex-to-muscle pathway derived from StTAs computed at the same sites (9.6 ± 2.1 ms). The results support the hypothesis that the longer time delays reported for the timing between cortical cell activation and muscle activation are due largely to the time required to bring motoneurons to firing threshold from a hyperpolarized state.

EXPERIMENTAL PROCEDURES

Behavioral Task

We trained a male rhesus macaque (Macaca mulatta) to perform a ramp-and-hold concentric wrist flexion and extension task (Figure 2.1). The monkey was seated in a custom primate chair within a sound-attenuating chamber with his arms comfortably restrained bilaterally. His right elbow was positioned at a 90̊ angle, and his right hand was positioned in a manipulandum that allowed horizontal concentric rotation about the wrist. To receive an applesauce reward, the monkey was required to produce alternating ramp-and-hold wrist movements to target positions of 40˚±10 in flexion and 30˚±15 in extension with 0˚ being alignment of the wrist with the forearm. To count as a successful trial, the monkey was required to hold against moderate resistance in both flexion and extension for a period of one second. Performance was guided by audio and visual cues.

Surgical Procedures

Following training an MRI-compatible stainless steel chamber allowing 30 mm diameter of dural exposure, and exploration of the underlying cortical area, was implanted stereotaxically over the primary motor cortex of the left hemisphere using procedures described in detail previously (Park et al., 2000). Briefly, the chamber was anchored to the skull using titanium screws and dental acrylic, and was centered over the hand area of M1 in the left hemisphere. In addition, threaded titanium nuts were attached

over the occipital aspect of the skull using titanium screws and dental acrylic. These nuts provided a point of attachment for a flexible head restraint system during recording (McKiernan et al., 1998, 2000).

Muscles of the right forearm, 5 flexors and 5 extensors, were each implanted with two multi-stranded stainless steel wires (Cooner Wire, AS632) using a transcutaneous technique described in detail previously (McKiernan et al., 2000). Briefly, all wires were stripped of ~2-3 mm of insulation and inserted transcutaneously into the target muscles a distance of ~2-3 cm, with ~5 mm separation of the two wires in each muscle. The wires terminated in connector modules (ITT Cannon, New Britain, CT) placed on the forearm. We tested the placement accuracy of each electrode pair by observing appropriate muscle twitches resulting from short stimulus trains. After confirming placement accuracy of all electrodes, medical adhesive tape was used to secure wires and the connectors to the forearm for the duration of the implant. The monkey wore a full-sleeved jacket (Lomir Biomedical, model PJ05) while in his home cage, with the right arm of the jacket reinforced with stainless steel mesh (Saf-T-Gard, Type 4.2 stainless steel mesh) to protect the implant.

We recorded multi-unit EMG activity from five extensor muscles: extensor carpi radialis (ECR), extensor digitorum communis (EDC), extensor digitorum 4,5 (ED4,5), extensor carpi ulnaris (ECU), extensor digitorum 2,3 (ED2,3); and five flexor muscles: flexor carpi radialis (FCR), flexor digitorum superficialis (FDS), palmaris longus (PL), flexor carpi ulnaris (FCU), flexor digitorum profundus (FDP).

Prior to each implant surgery, the monkey was administered ketamine (10 mg/kg, IM), atropine (0.04 mg/kg IM), medetomidine (0.05 mg/kg IM), and subsequently

isoflurane gas for the duration of the surgery. The monkey received prophylactic antibiotic (penicillin, 6000 U/kg, SC) 10 hours pre-surgery, 1 hour post-surgery and 3 days subsequent to the surgery. Following the surgery the monkey was given analgesics (buprenorphine, 0.01 mg/kg IM and carprofen, 5 mg/kg SC). All surgeries were performed in a facility accredited by the Association for Assessment and Accreditation of Laboratory Animal Care using full sterile procedures. All procedures conformed to the Guide for the Care and Use of Laboratory Animals, published by the United States Department of Health and Human Services and the National Institutes of Health.

Data Recording

We stimulated multiple locations in the arm representation of primary motor cortex of the left hemisphere (Figure 2.2) using glass and mylar insulated platinum-iridium electrodes with typical impedances of 0.7 - 1.5 MΩ (FHC Inc., Bowdoin, ME). We positioned the recording electrode using an X-Y positioner secured to the chamber for the duration of each recording session, and advanced the electrode into the brain using a manual hydraulic microdrive (FHC Corp.) until the electrode tip was located in cortical lamina V, or approximately 1.5 mm below the surface of the brain. Location of layer V was determined by depth, the appearance of large spikes, and finally by appropriate effects in StTA at 15μA and 15 Hz.

Stimulus Triggered Averages

StTAs were gathered for all implanted muscles from stimuli applied throughout all phases of the concentric wrist task. StTAs were used to help confirm positioning of the electrode in lamina V, to confirm electrode location stability for the duration of each recording session, and to determine minimum conduction time through the cortico-muscle pathway. EMG activity was typically filtered from 30 Hz to 1 kHz, digitized at 4 kHz and full-wave rectified. Individual stimuli for the StTAs were symmetrical biphasic pulses: initial negative pulse 0.2 ms in duration followed directly by a positive pulse 0.2 ms in duration. StTAs were based on a minimum of 500 trigger events. Averages were compiled using a 60 ms epoch, of which 20 ms prior to the trigger was considered baseline. StTAs were identified as having significant poststimulus effects if the peak or trough of the effect exceeded ±2 SD of the baseline for a period of ≥ 0.75 ms as described previously (Park et al., 2004). Strong poststimulus effects suggested the presence of the electrode tip in layer V.

Frequency-Modulated Stimulation Protocol

Once we confirmed that the electrode tip was situated in layer V, we recorded the baseline EMG activity of all muscles during the concentric wrist task for both extension and flexion phases. We then initiated a stimulation protocol using specific combinations of the following parameters: current intensity (10, 15, and 30 μA), stimulus train carrier frequency (50, 100, 150, 200, and 250 Hz), modulation frequency (4, 12, and 28 Hz), and extension- or flexion-triggered stimulation. Using a carrier frequency of 50 Hz often yielded average EMG records containing peaks corresponding to individual stimuli.

These peaks were riding on a baseline level of EMG that co-varied with modulation of the stimulus train frequency. The presence of individual stimulus-related peaks reflected incomplete summation of EPSPs and were not optimal for modulation-related timing measurements. Therefore the 50 Hz data were not included in the analyses, although for clarity 50 Hz data was used to illustrate our method of generating modulated stimulus trains (Figure 2.3). We used the same stimulation protocol at each cortical site whenever possible. For each stimulus parameter a minimum of 50 trials were collected to compute an average EMG response to modulated stimulation.

Figure 2.3A illustrates the circuit used to generate the frequency-modulated sinusoidal stimulus train. A waveform generator producing a sinusoidal output was triggered by either wrist flexion or extension. This signal modulated the simultaneously-triggered stimulus train carrier frequency created by a second waveform generator. The rising phase of this synthesized frequency-modulated signal triggered a Grass S-88 stimulator, which consequently delivered biphasic electrical pulses to the cortex via the microelectrode. Figure 2.3B illustrates two stimulus outputs superimposed. The VCG signal (black) modulated a carrier frequency, which resulted in a train of frequency-modulated stimulus triggers (red). Figure 2.3C is an expanded version of the middle cycle of the sequence in 2.3B, and demonstrates that the peak of the VCG signal is in sync with the peak frequency in the modulating stimulus train (shortest inter-spike interval). This VCG signal was used for analog cross-correlation analysis. A low stimulation frequency was used in this example for clear illustrative purposes.

Measurement of EMG cross-talk

We evaluated cross-talk between EMG electrodes by constructing EMG-triggered averages. This procedure used the motor unit potentials from one muscle as triggers for compiling averages of rectified EMG activity of all other muscles. The criterion established by (Buys et al., 1986) was used to eliminate effects that might have been affected by cross-talk. To be accepted as a valid poststimulus effect, the ratio of poststimulus facilitation between test and trigger muscle must exceed the ratio of their cross-talk peaks by a factor of two or more. Based on this criterion, no effect had to be eliminated.

Measurement of Latency

Once we acquired the EMG responses to sinusoidal stimulation, we applied an offline interpolation method to remove any stimulus artifact present in the raw EMG (Windows Neural Averager, L. Shupe, University of Washington, Seattle, WA).

We determined cortico-muscle transmission time by cross-correlating EMG activity with the sine wave (VCG signal) used to produce stimulus train modulation. The first ten cycles for each set of stimulus parameters were used to compute the cross-correlation. We rectified the raw EMG and smoothed it using a 2nd order Butterworth low-pass filter. We applied the same filter to the VCG signal to control for possible phase shift associated with filtering. Cross-correlation peaks with a magnitude of 15% or greater were considered significant and used in subsequent analyses (Houk et al., 1987, McKiernan et al., 2000).

Onset times of modulated EMG activity were measured relative to the onset of frequency-modulated stimulation by measuring the point at which the envelope of the EMG record surpassed the equivalent of ±2 SD above or below the mean of the baseline EMG activity. We used the 125 ms epoch preceding stimulus onset for the baseline.

Calculations and plots were computed with SigmaPlot 10.0.

RESULTS

Stimulus Triggered Averages

StTAs were acquired at each cortical site at which frequency-modulated stimulation was applied, using the same current intensities used for modulated stimulation. Acquiring StTAs allowed us to determine the optimal locations to apply the frequency-modulated stimulus protocol. It also provided a measure of the minimum conduction time for all cortico-muscle connections at a particular cortical site. The PStF onset and peak latencies measured in this study (Table 2.1) are comparable to poststimulus facilitation effects seen in previous studies of the forelimb (Park et al., 2004).

Sites that yielded strong PStF in StTAs were more likely to yield predominantly excitatory rather than inhibitory modulation when frequency-modulated stimulation was applied, while sites that yielded PStS were more likely to yield predominantly inhibitory modulation (Table 2.2). For example, the StTAs in Figure 2.4C revealed PStF in ED 4,5, and, at a longer latency, weak PStS in FDP. Applying frequency-modulated stimulation produced predominantly excitatory modulation in ED 4,5, and predominantly inhibitory modulation in FDP (Figure 2.4D-F). When FDP was silent (Figure 2.4D), applying stimulation produced no appreciable modulation. However when FDP was active (Figure 2.4E), stimulation produced inhibition associated with peaks in the frequency of stimulation. The sign of the effect from frequency-modulated stimulation can be most readily appreciated by looking at the response to the initial frequency peak at the onset of

the stimulus train. Note that the response is excitation for ED4,5 and suppression for FDP. Also of interest is the fact that the excitatory modulation of ED4,5 strengthens throughout the hold phase of the response while the inhibitory modulation in FDP is greatly diminished after the first two cycles.

Phase shifts derived from analogue cross-correlations

Cortical sites that yielded strong poststimulus effects in StTA records yielded robust EMG modulation in response to frequency-modulated stimulus trains applied at the same site. However the output EMG modulation was not always purely excitatory. At all carrier frequencies three fundamental modulation patterns in the EMG records were observed in response to stimulation: predominantly excitatory (pE), predominantly inhibitory (pI), and initially excitatory transitioning to inhibitory (tEI). Predominately excitatory responses yielded peaks in EMG activity that were directly related to corresponding peaks in stimulus frequency, i.e. as stimulus frequency increased, EMG activity increased (Figure 2.5A). Predominantly inhibitory responses were those that yielded the inverse of this pattern, i.e. as stimulus frequency increased, EMG activity decreased (Figure 2.5B). Responses categorized as tEI were those that shifted from excitatory to inhibitory over the course of the 750ms trial (Figure 2.5C). In rare cases within the tEI category (1.5%), responses began inhibitory and shifted to excitatory; these records were also included in the tEI category.

Using cross-correlation analysis we compared the timing (phase shift) of peaks in EMG activity relative to corresponding peaks in stimulus frequency. Given that most pI

and tEI effects did not modulate as clearly with sinusoidal stimulation as did pE effects, cross-correlation results for pI and tEI effects were more difficult to interpret. Therefore only records with pE responses were included in our cross-correlation analysis.

Average phase shifts between the frequency modulated stimulus train and EMG activity derived from analogue cross-correlation analysis are given in Table 2.3. The results are categorized by modulating frequency and carrier frequency. As there was no statistical difference in the phase shifts observed for different forearm muscles (one way ANOVA on ranks, $P = 0.485$), the latencies for all muscles were combined in the analysis. Higher carrier frequencies yielded fewer pE responses and correspondingly more pI and tEI responses, as evident from the number of records for each parameter, as each carrier frequency parameter was used an equal number of times for each modulation frequency pair . In addition, higher modulation rates and higher carrier frequencies yielded lower cross-correlation magnitudes. Higher frequencies would be expected to produce greater physiological spread and thus a greater probability of aggregating both excitatory and inhibitory effects that would interfere with the ability of the corticomotor system to follow higher frequencies.

Increasing stimulus intensity resulted in a significant decrease in phase shift of EMG modulation with respect to modulating stimulation (one way ANOVA on ranks, $P = <0.001$). pE responses for all frequency parameters with a stimulus intensity of 10 µA had a mean latency of 12.8 ± 4.3 ms (n = 184). Responses at 15 µA had a mean latency of 11.9 ± 5.6 ms (n = 273), and responses at 30 µA had a mean latency of 9.9 ± 6.1 ms (n = 245). One possible explanation for this is that higher intensities result in greater numbers of CM cells that are activated, and subsequently more rapid activation of motor units.

The overall mean phase shift, or latency, of pE EMG modulation relative to all frequency modulation parameters in this study was 11.5 ± 5.6 ms (n = 703). This latency approaches the minimum conduction time through the pathway from cortex to forearm muscles.

Onset latency measurements

We measured the onset latency of EMG activity following the onset of frequency-modulated stimulation for all pE M1 cortical sites in the study (Table 2.4). The mean onset latency for all stimulus parameters was 10.7 ± 4.4 ms (n = 657). There was a statistically significant difference in onset latency when the stimulus was applied in the presence or absence of background EMG (P = <0.001, Mann-Whitney). The mean onset latency when stimulation was applied in the presence of background muscle activity was 9.7 ± 3.3 ms (n = 371) compared to 12.1 ± 5.2 ms (n = 286) in the absence of background EMG activity.

Variety of responses to stimulation

EMG responses to stimulation observed in this study fell into three categories - pE, pI and tEI - as described earlier. However subtle variations within these categories are noteworthy. Figure 2.6A illustrates an example of a consistent level of excitatory modulation for the duration of the stimulation, whereas Figure 2.6B illustrates an extreme example of an excitatory response yielding to either strong inhibitory interactions or a

near complete inability to follow high frequency modulation for the duration of stimulation. Figure 2.6C illustrates a dynamic strengthening and subsequent attenuation in EMG activity throughout the duration of the stimulation. These responses convey an interesting competition between excitatory and inhibitory networks within the brain and spinal cord. Often this interplay leads the resulting EMG to transition from an excitatory response to an inhibitory response, possibly resulting from either greater latencies associated with the activation of inhibitory networks or stronger initial excitatory responses that eventually give way to building inhibitory tone.

DISCUSSION

The timing of muscle activity resulting from modulations in descending cortical output remains an underlying question of interest in the study of neural encoding. Many previous studies have reported consistently greater latencies between cortical activity and the onset of muscle activity during natural movements than would be expected from the minimum conduction time through the same pathway. Conduction studies using StTA and SpTA have reported minimum conduction times through the forelimb cortico-muscle pathway of 6.7 – 9.8 ms depending on the specific muscle tested (Cheney and Fetz, 1980, Lemon et al., 1986, McKiernan et al., 1998, Park et al., 2004). In contrast, numerous studies have reported latencies of 60-122 ms from population cortical activity to muscle activity during natural movement (Humphrey and Corrie, 1978, Cheney and Fetz, 1980, 1985, Baker and Lemon, 1998, McKiernan et al., 1998, Morrow and Miller, 2003, Park et al., 2004).

The long-duration stimulus-evoked EMG modulation reported in the present study differs from StTA and SpTA studies in that modulation is evident in individual trials and occurs over a period of 750 ms which simulates the time scale of natural, active movements. Therefore the EMG modulation observed is the result of the summed activity of corticospinal neurons modulated over time at stimulus frequencies and intensities that produce overt activation of muscle activity. In contrast, SpTA and StTA detect subliminal synaptic effects whose latency should reflect largely conduction time through the pathway to muscle.

There are several hypotheses regarding the nature of the observed discrepancy in timing. One hypothesis suggests that the disparity in timing may be due to plateau potentials in the dendritic currents of motor neurons, resulting from persistent inward currents (Morrow and Miller, 2003, Binder et al., 2011). These plateau potentials may act as a low-pass filter to both amplify and substantially delay the incoming signals. Plateau potentials could produce a consistent delay in the expression of cortical activity at the muscle level. Moreover, this delay would be present throughout the entire movement, rather than solely at movement onset. Plateau potentials could provide a possible explanation for the results obtained by Morrow and Miller (2003) in which they observed optimal fits between cortical activity and EMG activity using a phase shift of 50 ms.

A modeling study of plateau potentials by (Shapiro and Lee, 2007) may provide evidence for an alternative explanation regarding the disparity between results in the current study and results obtained by comparing the latency of natural cortical activity to EMG activity. This study suggests that bistable firing and synaptic amplification of motoneurons, previously proposed to involve one mechanism, may include two distinct mechanisms that would allow both slow and fast transmission by motoneurons. It is possible that in addition to slow L-type Ca2+ channels that are responsible for bistability of motoneuron dendrites, fast Na+ channels may be responsible for amplification of signals. If this were the case, the fast Na+ channels would be able to follow extremely rapid input such as that seen in this study.

Alternatively, the disparity may simply be due to the time required for the motoneurons to achieve firing threshold. This requires summation of converging excitatory postsynaptic potentials (EPSPs) from corresponding CM cells. This action

could pose a significant delay during the initiation of movement; however, the discrepancy in timing should be absent during active movement once the motoneurons are actively firing or near firing threshold. Therefore, during active movement the delay between CM cell activation and resulting EMG activity should approach the minimum conduction time through the pathway if time to achieve threshold is the mechanism.

The results in the current study suggest that once motoneurons are firing or are near firing threshold, the delay between the activity of CM cells and resulting muscle activity approaches the minimum conduction time through the pathway. The stimulus parameters used in our study resulted in overt activation of the cortico-muscle pathway. Nevertheless, we did see a small but significant difference in onset latency when stimulation was applied in the presence of background EMG activity, as opposed to quiescent background EMG activity. The fact that the difference was small is likely due to a fundamental difference between the activation of cortical neurons using stimulation compared to natural activation during voluntary movement. Our stimulation method would be expected to produce synchronous activation of cortical cells. As a consequence, at stimulus onset, a large number of cortical cells will be simultaneously activated yielding a large, relatively synchronous input volley to motoneurons bringing motor units to firing threshold quickly. In contrast, during natural voluntary movements, the onset of firing in different cortical cells is asynchronous with gradual recruitment of the requisite number of cells.

To more closely simulate natural activation of motor units by cortical stimulation, a logical extension of our study would be to not only modulate stimulus frequency, as we have done in this study, but also stimulus intensity. Modulating intensity would provide a

mechanism to simulate the range of cortical cell recruitment times relative to movement/EMG onset evident in studies of cortical cell activity during natural movements (for example, see (Cheney and Fetz, 1980), Figure 3).

Summary and Conclusions

Although the time delay between peaks in the frequency-modulated cortical stimulus train and corresponding EMG modulation varied somewhat with the stimulus parameters, the overall mean latency of excitatory modulation across all parameters determined via cross-correlation analysis (11.5 ± 5.6 ms) was only 1.9 ms longer than the conduction time through the cortex-to-muscle pathway derived from StTAs computed at the same sites (9.6 ± 2.1 ms). These results demonstrate that, during active movement, cortical output can modulate muscle activity at latencies approaching the minimum conduction time through the cortico-muscle pathway. The results support the hypothesis that the longer time delays reported for the timing between cortical cell activation and muscle activation are due largely to the time required to bring motoneurons to firing threshold from a hyperpolarized state.

Table 2.1. *Mean latencies and magnitudes of poststimulus effects obtained from StTAs*

	n	Onset (ms)	Peak (ms)	Magnitude, %
PStF	253	9.6 ± 2.1	12.6 ± 2.0	72.5 ± 92.6
PStS	38	14.2 ± 2.8	17.7 ± 5.0	-21.8 ± 7.0

Values are means ± SD; n = number of effects measured. Stimulus intensities used to acquire StTAs were 10, 15, and 30 µA. Magnitude was measured as the peak increase above baseline for poststimulus facilitation (PStF) or decrease below baseline for poststimulus suppression (PStS) effects expressed as a percent of baseline.

Table 2.2. *Comparison of effects from sinusoidal stimulation and stimulus triggered averaging*

	Sinusoidal Stimulation Effect			
	pE	pI	tEI	Total
Poststimulus Effect	*n*	*n*	*n*	*n*
PStF	488	79	332	899
PStS	21	34	20	75
PStF/PStS	64	17	51	132
Weak or No PStE	129	157	91	377
Total	702	287	494	1493

Values in the table are the total number of sinusoidal modulation effects at each site corresponding to different types of poststimulus effects obtained from the same sites. n = number of measurements. Stimulus intensities used were 10, 15, and 30 µA. EMG modulation effects were considered significant and included if the envelope of the EMG record surpassed ±5 SD above or below the mean of the baseline EMG activity. pE is predominantly excitatory, pI is predominantly inhibitory and tEI is initially excitatory transitioning to inhibitory.

Table 2.3. *Mean latency values derived from analogue cross-correlation analysis*

Modulation Freq, Hz	Carrier Freq, Hz	Freq Range, Hz	Latency, ms	Magnitude, %
4	150	63 - 263	16.2 ± 7.8 (n = 109)	46.1 ± 13.3
12	100	63 - 167	8.2 ± 4.5 (n = 297)	38.5 ± 14.7
12	200	81 - 357	8.6 ± 5.5 (n = 23)	28.7 ± 10.7
28	150	108 - 230	12.2 ± 2.3 (n = 192)	24.9 ± 7.9
28	250	104 - 434	15.9 ± 1.9 (n = 81)	19.1 ± 3.4
All	All	All	11.5 ± 5.6 (n = 703)	33.4 ± 14.9

Values are means ± SD; n = number of cortical site–muscle pairs measured. Data is based on predominantly excitatory (pE) EMG modulation. Stimulus intensities used were 10, 15, and 30 µA. Magnitude % = peak percent increase (PPI) above baseline.

Table 2.4: *Mean onset latencies for pE responses in the presence and absence of background EMG activity.*

Modulation Frequency, Hz	Carrier Frequency, Hz	Background EMG	Mean Onset, ms
4	150	Present	8.7 ± 2.4 (n = 55)*
4	150	Absent	11.4 ± 5.5 (n = 53)
12	100	Present	8.9 ± 3.4 (n = 159)*
12	100	Absent	10.9 ± 5.4 (n = 114)
12	200	Present	7.8 ± 1.9 (n = 8)*
12	200	Absent	15.9 ± 5.8 (n = 14)
28	150	Present	10.3 ± 3.2 (n = 104)*
28	150	Absent	12.4 ± 4.2 (n = 75)
28	250	Present	12.4 ± 2.7 (n = 45)*
28	250	Absent	15.7 ± 3.4 (n = 30)
All	All	Present	9.7 ± 3.3 (n = 371)*
All	All	Absent	12.1 ± 5.2 (n = 286)

Values are means ± SD; n = number of measurements. Data is based on predominantly excitatory (pE) muscle modulation. Stimulus intensities used were 10, 15, and 30 µA. *Using the same stimulus parameters, mean onset time for modulation in the presence of background EMG is statistically shorter than onset of modulation in the absence of background EMG (Mann-Whitney, $P < 0.001$).

Figure 2.1. Monkey performing the ramp-and-hold concentric wrist flexion and extension task.

Concentric wrist flexion and extension task

Figure 2.2. Unfolded map of the monkey's M1 forelimb representation in the left hemisphere with a view of the dorsal surface of the precentral gyrus and the rostral wall of the central sulcus. Anterior, posterior, medial and lateral are indicated by the compass rose. Sites of frequency-modulated sinusoidal stimulation are indicated by the yellow dots, and are numbered in chronological order of stimulation. The color-coded muscle representation map was obtained from a previous StTA mapping study in this monkey. Distal forearm facilitation in M1 is represented as blue, proximal forearm facilitation as red, and proximal-distal co-facilitation as purple.

Unfolded map of M1 forelimb representation

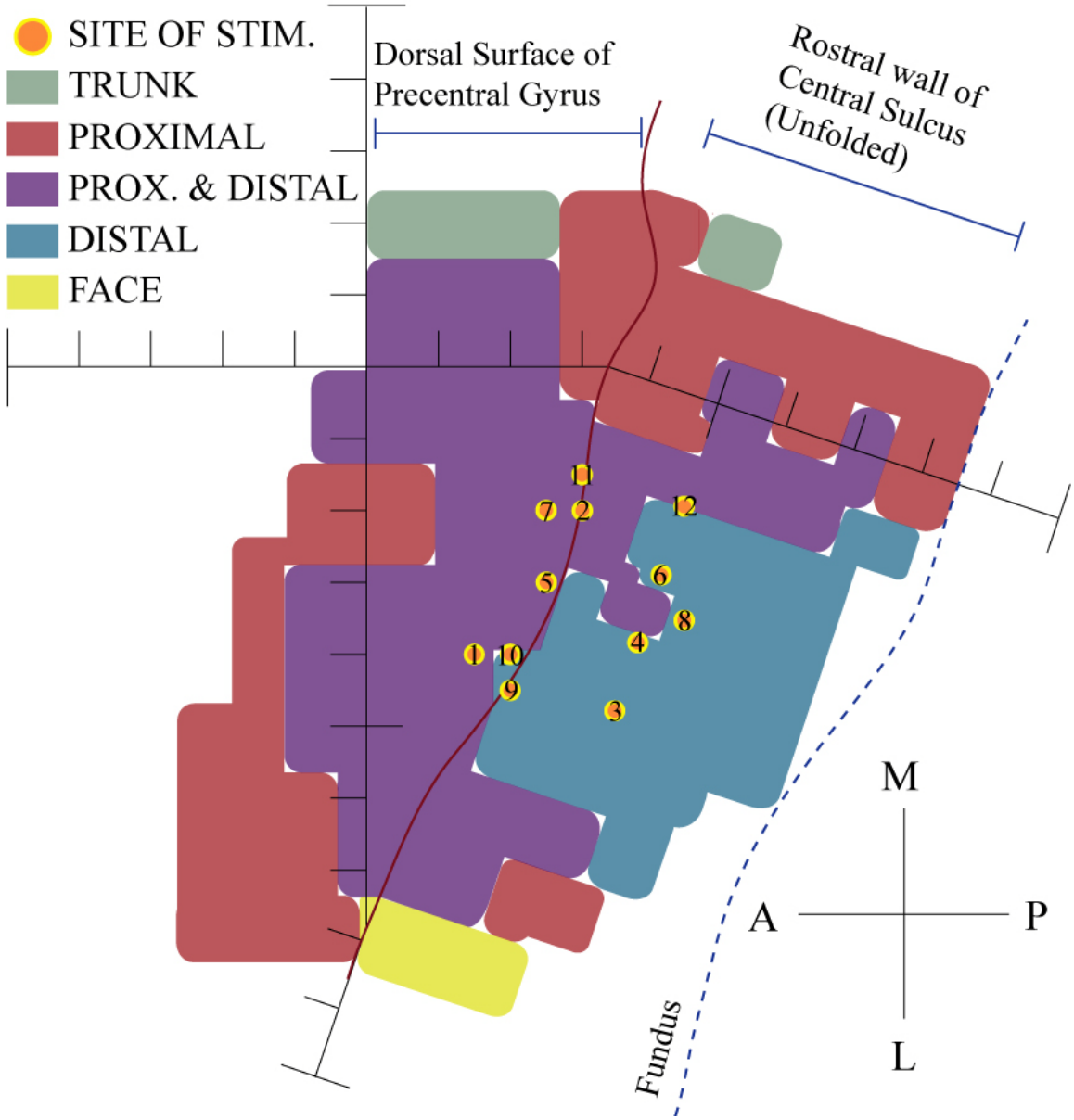

Figure 2.3. *A*: Basic circuit used to generate frequency-modulated stimulus trains. *B*: Modulated stimulus output train. The black waveform is the voltage controlled generator signal (VCG), which modulates a carrier frequency to yield the frequency-modulated stimulus pulse train (red) used to trigger the stimulator. The stimulus train in this example modulates from 24 to 82 Hz around a carrier frequency of 50 Hz. The rate of modulation was 4 Hz. *C*: An expanded version of the middle cycle represented in *B*. The shortest inter-spike interval (ISI) is noted.

Frequency-modulated stimulus generator circuit

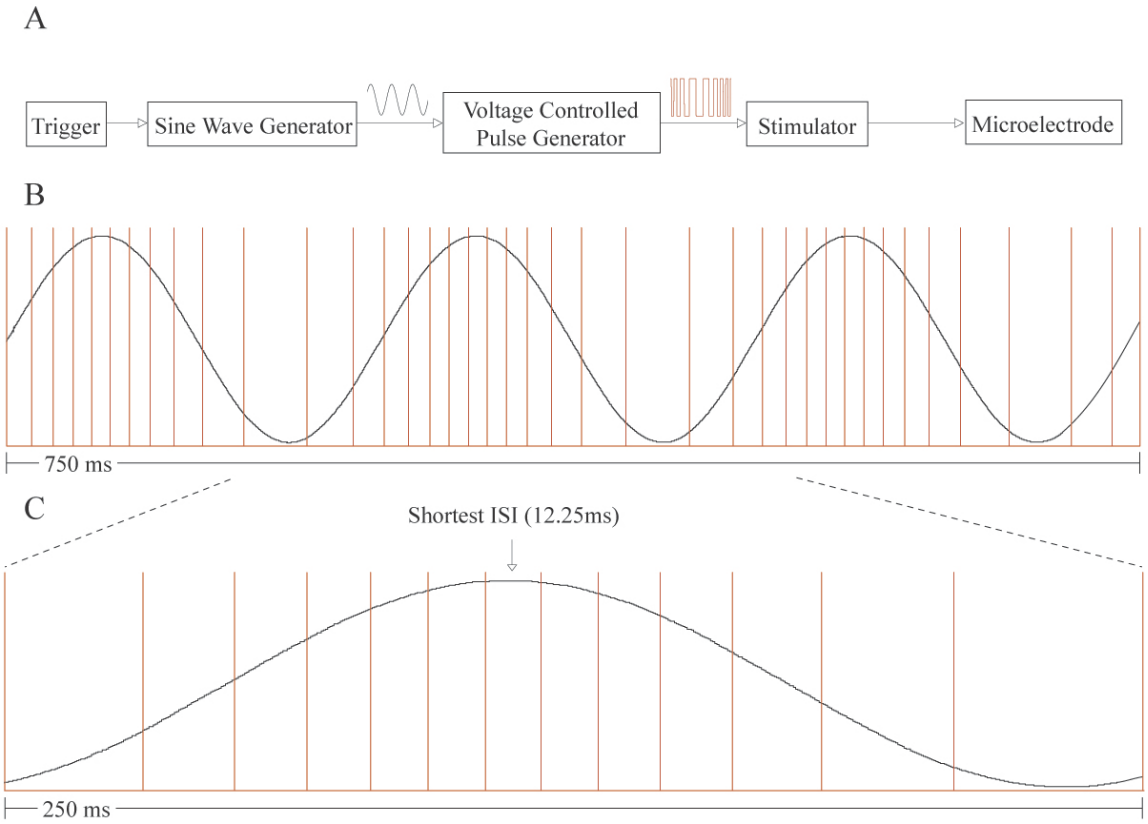

Figure 2.4. Baseline muscle activity and frequency-modulated activation of the same muscles. All records included in this figure were obtained from cortical site 5 (Figure 2.2). *A-B*: ED 4,5 and FDP EMG activity associated with wrist extension and flexion, respectively, in the absence of stimulation. For muscle abbreviations, see Methods. Wrist position record (gray line) is superimposed on each EMG record, and ranges from 40°±10 in flexion to 30°±15 in extension. *C*: Stimulus triggered averages for ED 4,5 and FDP acquired at 30 µA. The stimulus is shown as a light gray line superimposed on the EMG records. *D-E*: wrist extension and flexion respectively with frequency-modulated stimulation (*F*) beginning midway through the dynamic phase of movement. The period of stimulation is represented by gray shading. The number in parentheses under each set of records is the number of events averaged.

Baseline and frequency-modulated muscle activity

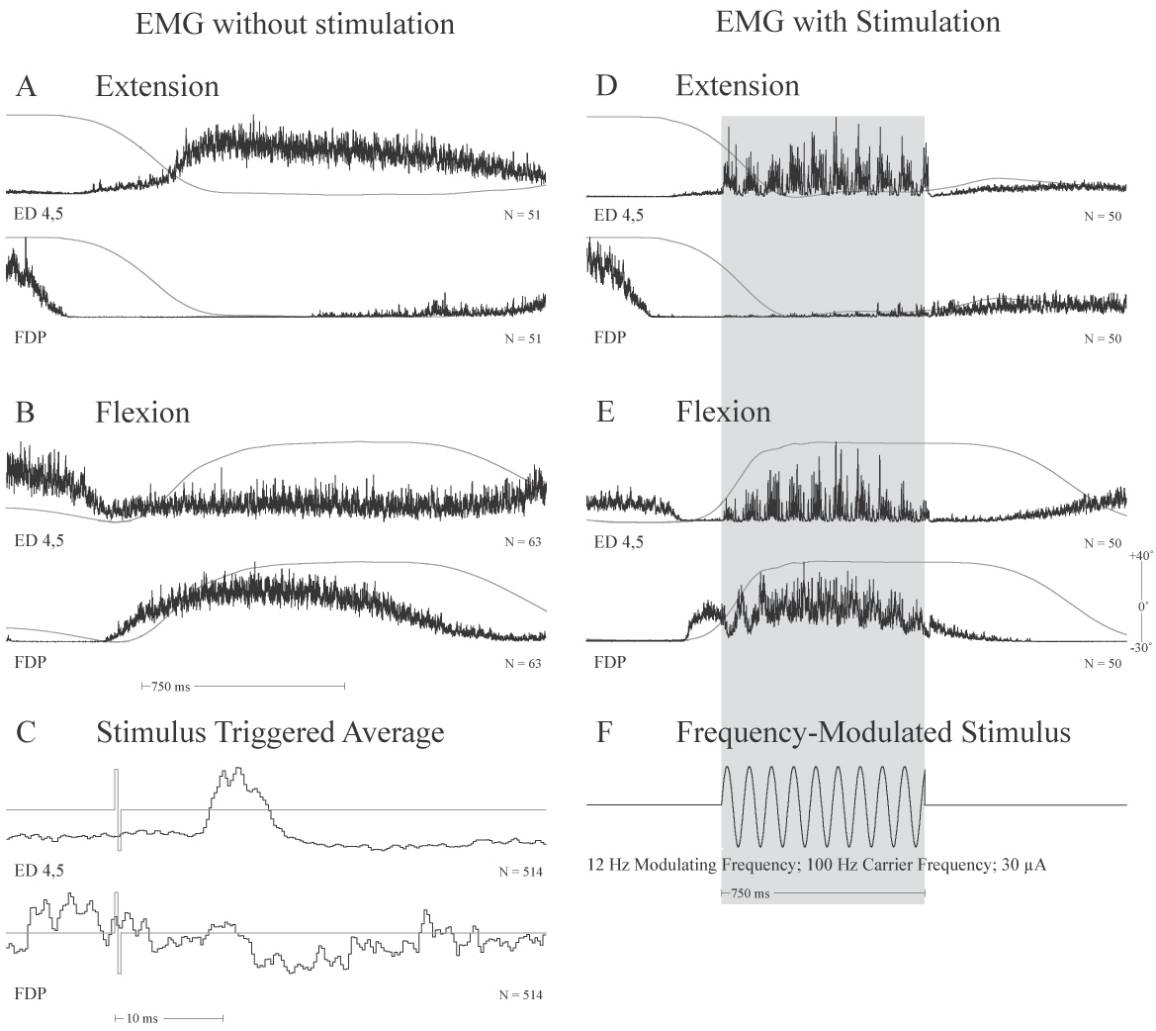

Figure 2.5. *A*: pE, or predominantly excitatory response. EMG activity increases in response to increasing stimulus frequency. *B*: pI, or predominantly inhibitory response. EMG activity decreases in response to increasing stimulus frequency. *C*: tEI, or excitation transitioning to inhibition. EMG activity initially responds with an increase in activity in response to increasing stimulus frequency, but gradually transitions to inhibition as the stimulus train continues. For muscle abbreviations, see Methods. Wrist position record (gray line) is superimposed on each EMG record, and ranges from 40°±10 in flexion to 30°±15 in extension. The 12 Hz signal used to modulate the stimulus train is superimposed on the EMG records (red line).

Fundamental responses to stimulation

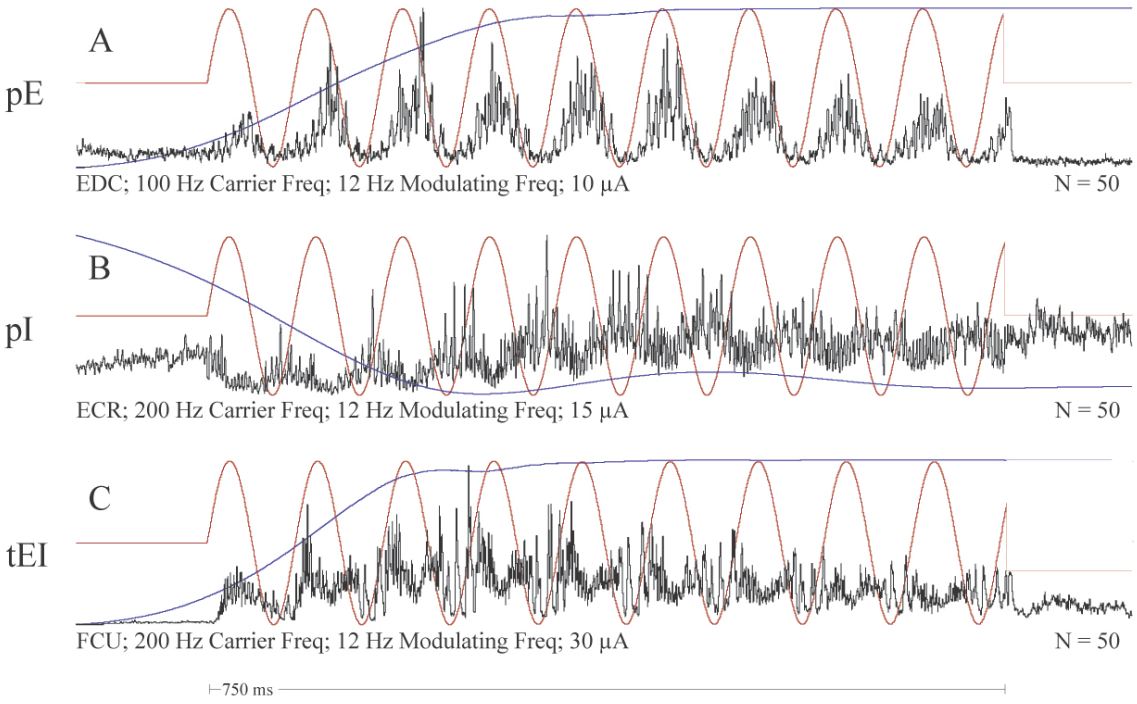

Figure 2.6. *A*: Consistent modulation throughout stimulation. *B*: Strong excitatory responses followed by almost complete loss of modulation after about 10 cycles. C: Waxing and waning of EMG excitatory responses throughout the stimulus train. For muscle abbreviations, see Methods. Wrist position record (gray line) is superimposed on each EMG record, and ranges from 40˚±10 in flexion to 30˚±15 in extension. The stimulus modulation signal is shown as a light red line superimposed on the EMG records.

Variations in response to sinusoidal stimulation

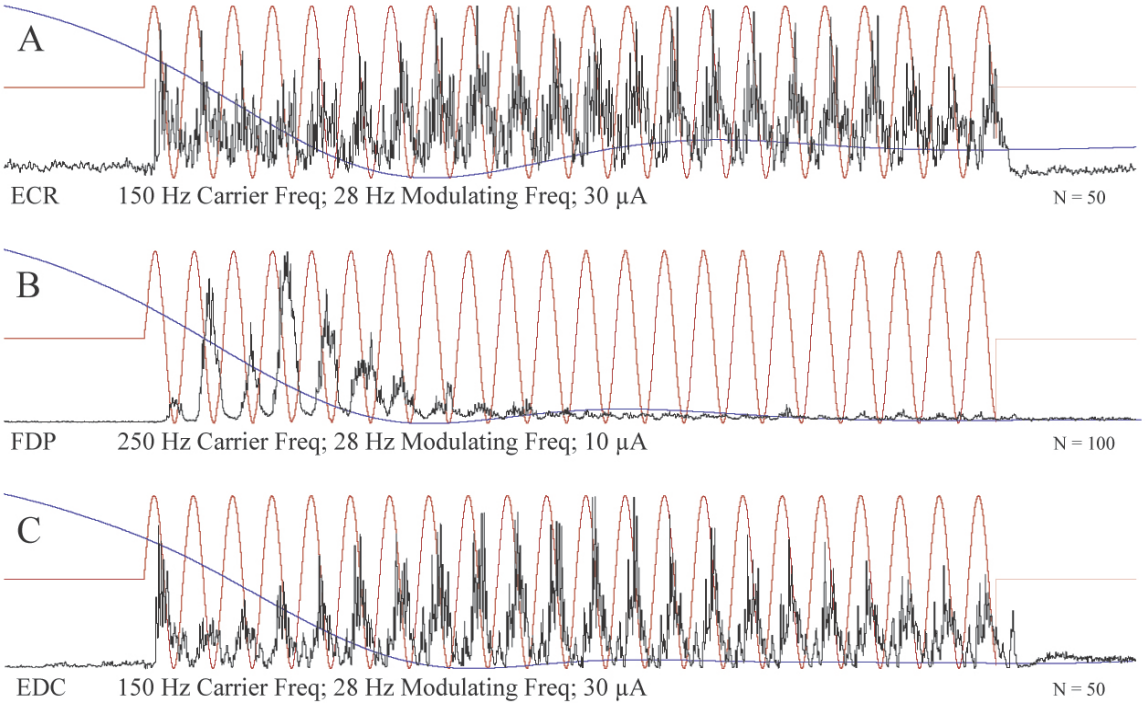

CHAPTER III:

OPTIMAL STIMULUS PARAMETERS FOR M1 RL-ICMS-EVOKED FORELIMB TRANSLOCATION WITH SUBSEQUENT STABILIZATION

ABSTRACT

The goal of this study was to investigate the relationship between RL-ICMS parameters applied to the rhesus macaque primary motor cortex (M1) and the resulting muscle activation and evoked movement. This will enable appropriate selection of stimulus parameters for systematic mapping of forelimb movements in terms of spatial end-points as well as muscle synergies. We applied stimulation to M1 as combinations of frequency (30 - 400 Hz), amplitude (30 - 200 µA) and duration (0.5 - 2 s) while concurrently recording EMG activity from 24 forelimb muscles and movement kinematics using a Vicon motion capture system. Our results suggest a relatively narrow range of stimulus parameters that were both effective and safe for evoking forelimb translocation with subsequent stabilization at a spatial end-point. The range of parameters were 70 - 130 Hz, 70 - 130 µA and 750 - 1000 ms. The mean end-point time of stimulus evoked movements was 479.0 ± 178.9 msec. The median successful frequency normalized for success rate was 110 Hz, and the median successful amplitude was 110 µA. Attenuated parameters resulted in inconsistent, truncated or undetectable movements, while intensified parameters increased the potential for large-scale physiological spread and adverse focal motor effects. Establishing cortical stimulation parameters that yield consistent forelimb movement end-points forms the basis for a systematic and complete mapping of M1 cortex in terms of evoked movement end-points and associated muscle synergies. The results add to our understanding of how the central nervous system encodes movement, and could aid in the development of neuroprosthetic devices.

INTRODUCTION

The goal of the present study was to investigate the relationship between stimulus parameters applied to the macaque primary motor cortex (M1) and the resulting muscle activation patterns and evoked movements. Cortico-motor connectivity between neurons in M1 and muscles has been mapped previously using various forms of electrophysiological methods, tracer studies, and histological approaches (Penfield and Boldrey, 1937, Woolsey et al., 1952, Cheney and Fetz, 1985, Donoghue et al., 1992, Rathelot and Strick, 2006). While early clinical electrophysiological approaches utilized surface stimulation of the cortex to evoke grossly observable responses (Penfield and Boldrey, 1937, Woolsey et al., 1952), the introduction of intracortical microstimulation (ICMS) has permitted more refined mapping of cortical output to muscles (Asanuma and Sakata, 1967). Short trains of high frequency ICMS (RS-ICMS) have been used to evoke twitch-like responses for cortical mapping and other purposes (Asanuma et al., 1976, Strick and Preston, 1978). More recently this method of ICMS has been modified by applying ICMS trains with longer durations (500 ms) that more closely match the timescale of natural movements (Graziano et al., 2002, Graziano et al., 2005, Ethier et al., 2006). These long-duration repetitive trains (RL-ICMS) produced natural appearing movements of activated limbs characterized by having a common spatial end-point for a particular cortical site regardless of the starting position of the limb.

In the current study, our aim was to determine the optimal parameters for RL-ICMS. Stimulation of M1 using optimal parameters should yield translocation and subsequent stabilization of the forelimb at discrete spatial end-points. We applied

stimulation as combinations of frequency (30 - 400 Hz), amplitude (30 - 200 uA) and duration (0.5 - 2 s) to M1 while concurrently recording the EMG output to 24 forelimb muscles as well as the stimulus-evoked limb kinematics using a Vicon motion capture system. Our results suggest a relatively narrow range of optimal stimulus parameters for M1 that are both safe and effective for evoking movement and subsequent stabilization of the forelimb at a spatial end-point. The optimal parameters were 70 - 130 Hz, 70 - 130 µA and 750 - 1000 ms. The mean end-point arrival time was 479.0 ± 178.9 msec. The median successful frequency and stimulus intensity for all successful trials were 110 Hz and 110 µA, respectively. Attenuated parameters resulted in inconsistent, truncated or undetectable movements, while intensified parameters increased the potential for large-scale physiological spread and adverse focal motor effects. Establishing stimulation parameters for M1 that yield consistent forelimb movements to stable spatial end-points forms the basis of a systematic and complete mapping of forelimb movement representations elicited from the primary motor cortex. The results will add to our understanding of how RL-ICMS applied to the motor cortex affects motor output, and could aid in the future development of more advanced neuroprosthetic devices.

EXPERIMENTAL PROCEDURES

Behavioral Task

Data were collected from two male rhesus macaques (*Macaca mulatta; ~9 kg each, ages 12 and 4*) performing a reach and prehension task that required co-activation of proximal and distal forelimb muscles, while also yielding discrete spatial locations to cue stimulus trains (Figure 3.1). Training procedures and the behavioral task have been described in detail previously (Belhaj-Saif et al., 1998, McKiernan et al., 1998). Briefly, the monkey was seated in a custom primate chair within a sound-attenuating chamber with his left arm comfortably restrained while his right arm retained freedom of movement. To discourage the monkey from interfering with reflective motion capture spheres attached to his arm, a custom face mask barrier was installed on the chair that contained a small hole through which the monkey could feed himself. In order to receive a food reward the monkey initiated the task with his right hand by depressing a homeplate lever (Figure 3.1A) located at waist height directly in front of him for 1 second duration, triggering the release of a food pellet into a food well (Figure 3.1B) located at shoulder height. Following the retrieval and consumption of the food reward (Figure 3.1C), the monkey returned his hand to the homeplate for subsequent trials. Performance was guided by audio and visual cues.

Surgical Procedures

Following training, an MRI-compatible stainless steel chamber allowing 30 mm diameter of dural exposure, and exploration of the underlying cortical area, was implanted stereotaxically over the primary motor cortex of the left hemisphere of each monkey using procedures described in detail previously (Park et al., 2000). Briefly, the chamber was anchored to the skull using titanium screws and dental acrylic, and was centered over the hand area of M1 in the left hemisphere. In addition, threaded titanium nuts were attached over the occipital aspect of the skull using titanium screws and dental acrylic. These nuts provided a point of attachment for a flexible head restraint system during data collection (McKiernan et al., 1998, 2000). The chambers were centered at anterior 17.7 mm, lateral 27.2 mm and 26 º to the sagittal plane for Monkey X, and anterior 16 mm, lateral 22 mm 30 º to the sagittal plane for Monkey A.

Twenty four muscles of the right shoulder and forelimb were each implanted with two multi-stranded stainless steel wires (Cooner Wire, AS632). Both monkeys were implanted under sterile conditions using a cranial subcutaneous implant technique described previously (Park et al., 2000). Briefly, all wires were stripped of ~2-3 mm of insulation and tunneled subcutaneously from a cortical connector (Amphenol, Wallingford, CT) to each muscle, where the wires were inserted into the muscles a distance of ~2-3 cm, with a ~5 mm separation of the two wires in each muscle. The cortical connector module was secured with dental acrylic near the cortical recording chamber. We tested the placement accuracy of each electrode pair by observing appropriate muscle twitches that resulted from applying short stimulus trains (Grass SD9 Stimulator). EMG activity was recorded from five shoulder muscles: pectoralis major (PEC), anterior deltoid (ADE), posterior deltoid (PDE), teres major (TMAJ) and

latissimus dorsi (LAT); seven elbow muscles: biceps short head (BIS), biceps long head (BIL), brachialis (BRA), brachioradialis (BR), triceps long head (TLON), triceps lateral head (TLAT) and dorsoepitrochlearis (DE); five wrist muscles: extensor carpi radialis (ECR), extensor carpi ulnaris (ECU), flexor carpi radialis (FCR), flexor carpi ulnaris (FCU) and palmaris longus (PL); five digit muscles: extensor digitorum communis (EDC), extensor digitorum 2 and 3 (ED23) extensor digitorum 4 and 5 (ED45), flexor digitorum superficialis (FDS) and flexor digitorum profundus (FDP); and two intrinsic hand muscles: abductor pollicis brevis (APB) and first dorsal interosseus (FDI).

All surgeries were performed under deep general anesthesia and aseptic conditions. Prior to each implant surgery, the monkey was administered ketamine (10mg/kg IM), atropine (0.04 mg/kg IM), and medetomidine (0.05 mg/kg IM) for transportation purposes, and subsequently isoflurane gas for the duration of the surgery. Each monkey received prophylactic antibiotic (penicillin, 6000 U/kg SC) 10 hours pre-surgery, 1 hour post-surgery, and 3 days following surgery. Postoperatively, the monkeys were given analgesics (buprenorphine, 0.01 mg/kg IM and carprofen, 5 mg/kg SC). All surgeries were performed in a facility accredited by the Association for Assessment and Accreditation of Laboratory Animal Care using full sterile procedures. All procedures conformed to the Guide for the Care and Use of Laboratory Animals, published by the United States Department of Health and Human Services and the National Institutes of Health.

Recording Forelimb Kinematics

Limb kinematics were monitored and recorded using a Vicon motion capture system. For the purposes of this study, a virtual sphere located on the dorsal tubercle of the radius was calculated and used to evaluate limb kinematics as well as the spatial end-point resulting from RL-ICMS applied to each cortical site (Figure 3.1). The 3-dimensional coordinates of this virtual sphere were calculated using a Point Cluster technique described previously (Andriacchi et al., 1998, Senesh and Wolf, 2009). Briefly, a cluster of reflective spheres were attached to the forearm of each monkey. The three-dimensional coordinates of the spheres in each cluster, as measured using the Vicon system, were used to triangulate the coordinates of the virtual sphere located on the dorsal tubercle of the radius, which was identified during static trials at the start of each recording session. The dorsal tubercle of the radius was used as a surrogate for end-point position of the hand in space. Utilizing subsets of the numerous wrist markers to calculate the spatial position of the reference point (dorsal tubercle of the radius) reduced the need for the wrist to be within view of any particular set of Vicon cameras in order to be monitored.

RL-ICMS Protocol

One-thousand, three-hundred and sixty-five RL-ICMS trains were applied to 19 distinct cortical sites within the right forelimb representation of M1 in the left hemisphere (Figure 3.2A and 3.2B) of two rhesus macaques performing a reach and prehension task over the course of the study. Stimulation was applied through glass insulated platinum-iridium electrodes suitable for single unit recording (FHC Inc., Bowdoin, ME), with

typical impedances of 0.7 - 1.5 MΩ at the start of each recording session. We positioned the electrodes using an X-Y positioner secured to the chamber for the duration of each recording session, and advanced the electrode into the brain using a manual hydraulic microdrive (FHC Corp.) until the electrode tip was located in cortical lamina V, or approximately 1.5 mm below the surface of the brain. Location of layer V was determined by depth, audio cues (Grass AM8 Audio Monitor), visual cues (oscilloscope display of large spike waveforms), and finally by poststimulus effects in StTAs at 15μA and 10 Hz. Stimulation was applied when the monkey's hand was at one of three task positions (Figure 3.1), and the location that was furthest from the stimulus-evoked spatial end-point was chosen once a test stimulation trial elicited a detectable movement. Because position 3.1B (feeder) was on the periphery of the monkey's work space, this location was used most frequently for stimulation onset.

At each cortical site we applied systematic combinations of frequency (30 - 400 Hz), amplitude (30 - 200 μA) and duration (0.5 - 2 s) in order to delineate parameters that yielded forelimb movement with subsequent stabilization from parameters that did not. Individual stimuli for each stimulus train were symmetrical biphasic pulses: initial negative pulse 0.2 ms in duration followed directly by a positive pulse 0.2 ms in duration. Stimulus train duration of 1 second was revealed early in the study to be an optimal epoch for assessing the adequacy of the other parameters. A 0.5 second stimulus train duration often resulted in movements that were truncated relative to spatial end-points achieved with longer durations and was therefore too short to determine a spatial end-point for many elicited movements. Stable end-points were always achieved with stimulus durations of one second or less so longer durations were unnecessary and

increased the risk of adverse focal motor effects. We should also note that while we initially explored frequencies ranging from 200 - 400 Hz as well as amplitudes ranging from 150 - 200 μA, we concluded that these parameter ranges were unnecessary for achieving a stable stimulus-evoked end-point, and that these frequencies also increased the potential for adverse focal motor effects. Therefore each parameter set collected for data analysis in this study was a combination of frequency (50 - 170 Hz), amplitude (30 - 150 μA) and a one second stimulus duration. Five trials were conducted for each RL-ICMS parameter set.

Determining successful stimulus parameters for evoked movements

The RL-ICMS-evoked kinematics of the dorsal tubercle of the radius were used to assess successful spatial end-points achieved through stimulation of M1. RL-ICMS-evoked movement trials were deemed successful if the stimulus parameters applied to the M1 site were sufficient to translocate the monkey's forelimb to a spatial location distinct from its location at the initiation of stimulation and sufficient to maintain the limb at the stimulus-evoked location for the duration of stimulation. Attenuated parameters resulted in incomplete, truncated, or undetectable movements of the forelimb, often resulting in the monkey overcoming the stimulated movement and returning to the voluntary movement task. Intensified parameters deemed successful yielded similar end-points from those achieved with less intense yet successful parameters. However, intensified parameters increased the potential for secondary movements during the stimulus train following arrival at an initial end-point, as well as the potential for adverse focal motor

effects. Secondary movements and adverse focal motor effects are possibly due to extensive physiological spread along horizontal cortical collaterals exacerbated by excessive stimulus frequency. Therefore, our goal was to delineate the safe and effective range of parameters that yielded movement and subsequent stabilization of the forelimb for the duration of stimulation.

The specific success criteria we used required, firstly, that movement occur within the first 500 ms of stimulation onset to indicate adequate stimulus-induced movement. Next, our criteria required that movement velocity reach a level greater than or equal to 40% of the maximum mean stimulus-induced velocity. The mean stimulus-induced velocity was calculated from all successful trials included in this study. Once this criterion is met, the induced movement velocity must then cross a threshold of less than or equal to 25% of the maximum mean stimulus-induced velocity. Finally, once this lower threshold is crossed, the velocity of the movement must remain below this 25% threshold for the remainder of the applied stimulus train (Figure 3.3). Time to spatial end-point stabilization for successful trials was measured at the point where the stimulus-evoked velocity crossed a threshold of ≤25%. These criteria yielded objective success evaluation that closely matched visual subjective assessment.

Stimulus Triggered Averages

Stimulus triggered averages (StTAs) were gathered for all implanted muscles from stimuli applied throughout all phases of the reach and prehension task. StTAs were used to help confirm positioning of the electrode in lamina V and to determine cortico-

muscle connectivity of corticospinal cells directly surrounding the electrode tip. StTAs were obtained at 10 Hz and at current intensities that matched those used for each RL-ICMS train applied at the same site. In addition muscle facilitation maps (Figures 3.2A and 3.2B) utilized StTAs collected at 15 and 30 µA and were based on mapping at 1 mm intervals on the surface of the precentral gyrus and 0.5 mm vertical intervals down the bank of the central sulcus. EMG activity was filtered from 30 Hz to 1 kHz, digitized at 4 kHz and full-wave rectified. Individual stimuli for the StTAs were symmetrical biphasic pulses: initial negative pulse 0.2 ms in duration followed directly by a positive pulse 0.2 ms in duration. StTAs were based on a minimum of 1000 trigger events. Averages were compiled using a 60 ms epoch, of which 20 ms prior to the trigger was considered baseline. StTAs were identified as having a significant PStE if the peak or trough of the effect exceeded ±5 SD of the baseline for a period of≥ 0.75 ms as described previously for moderate-to-large effects (Park et al., 2004).

Measurement of EMG cross-talk

We evaluated cross-talk between EMG electrodes by constructing EMG-triggered averages. This procedure used the motor unit potentials from one muscle as triggers for compiling averages of rectified EMG activity of all other muscles. Criteria established previously (Buys et al., 1986) were used to eliminate effects that might have been affected by cross-talk. To be accepted as a valid PStE, the ratio of PStF between the test and trigger muscles must have exceeded the ratio of their cross-talk peaks by a factor of two or more. Based on this criterion, FDI in monkey X was removed from the analysis.

RESULTS

Success rate for parameter pairings

The ratio of successful RL-ICMS-evoked movement trials to total trials was calculated for each frequency and current intensity parameter pairing. A successful trial was defined as one in which RL-ICMS produced translocation of the arm to a new end-point position which remained stable for the duration of stimulation (see Methods for more detail). At each cortical site tested, five stimulation trials per parameter pairing were applied. Based on numerous preliminary studies, optimal train duration was determined to be one second. Shorter durations were sometimes insufficient to reach an end-point and longer durations always exceeded the time needed to reach an end-point position.

Figure 3.4 illustrates the success rate for each parameter pairing color coded as a ratio of successful trials to total trials for each pairing. The results suggest a relatively narrow range of stimulus parameters that yield clear and stable forelimb movement end-points from RL-ICMS applied to M1 cortex. The successful stimulus frequency range was 70- 130 Hz coupled with a stimulus intensity range of 70 - 130 µA. Using these parameters, the mean time from stimulus onset to reach an end-point position was 479.0 ± 178.9 ms. The mean successful frequency, calculated using a weighted average based upon the ratio of successful to total trials for each parameter pairing, was 115.2 ± 22.3 Hz and the mean successful stimulus intensity was 108.8 ± 23.7 µA. Additionally, the median successful frequency for all trials was 110 Hz and the median intensity was 110

µA. Attenuated parameters resulted in inconsistent, truncated, or undetectable movements of the forelimb, often resulting in the monkey superseding the stimulated movement with voluntary movement and returning to the volitional movement task. Intensified parameters beyond the optimal range identified above increased the potential for physiological spread and adverse focal motor effects, and therefore were avoided.

Success rate for parameter pairings for an individual site

Figure 3.5 illustrates stimulus parameter pairings that led to successful spatial end-points at an individual cortical site. In this example, 245 stimulation trials were applied to cortical site 5 of monkey X (Figure 3.2B). From one M1 cortical site to another, the range of stimulus parameters that evoked successful spatial end-points varied to some degree, however the deviation was relatively minimal. At each cortical site at which stimulation was applied in this study, a locus of successful stimulus parameter pairings was evident. In this example the parameters that resulted in the most prominent successful spatial end-points were 80 - 130 Hz and 110 - 120 µA, with a mean time to spatial end-point stabilization of 469 ± 156 msec.

Effect of stimulus parameters on peak movement velocity

While the stimulus-evoked spatial end-point did not deviate significantly from one successful parameter to another for each cortical site, the velocity with which the forelimb traveled to the spatial end-point varied directly with stimulus parameters. Figure

3.6 illustrates a density plot of stimulus parameter pairings color coded as the peak stimulus-induced velocity for each parameter pairing averaged over the number of trials listed in the corner of each square. A stimulation duration of one second was applied for each parameter pairing, and only trials that yielded successful spatial end-points were included. A clear trend is evident that as frequency and amplitude were increased, the peak stimulus-evoked movement velocity increased as well.

RL-ICMS effect on M1 not directly affected by stimulation

Successful spatial end-points as calculated in this study were unattainable at a number of sites in M1. RL-ICMS applied to M1 cortical sites that were either solely proximal or solely distal facilitation, as determined with StTA mapping, had a greater likelihood than proximal-distal co-facilitation (PDC) sites to yield co-activated movements resulting from a combination of stimulated and voluntary activity. For example, if we applied stimulation to an area assessed by StTA to yield distal forelimb facilitation, the likelihood of achieving a spatial end-point of the wrist marker was reduced in comparison to sites in or close to PDC sites. This appeared to be due to the monkey's ability to retain control of the joint associated with the muscles that were not directly affected by stimulation. At such purely distal-representation sites, the monkey preserved the ability to move his shoulder and/or elbow, while his distal muscles were fully stimulus-activated and apparently locked in the stimulus-evoked posture. This resulted in the monkey being able to move the virtual sphere located on a distal point of his wrist continuously during stimulation, thereby reducing the likelihood of achieving a

successful spatial end-point. However not every proximal- or distal-only site based on StTA effects responded in this manner, as some sites in these areas yielded both proximal and distal muscle activation when the RL-ICMS was applied. This could be the result of physiological spread amongst stimulated neural networks that connect proximal to distal muscles for coordinated limb activation.

Data in the present study were acquired at cortical sites that yielded both proximal and distal RL-ICMS-evoked muscle activity, resulting in stimulation leading the arm to consistent spatial end-points.

DISCUSSION

The goal of this study was to determine the optimal RL-ICMS parameters applied to M1 that yield translocation and subsequent stabilization of the forelimb at a fixed end-point within the monkey's work space. The use of RL-ICMS to study motor output has gained traction as an additional technique to include with other electrical stimulation methods such as TMS, RS-ICMS and StTA in studying cortical encoding of limb movements, as well as in the study of cortical eye fields (Tehovnik and Lee, 1993, Thier and Andersen, 1998, Graziano et al., 2002, Graziano et al., 2005, Ethier et al., 2006). Delineating stimulation parameters that translocate the limb and subsequently stabilize it at a spatial end-point, by way of replacing volitional descending cortico-motor commands with stimulated commands, will enable appropriate selection of stimulus parameters for systematically mapping the representation of RL-ICMS-induced movements elicited from the rhesus macaque primary motor cortex (M1).

Mechanism of stimulus-evoked movement

In this study we determined the optimal RL-ICMS parameters that when applied to M1 cortex would supplant volitional movement of the forelimb with movement induced by stimulation. This replacement of volitional movement with stimulated movement requires two steps: eliminating the subject's voluntary efferent output to target muscles of the forelimb, and replacing these commands with those imposed by stimulus-evoked activity. Elimination of volitional descending signals may be a result of the

applied stimulus pulses antidromically interrupting natural efferent input to corticospinal neurons by causing the cell and axons to fire at a rate that approaches or eclipses the cell's natural firing rate during active movement. Firing rates of layer V cortical cells in cat motor cortex reveal the ability to fire at peak rates of 150-200 Hz in the presence of the $GABA_A$ antagonist Bicuculline methiodide (BIC), while the study's average firing rate range was 70-100 Hz (Capaday et al., 2011).

This phenomenon of replacement has been shown to occur in M1 as well as in subcortical areas such as the subthalamic nucleus with deep brain stimulation (Garcia et al., 2005, Griffin et al., 2011). Replacement, or "hijacking," of corticospinal cell activity likely occurs in direct response to application of stimulus frequencies that exceed the natural movement related firing rates of cortical neurons and afferent inputs (Griffin et al., 2011). The stimulus rates found to be optimal in this study (70-130 Hz) are similar to the expected average maximum firing rates of cortical cells and axons and, therefore, would be expected to be effective in blocking and replacing natural movement related activity. However, in order to evoke complete movements using stimulation, recruitment of an ample number of corticospinal cells to activate a muscle synergy is necessary. This is a function of stimulus intensity. The stimulus intensity range found to be effective in this study in producing RL-ICMS evoked translocation to a new stable end-point position was 70–130 µA. The following equation can be used to calculate the spread of effective stimulus current within the cortex

$$r = \sqrt{i/k}$$

where r is the radius of the stimulus-activated cortex volume, i is the stimulus intensity and k is the current-distance constant. Based on a minimal excitability constant of 250

$\mu A/mm^2$ for the largest cortical neurons (Cheney and Fetz, 1985, Tehovnik et al., 2006) or an intermediate excitability of 1292 $\mu A/mm^2$ (Tehovnik et al., 2006), the area of activated cortical tissue can be estimated to be 0.88 - 1.63 mm^2 or 0.17 - 0.32 mm^2, respectively. Of course, this does not take into account trans-synaptic activation via physiological spread of stimulus current which is undoubtedly substantial at the RL-ICMS frequency range that was found to produce successful stimulus evoked movements; therefore, the number of neural elements activated becomes difficult to estimate (Cheney and Fetz, 1985).

RL-ICMS assuredly activates numerous connections aside from the corticospinal-to-motor unit pathway that ultimately evokes movement. For instance, cortico-cortical interactions due to antidromic activation of axon collaterals; cortico-striatal; cortico-bulbar, including possible activation of cortico-cerebellar loops; and gamma motoneurons and muscle spindle afferents. These connections might all play some role in achieving a stimulus-evoked spatial end-point. However, we suggest that the primary neural elements mediating RL-ICMS evoked movements are corticospinal and corticomotoneuronal linkages to motoneurons due to their strength and abundance (Jackson et al., 2003, Smith and Fetz, 2009). Additionally, trans-synaptic activation through axon collaterals to corticospinal cells with common output targets, as well as activation along cortical networks that exhibit strong synaptic connectivity, are likely involved.

Co-activation of multiple neural network ensembles with strong output connections to muscles likely results in a movement achieved through equilibrium of co-activated muscles acting along the length-tension relationships of all muscles activated.

We believe the parameters used in RL-ICMS are unlikely to act upon any individual neural network that may be responsible for a complex volitional movement, rather stimulation activates numerous co-localized networks that contain descending fibers which result in movement equilibrium of all descending input to the muscles. The resulting movement would likely equal that of no individual neural network responsible for activation of a natural-movement muscle ensemble, however the equilibrium achieved through activation of numerous networks could appear complex by the nature of random muscle ensemble activation. For example, movements resulting in the monkey's hand ending near the mouth with his wrist supinated could appear as though a natural feeding movement, whereas a similar endpoint however with the wrist pronated would appear unnatural and awkward. Both of these examples were observed. With this taken into account, mapping output of even combinations of local neural networks neighboring the electrode reveals important information about topographical cortico-cortical connections and the descending cortical mechanism from M1 to muscle ensembles.

Effect of stimulus parameters on muscles not directly affected by stimulation

This study may add to our understanding of the broad-scope effects that result from RL-ICMS parameters applied to M1 that are sufficient for translocation of the forelimb. One possible mechanism for the action of RL-ICMS is that stimulation antidromically activates premotor areas associated with the integration of planned movement, thereby inhibiting any voluntary motor activity regardless of whether or not stimulation directly acts upon cortico-motor efferents. Another possibility is that

stimulation activates local neural components and cortical collaterals associated with descending input, while upstream cortical areas remain relatively unaffected. The results of the current study suggest the latter possibility in that muscles not directly affected by stimulation can preserve voluntary activity. As a result the monkey retains the ability to voluntarily activate these unaffected muscles. For example in the current study, when RL-ICMS applied to M1 replaced voluntary activity of distal muscles only, the ability to voluntarily activate proximal muscles was preserved. Indeed, in such trials the monkey would often move the unaffected joints variably on a trial-to-trial basis in an apparent attempt to reposition the hand in a voluntary trajectory, often toward an unclaimed food reward. This suggests that stimulation acts primarily orthodromically along descending cortical efferents, while premotor areas and other more upstream regions involved in motivation and planning of movements remained relatively unaffected.

Successful parameter ranges that evoked movement varied little within M1.

The range of successful stimulus parameters that evoked translocation of the forelimb to, and subsequent stabilization at, a spatial end-point varied relatively little from one cortical site to the next within M1. The small variations that we did observe could be due to the quantity of cortico-muscle efferents in the vicinity of the stimulating electrode, as well as horizontal connections activated trans-synaptically. It is not unexpected that the requisite frequency for activation was similar from site to site, as any frequency greater than the threshold required to replace spontaneous neural activity with stimulus-induced activity should suffice (Griffin et al., 2011). As well, the current

intensity needed to activate the requisite number of motor units to cause overt movement requires the activation of a sufficient number of descending cortical efferents to motoneurons in the spinal cord, suggesting minimal variation in the cortical density of descending efferents over the sites included in this study.

Effect of stimulus parameters on evoked movement velocity

We found that increasing the stimulus parameters of frequency and amplitude both had a direct effect on the forelimb movement velocity to the equilibrium spatial end-point. This finding suggests that increasing the rate at which descending inputs are recruited through physical and physiological current spread has a direct impact on the rate at which descending cortical output affects the activity of motor units and subsequent muscle fibers.

Comparison of stimulus parameters in the current to previous studies

Our results suggest that optimal RL-ICMS parameters for evoking translocation of the forelimb to new stable end-point positions had a relatively narrow range: 70 - 120 Hz, 70 - 120 μA and 1000 ms, (using bipolar 0.2 ms pulses). These parameters have similarities to stimulus parameters used in previous studies to evoke prolonged movement of a limb or eye saccades, however there are some significant differences. To elicit smooth and stable eye saccades, parameters of 500 Hz, 100 - 200 μA, 100 ms, with bipolar pulses 0.1 ms duration have been found to be effective (Thier and Andersen,

1998). To evoke limb movement in an anesthetized cat, parameters of 333 Hz, 10-100 µA, 500 ms, with 0.2 µs pulses were used (Ethier et al., 2006). For eliciting movements in the monkey forelimb, Graziano et al. (2002a) used 200 Hz, 100 µA and a stimulus train duration of 500 ms with bipolar 0.2 ms pulses. Some of the variability in stimulus parameters used between studies possibly reflect the various cortical locations, animal species and anesthetizing agents used. The stimulus duration used in the current study (1000 ms) was longer than those used in previous mapping studies due to the fact that the latency of stimulus onset to arrival of the forelimb at a stable spatial end-point had a wide range, with many movements exceeding stimulation durations used in previous studies.

Interestingly, frequency parameters that have been empirically adopted to therapeutically treat diseases such as Parkinson's Disease by way of deep brain stimulation (DBS) are in the range of 120-180 Hz (Garcia et al., 2005). The similarity in frequency used in DBS and the current study likely reflects the goal in both studies to replace the neural activity of target cells with artificial stimulation. This requires the frequency of applied pulses to exceed the neuron's spontaneous rate of firing.

Summary and Conclusions

Our results suggest a relatively narrow range of stimulus parameters applied to M1 that are both safe and effective for evoking translocation and subsequent stabilization of the stimulated limb at a spatial end-point: 70 - 130 Hz, 70 - 130 µA and 1000 ms, with a mean spatial end-point time of 469 ± 156 ms. The mean successful frequency, normalized for all trials recorded in the study, was 115.2 ± 22.3 Hz, and the mean

successful amplitude was 108.8 ± 23.7 µA. Additionally, the median successful frequency and amplitude for all trials were 110 Hz and 110 µA respectively. Attenuated parameters resulted in inconsistent, truncated or undetectable movements, while intensified parameters increased the potential for large-scale physiological spread and adverse focal motor effects. Establishing cortical stimulation parameters that yield consistent stimulus-evoked end-points provides a foundation for a systematic and complete mapping of movement space and associated muscle synergies in primary motor cortex. The results will add to our understanding of how the central nervous system encodes movement, and could aid in the development of neuroprosthetic devices.

Figure 3.1. Red arrows represent the movement sequence required to perform the task: Monkey holds homeplate lever (A) until a food reward drops and he retrieves a pellet from the food dispenser (B) and feeds himself (C). In this illustration, RL-ICMS is applied when the monkey's hand arrived at the food dispenser (B), subsequently driving his right forelimb to a spatial end point. Vicon motion capture reflective spheres (multi-colored spheres on the upper and lower forelimb) of the lower forelimb were used to calculate the 3D coordinates of the dorsal tubercle of the radius (large green sphere). Illustrated are RL-ICMS-evoked example trajectories (solid green lines) and example voluntary movement trajectories following stimulation end (dashed green lines).

Monkey performing reach and prehension task

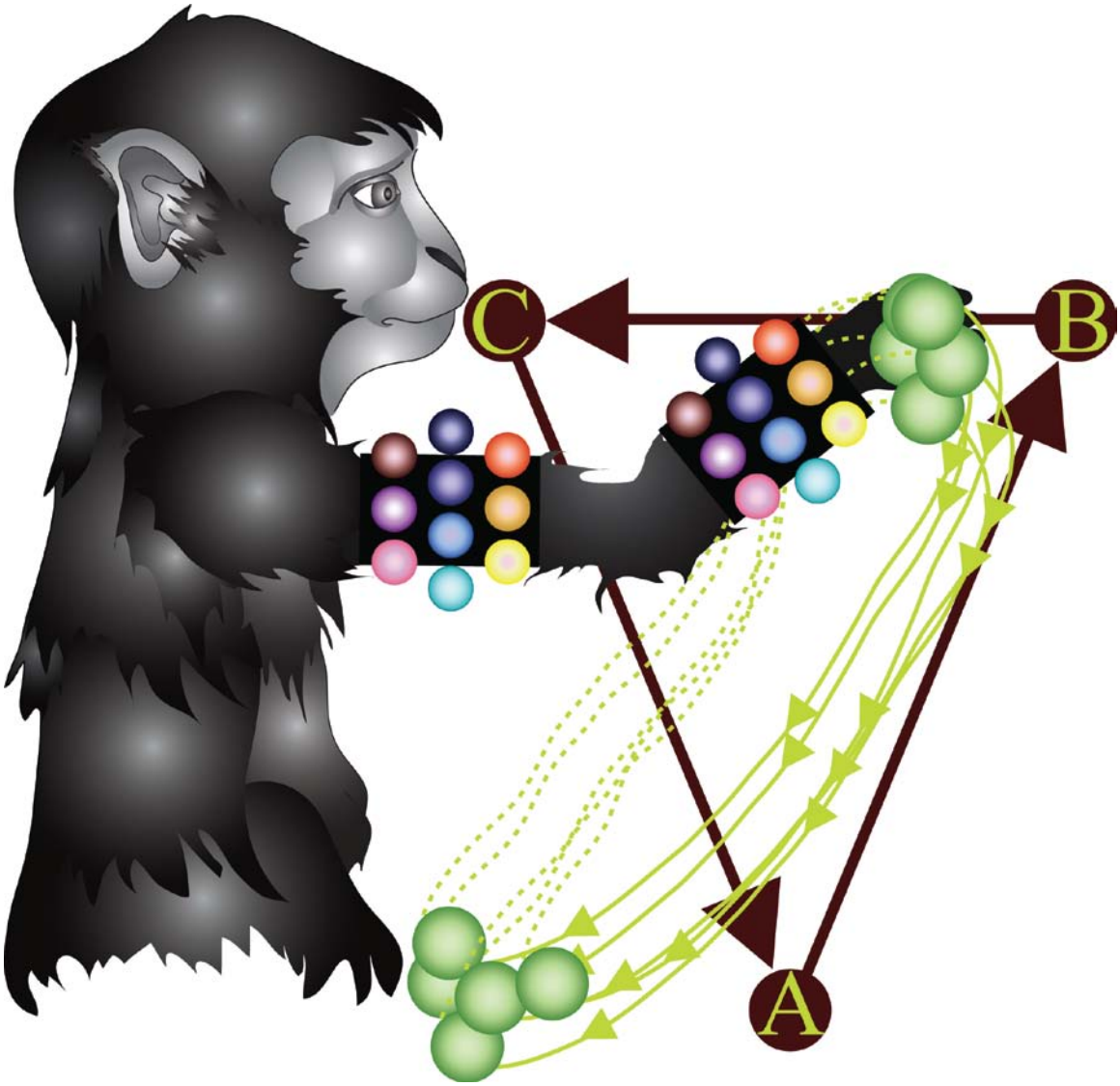

Figure 3.2A. Unfolded map of monkey A's M1 forelimb representation in the left hemisphere with a view of the dorsal surface of the precentral gyrus and the rostral wall of the central sulcus. Cortical site locations used for stimulus parameter analyses are included. Anterior, posterior, medial and lateral are indicated by the compass rose. Sites of stimulation are indicated by the orange dots. The color-coded muscle representation map is StTA-derived. Distal forearm facilitation in M1 is represented as blue, proximal forearm facilitation as red, and proximal-distal co-facilitation as purple.

.

Monkey A's M1 forelimb representation with stimulus parameter sites

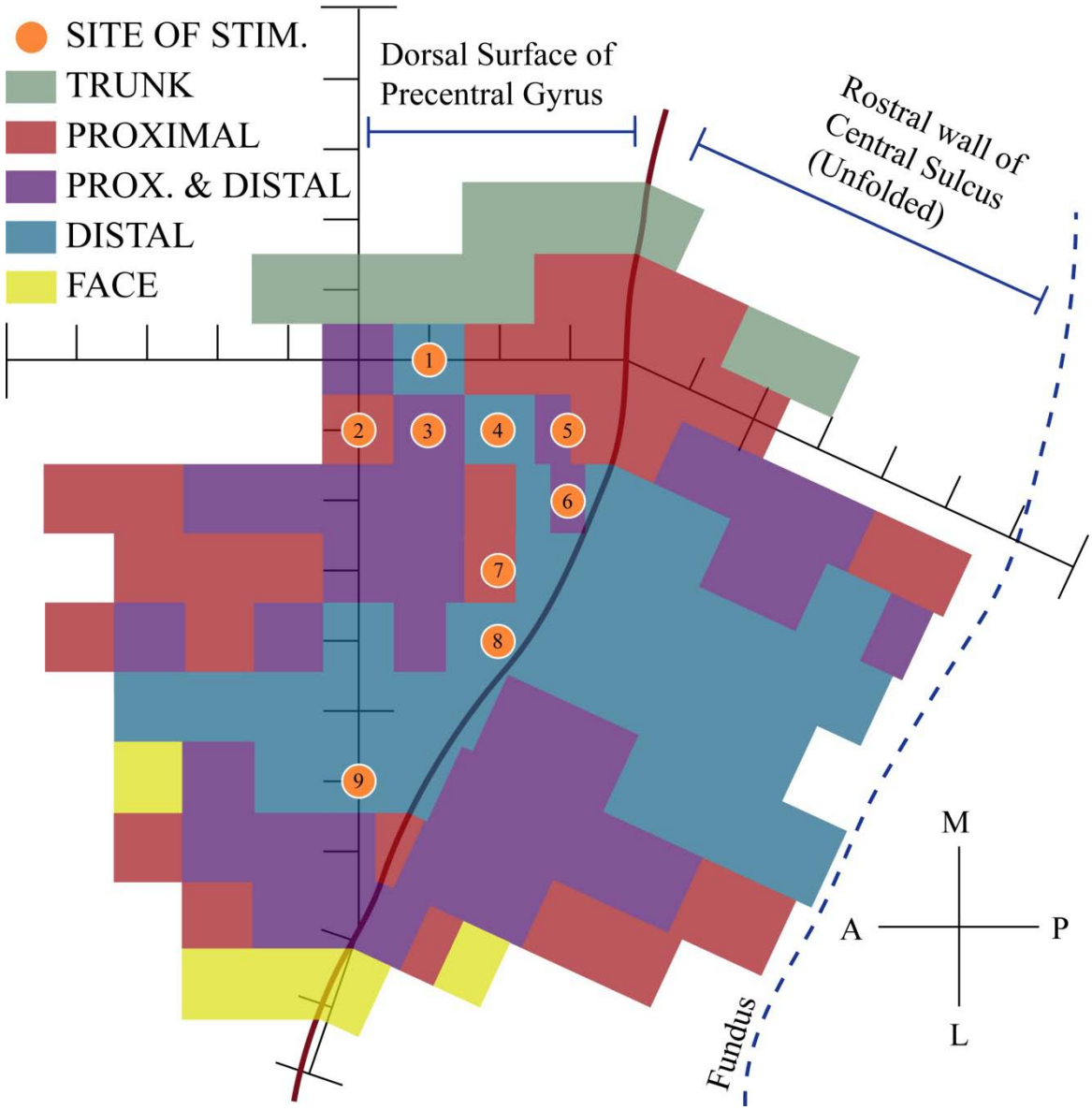

Figure 3.2B. Unfolded map of monkey X's M1 forelimb representation in the left hemisphere with a view of the dorsal surface of the precentral gyrus and the rostral wall of the central sulcus. Cortical site locations used for stimulus parameter analyses are included. Anterior, posterior, medial and lateral are indicated by the compass rose. Sites of stimulation are indicated by the orange dots. The color-coded muscle representation map is StTA-derived. Distal forearm facilitation in M1 is represented as blue, proximal forearm facilitation as red, and proximal-distal co-facilitation as purple.

Monkey X's M1 forelimb representation with stimulus parameter sites

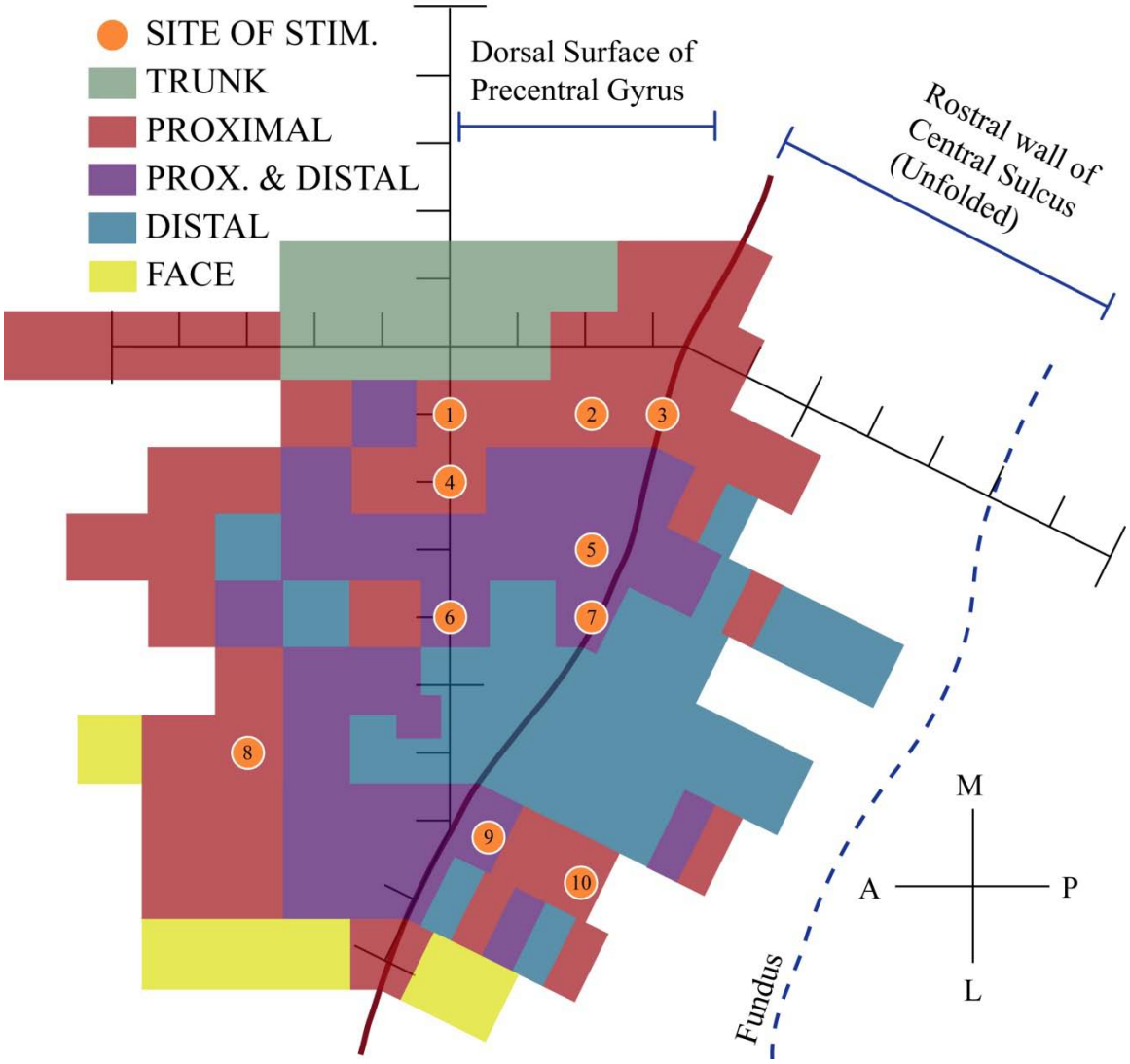

Figure 3.3. Velocity profiles of the monkey's wrist (dorsal tubercle of the radius) in space during three separate trials. A successful trial is defined as stimulation resulting in translocation of the limb to a spatial end-point with subsequent stabilization for the duration of the stimulation ($\leq 25\%$ maximum mean stimulus-induced velocity).

Velocity profile examples

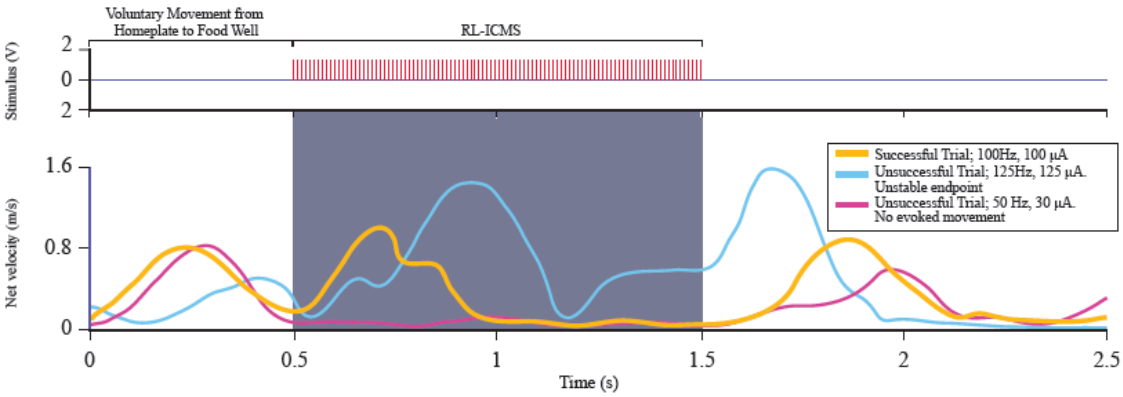

Figure 3.4. Density plot of stimulus parameter pairings color coded as a ratio of successful trials to total trials for each pairing. Stimulus train duration was one second for each parameter pairing. Total trials for each parameter pairing are listed in the corner of each square. On the ratio scale, 1.0 is equal to a success rate of 100% for that stimulus parameter combination. Abbreviation: NT, parameters not tested.

Success rate for RL-ICMS parameter pairings

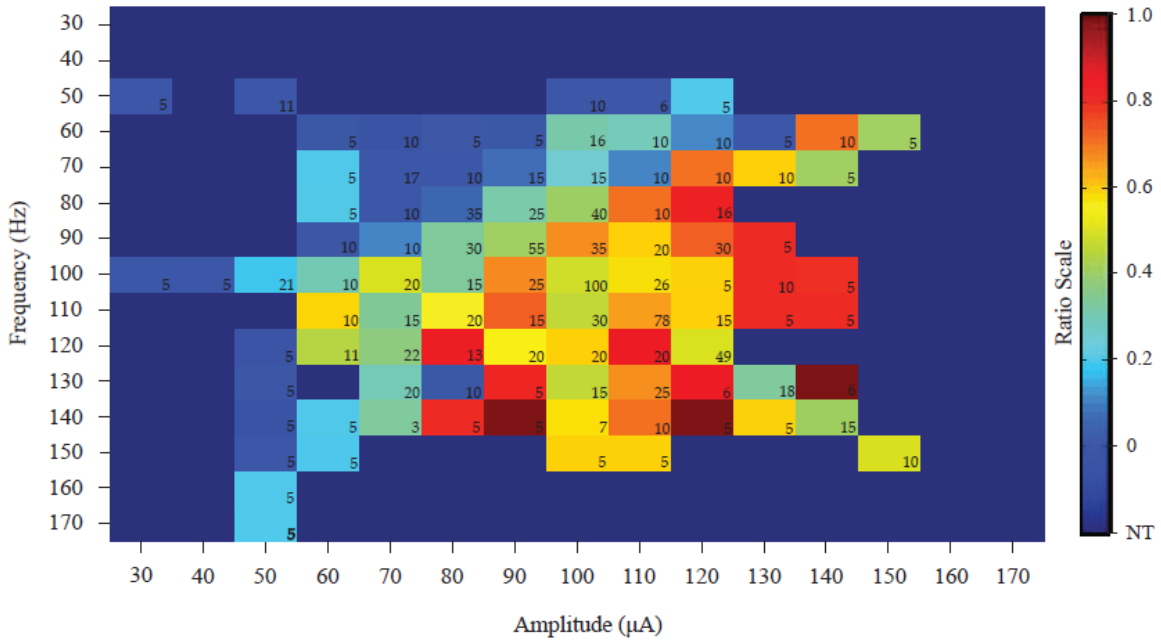

Figure 3.5. Density plot of stimulus parameter pairings color coded as a ratio of successful trials to total trials for each pairing. Data for this example were collected from stimulation site five in monkey X. Stimulus train duration was one second for each parameter pairing. Total trials for each parameter pairing are listed in the corner of each square. On the ratio scale, 1.0 is equal to a success rate of 100% for that stimulus parameter combination. Abbreviation: NT, parameters not tested.

Success rate for RL-ICMS parameter pairings at one cortical site

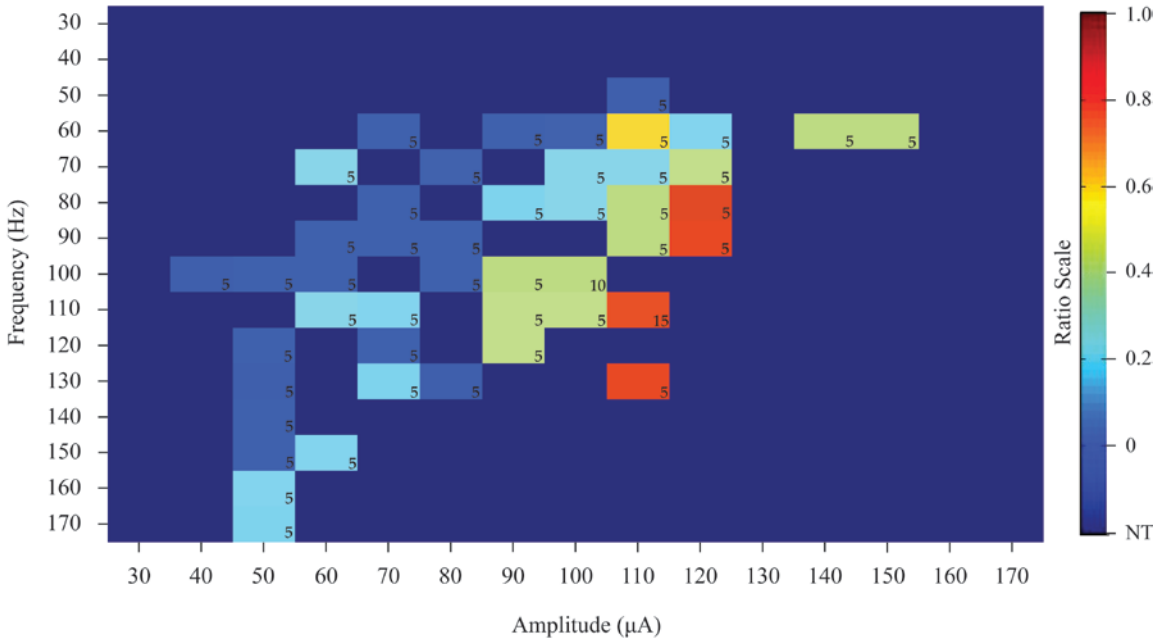

Figure 3.6. Density plot of stimulus parameter pairings color coded as the maximum velocity for each pairing averaged over the number of trials listed in the corner of each square. Only successful trials were included. Stimulus train duration was one second for each parameter pairing.

Peak velocity for successful RL-ICMS parameter pairings

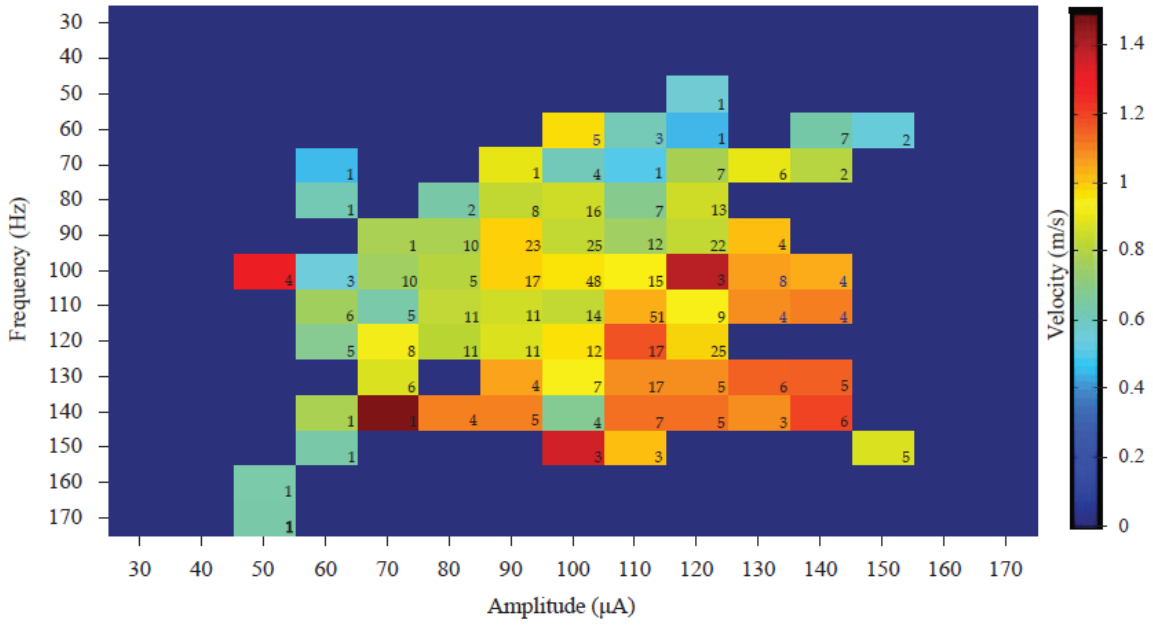

CHAPTER IV:

COMPREHENSIVE SPATIAL END-POINT MAP ELICITED FROM THE CORTICAL FORELIMB REPRESENTATION OF PRIMARY MOTOR CORTEX

ABSTRACT

The purpose of this study was to acquire a comprehensive map of the representation in primary motor cortex (M1) of forelimb movement end-points elicited with repetitive long-duration intracortical microstimulation (RL-ICMS). Previous studies have utilized RL-ICMS to investigate both oculuomotor and forelimb movements (Ethier et al 2006; Graziano et al 2002; Thier and Andersen 1998). The present study expands upon previous findings by producing a systematic and comprehensive RL-ICMS-evoked spatial end-point map of M1 utilizing a subset of stimulus parameters, typically 100-120 Hz, 100-120 µA and one second duration, determined previously (Chapter III) to be optimal for eliciting stable spatial end-points of the forelimb. We recorded the EMG activity of 24 forelimb muscles concurrently along with movement kinematics and end-point positions of the wrist using a Vicon motion capture system. Forelimb muscle representation in M1 was derived from effects in stimulus-triggered averages (StTA) of EMG activity (Park et al, 2001). The results reveal RL-ICMS-evoked forelimb spatial end-points that encompass a considerable range of locations throughout the forelimb work space at or below head level. Cortical sites yielding successful RL-ICMS-evoked forelimb translocation with subsequent stabilization at an end-point were located primarily in or near cortical output zones that produced facilitation of both proximal and distal muscles based on StTA. Sites comprising exclusively proximal or distal muscle facilitation, as well as sites on the border of the M1 forelimb representation, were less likely to yield complete movements to stable spatial end-points. Additionally, stable end-points generated by stimulation of adjacent M1 cortical sites tended to be spatially

contiguous in the monkey's work space. This yielded an overall cortical map of end-point positions in which the monkey's three-dimensional workspace was represented in a relatively orderly fashion across the two-dimensional surface of M1 cortex. While there were distinct cortical topographical differences of end-point representations between monkeys, there were also clear similarities such as hand-to-mouth postures elicited from sites neighboring the M1 face representation in both monkeys. These results reveal an extensive movement reportoire that can be elicited by applying RL-ICMS to M1, and add to our understanding of cortical encoding of motor output.

INTRODUCTION

The purpose of this study was to acquire a comprehensive map of the representation in primary motor cortex (M1) of forelimb movement end-points elicited with repetitive long-duration intracortical microstimulation (RL-ICMS). Cortico-motor connectivity between neurons in M1 and corresponding muscles has been mapped previously using multiple electrophysiological techniques (Penfield and Boldrey, 1937, Woolsey et al., 1952, Evarts, 1964, Asanuma and Sakata, 1967, Cheney and Fetz, 1980, 1985). While early electrophysiological approaches in patients and monkeys utilized surface stimulation of the cortex to evoke large scale observable responses (Penfield and Boldrey, 1937, Woolsey et al., 1952), the introduction of intracortical microstimulation (ICMS) permitted more refined mapping of cortical output to muscles (Asanuma and Sakata, 1967). These short-duration trains of high frequency ICMS (RS-ICMS) have been used to evoke twitch-like responses for cortical mapping and other purposes.

Recently research groups have combined the approach of using long-duration stimulation used in some early studies to evoke movements in patients and monkeys (Penfield and Boldrey, 1937, Woolsey et al., 1952) with the use of focal ICMS to investigate both oculuomotor and forelimb evoked movements on a timescale that closely matches the duration of voluntary movement over the evoked trajectory (Ethier et al 2006; Graziano et al 2002; Thier and Andersen 1998). RL-ICMS trains applied to the motor cortex produced natural-appearing movements of affected limbs characterized by the limb having a common end-point posture resulting from stimulation at a particular cortical site, regardless of the starting position of the limb (Graziano et al., 2002). These

groups explored broad areas of the motor cortex using the same basic stimulation approach as in the present study, though with different stimulation parameters (Graziano et al., 2002, Ethier et al., 2006).

The present study expands upon previous findings by producing a systematic and comprehensive RL-ICMS-evoked spatial end-point map of M1 utilizing a subset of stimulus parameters, typically 100-120 Hz, 100-120 µA and 1 second duration, determined previously in our lab (Chapter III) to be optimal for eliciting forelimb movements with stable spatial end-points. Concurrently, we recorded the EMG activity of 24 forelimb muscles as well as movement kinematics and end-point positions of the wrist using a Vicon motion capture system. Forelimb muscle representation in M1 was derived from effects in stimulus-triggered averages (StTA) of EMG activity (Park et al, 2001). From the data, we produced two-dimensional topographical cortical maps representing the elicited forelimb movement in three-dimensional space. In addition, we provide maps illustrating the extent of the monkey's work space represented by stimulus-evoked movement end-points. The results of this study reveal an extensive movement reportoire that can be elicited by applying RL-ICMS to M1 cortex. Although not all regions of the work space are equally reprsented by RL-ICMS evoked end-point locations, our results reveal a trend toward an orderly representaton in the cortex of end-point positions in the work space. These findings add to our understanding of cortical encoding of motor output.

EXPERIMENTAL PROCEDURES

Behavioral Task

Data were collected from two male rhesus macaques (*Macaca mulatta; ~9 kg each, ages 4 and 12*) performing a reach and prehension task that required co-activation of proximal and distal forelimb muscles, while also yielding discrete spatial locations at which stimulus trains could be cued (Figure 4.1). Training procedures and the behavioral task have been described in detail previously (Belhaj-Saif et al., 1998, McKiernan et al., 1998). Briefly, the monkey was seated in a custom primate chair (Figure 4.2) within a sound-attenuating chamber with his left arm comfortably restrained while his right arm retained freedom of movement. To discourage the monkey from interfering with reflective motion capture spheres attached to his arm during each recording session, a custom face mask barrier was installed on the chair that contained a small hole through which the monkey could feed himself. In addition, a removable waist plate was left secured to inhibit the monkey from interfering with the spheres using his feet. In order to receive a food reward the monkey initiated the task with his right hand by depressing a homeplate lever (Figure 4.1A) located at waist height directly in front of him for 1 second duration, triggering the release of a food pellet into a food well (Figure 4.1B) located approximately at shoulder height. Following the retrieval and consumption of the food reward (Figure 4.1C), the monkey returned his hand to the homeplate lever to initiate subsequent trials. Performance was guided by audio and visual cues.

Surgical Procedures

Following training, an MRI-compatible stainless steel chamber allowing 30 mm diameter of dural exposure, and access to the underlying cortical area, was implanted stereotaxically over the primary motor cortex of the left hemisphere of each monkey using procedures described in detail previously (Park et al., 2000). Briefly, the chamber was anchored to the skull using titanium screws and dental acrylic, and was centered over the hand area of M1 in the left hemisphere. In addition, threaded titanium nuts were attached over the occipital aspect of the skull using titanium screws and dental acrylic. These nuts provided a point of attachment for a flexible head restraint system during data collection (McKiernan et al., 1998, 2000). The chambers were centered at anterior 17.7 mm, lateral 27.2 mm and 26 º to the sagittal plane for Monkey X, and anterior 16.0 mm, lateral 22.0 mm and 30 º to the sagittal plane for Monkey A.

Twenty-four muscles of the right shoulder and forelimb were each implanted with two multi-stranded stainless steel wires (Cooner Wire, AS632). Both monkeys were implanted under sterile conditions using a cranial subcutaneous implant technique described previously (Park et al., 2000). Briefly, all wires were stripped of ~2-3 mm of insulation and tunneled subcutaneously from a cortical connector (Amphenol, Wallingford, CT) to each muscle, where the wires were inserted into the muscles a distance of ~2-3 cm, with a ~5 mm separation of the two wires in each muscle. The cortical connector module was secured with dental acrylic near the cortical recording chamber. We tested the placement accuracy of each electrode pair by observing appropriate muscle twitches that resulted from applying short stimulus trains (Grass SD9

Stimulator). EMG activity was recorded from five shoulder muscles: pectoralis major (PEC), anterior deltoid (ADE), posterior deltoid (PDE), teres major (TMAJ) and latissimus dorsi (LAT); seven elbow muscles: biceps short head (BIS), biceps long head (BIL), brachialis (BRA), brachioradialis (BR), triceps long head (TLON), triceps lateral head (TLAT) and dorsoepitrochlearis (DE); five wrist muscles: extensor carpi radialis (ECR), extensor carpi ulnaris (ECU), flexor carpi radialis (FCR), flexor carpi ulnaris (FCU) and palmaris longus (PL); five digit muscles: extensor digitorum communis (EDC), extensor digitorum 2 and 3 (ED23) extensor digitorum 4 and 5 (ED45), flexor digitorum superficialis (FDS) and flexor digitorum profundus (FDP); and two intrinsic hand muscles: abductor pollicis brevis (APB) and first dorsal interosseus (FDI).

All surgeries were performed under deep general anesthesia and aseptic conditions. Prior to each implant surgery, the monkey was administered ketamine (10mg/kg, IM), atropine (0.04 mg/kg, IM), and medetomidine (0.05 mg/kg, IM) for transportation purposes, and subsequently isoflurane gas for the duration of the surgery. Each monkey received prophylactic antibiotic (penicillin, 6000 U/kg) SC 10 hours pre-surgery, 1 hour post-surgery, and 3 days following surgery. Postoperatively, the monkeys were given analgesics (buprenorphine, 0.01 mg/kg IM and carprofen, 5 mg/kg SC). All surgeries were performed in a facility accredited by the Association for Assessment and Accreditation of Laboratory Animal Care using full sterile procedures. All procedures conformed to the Guide for the Care and Use of Laboratory Animals, published by the United States Department of Health and Human Services and the National Institutes of Health.

Stimulus Triggered Averages

StTAs were acquired for all implanted muscles from stimuli applied throughout all phases of the reach and prehension task, and were used to help confirm positioning of the electrode in lamina V as well as to determine cortico-muscle connectivity of corticospinal cells directly surrounding the electrode tip. Stimulation was applied through glass insulated platinum-iridium electrodes suitable for single unit recording (FHC Inc., Bowdoin, ME), with typical impedances of 0.7 - 1.5 MΩ at the start of each recording session. We positioned the electrodes using an X-Y positioner secured to the chamber for the duration of each recording session, and advanced the electrode into the brain using a manual hydraulic microdrive (FHC Corp.) until the electrode tip was located in cortical lamina V, or approximately 1.5 mm below the surface of the brain. Location of layer V was determined by depth, audio cues (Grass AM8 Audio Monitor), visual cues (oscilloscope display of large spike waveforms), and finally by post-stimulus effects (PStEs) in StTAs at 15µA and 10 Hz.

StTAs were obtained at 10 Hz and at current intensities that matched those used for each RL-ICMS train applied at the same cortical site. In addition muscle facilitation maps (Figures 4.3A and 4.3B) utilized StTAs collected at 15 and 30 µA and were based on mapping at 1 mm intervals on the surface of the precentral gyrus and 0.5 mm vertical intervals down the bank of the central sulcus as described previously (Park et al., 2001). Acquiring boundaries of M1 ensured complete RL-ICMS mapping of M1. EMG activity was filtered from 30 Hz to 1 kHz, digitized at 4 kHz and full-wave rectified. Individual stimuli for the StTAs were symmetrical biphasic pulses: initial negative pulse 0.2 ms in

duration followed directly by a positive pulse 0.2 ms in duration. StTAs were based on a minimum of 1000 trigger events. Averages were compiled using a 60 ms epoch, of which 20 ms prior to the trigger was considered baseline. StTAs were identified as having significant PStEs if the peak or trough of the effect exceeded ±5 SD of the baseline for a period of ≥ 0.75 ms as described previously for moderate-to-large effects (Park et al., 2004).

RL-ICMS Protocol

RL-ICMS trains were applied to 251 distinct cortical sites (Figures 4.3A and 4.3B) in the left hemisphere of two rhesus macaques performing a reach and prehension task over the course of the study. Stimulation was applied when the monkey's hand was at one of three positions of the task (Figure 4.1). A stimulus onset location that was furthest from the stimulus-evoked spatial end-point was chosen once a test trial elicited a detectable movement. Because position 4.1B (feeder) was on the periphery of the monkey's work space, this starting location for stimulation was used most frequently. Starting location for stimulation had no noticeable effect on the spatial end-points elicited in the present study, consistent with previous studies (Graziano et al., 2002, Graziano et al., 2005).

Cortical sites within M1 of each monkey were mapped in random order at a resolution of 1 mm^2 on the surface of the gyrus and 0.5 mm along descending tracks in the rostral bank of the central sulcus. M1 of one monkey was fully mapped before proceeding to the next. We applied systematic combinations of frequency and amplitude

with a stimulus train duration of one second until either a combination of parameters was qualitatively assessed visually to yield a successful spatial end-point, or it was determined no spatial end-point could be elicited. Sites that did not yield spatial end-points yielded either little or minimal movement upon stimulation, or affected distal or proximal muscles independently thereby allowing voluntary movement of the unaffected muscles during stimulation which then yielded unstable movement end-points.

Data from previous work (Chapter III) demonstrated that the median parameters that elicit translocation with subsequent stabilization of the forelimb at spatial end-points are 110 Hz, 110 µA, and a one second stimulus train duration. These parameters were used for the majority of the trials that yielded successful end-points achieved throughout the present study (63.4% and 75.0% for monkeys A and X respectively), with the remaining sites requiring stimulation parameters in the ranges of 90 - 150 Hz and 90 - 150 µA. For each RL-ICMS parameter set we conducted 5 trials. Real-time qualitative assessment of successful spatial end-points for each site were determined by subjective visual evaluation. Kinematic data were later used in offline analyses to quantitatively map successful spatial end-points.

Recording Forelimb Kinematics

Limb kinematics were monitored and recorded using a Vicon motion capture system. For data collected in the present study, a virtual sphere located on the dorsal tubercle of the radius (Figure 4.1, green sphere) was calculated and used to evaluate RL-ICMS-evoked forelimb kinematics and the spatial end-point positions elicited from each

cortical site. The three-dimensional coordinates of this virtual sphere were calculated using a Point Cluster technique described previously (Andriacchi et al., 1998, Senesh and Wolf, 2009). Briefly, a cluster of 10 reflective spheres were attached to the forearm of each monkey. The three-dimensional coordinates of the spheres in each cluster, as measured using the Vicon system, were used to triangulate the coordinates of the virtual sphere located on the dorsal tubercle of the radius, which was identified during static trials at the start of each recording session. The dorsal tubercle of the radius was used as a surrogate for end-point position of the hand in space. Utilizing subsets of the numerous wrist markers to calculate the spatial position of the reference point (dorsal tubercle of the radius) reduced the need for the wrist to be within view of any particular set of Vicon cameras in order to be monitored. The monkey's work space was represented as a cube subdivided into 27 voxels. Each voxel (154.2 x 126.1 x 98.7 mm) was color-coded to enable visualization of subdivisions within the monkey's work space (Figure 4.4A).

Determining successful spatial end-points for RL-ICMS-evoked movements

RL-ICMS-evoked kinematics of the dorsal tubercle of the radius were used to assess successful spatial end-points of the wrist achieved through stimulation of M1. RL-ICMS-evoked movement trials were deemed successful if the stimulus parameters applied to the M1 site were sufficient to translocate the monkey's forelimb to a spatial location distinct from its location at the initiation of stimulation and sufficient to maintain the limb at the stimulus-evoked posture for the duration of stimulation. The specific success criteria we used required, firstly, that movement occur within the first 500 ms of

stimulation onset to indicate adequate stimulus-induced movement. Next, our criteria required that movement velocity reach a level greater than or equal to 40% of the maximum mean stimulus-induced velocity. The mean stimulus-induced velocity was calculated from all successful trials included in this study. At a few sites, we based the velocity criterion on a smaller subset of trials, due to a few clear stimulus-evoked movements translocating to end-points at a slower rate than the majority of trials. Once this criterion is met, the induced movement velocity must then cross a threshold, on the slowing phase, of less than or equal to 25% of the maximum mean stimulus-induced velocity. Finally, once this lower threshold is crossed, the velocity of the movement must remain below this 25% threshold for the remainder of the applied stimulus train. Time to spatial end-point stabilization for successful trials was measured at the point where the stimulus-evoked velocity crossed a threshold of ≤25%. This time point was used to characterize the spatial end-point coordinates associated with stimulus-evoked movement for each cortical site. These criteria enabled the identification of successful RL-ICMS-evoked movements and objective evaluation of associated spatial end-points. These objective end-points closely matched end-points identified using real-time subjective visual assessment.

Measurement of EMG cross-talk

We evaluated cross-talk between EMG electrodes by constructing EMG-triggered averages. This procedure used the motor unit potentials from one muscle as triggers for compiling averages of rectified EMG activity of all other muscles. Criteria established

previously (Buys et al., 1986) were used to eliminate effects that might have been affected by cross-talk. To be accepted as a valid PStE, the ratio of PStF between the test and trigger muscles must have exceeded the ratio of their cross-talk peaks by a factor of two or more. Based on this criterion, FDI in monkey X was removed from the analysis.

RESULTS

RL-ICMS-induced forelimb spatial end-points evoked from M1

Long-duration ICMS was applied at each cortical site that yielded StTA-derived PStE in an attempt to obtain a comprehensive map of stimulus evoked forelimb postures and end-points represented in M1cortex. At each cortical site, we began stimulation with optimal parameters determined previously (110 Hz and 110 µA, Chapter III). If successful stimulus evoked movements were not obtained, stimulus parameters were systematically adjusted until a clear spatial end-point was achieved or until we determined no stable end-point could be obtained. We concluded that end-points were not inducible if sufficient movement was not evoked at stimulation parameters up to 150 Hz and 150 µA, and/or stimulation affected only proximal or only distal muscles which allowed for the monkey to voluntarily move the unaffected muscles and associated joints for the duration of stimulation. For all cortical sites in the present study, the range of parameters used to evoke a stable forelimb end-point posture was 90-150 Hz for frequency and 90-150 µA for intensity. The combination of 110 Hz and 110 µA produced successful movements and stable end-points in 63.4% and 75.0% of the successful trials in monkey A and monkey X respectively.

Cortical representation maps of forelimb spatial end-points elicited from each cortical site were constructed (Figures 4.5A and 4.5B), with the color at each site corresponding to an evoked movement end-point within a color-coded voxel representing a portion of the volume within the monkey's work space (Figure 4.4A). The calculated

end-point coordinates for each site were the mean coordinates calculated from the total successful RL-ICMS-evoked movement trials elicited from that site. We found that cortical sites yielding successful RL-ICMS-evoked forelimb movements with subsequent stabilization at a spatial end-point tended to be located within or near cortical output zones that produced StTA-derived facilitation of both proximal and distal muscles. However cortical sites yielding successful spatial end-points did not perfectly overlap with the proximal-distal cofacilitation zone. This undoubtedly reflects the use of higher stimulus currents with RL-ICMS (90-150 µA) compared to the currents applied during StTA mapping (15-30 µA), which resulted in activation of a larger number of corticospinal neurons (Tehovnik et al., 2006). In addition, the higher stimulus frequencies used with RL-ICMS would have resulted in greater physiological spread through collatoral connections further eroding the map boundaries observed with StTA (Tehovnik et al., 2006).

Cortical sites comprised of exclusively StTA-derived proximal or distal muscle facilitation such as distal forelimb facilitation sites down the bank of the central sulcus, as well as proximal facilitation sites on the border of the M1 forelimb representation, were less likely to yield complete movements to stable spatial end-points. Stimulus-evoked activation of exclusively proximal or distal muscles left open the possibility that the unaffected muscles and associated joints could be voluntarily activated by the monkey during stimulation, thereby allowing the monkey to move his wrist end-point throughout the duration of stimulation. Although problematic for identifying a stable end-point, the fact that the monkey retained the ability to voluntarily control muscles at joints not affected by RL-ICMS is relevant to understanding the extent of disruption of the internal

motor program by repetitive stimulation. In addition to its direct effect on neural elements within the local cortical tissue surrounding the electrode tip, RL-ICMS-mediated activation of neurons might propagate through antidromic and orthodromic activation of fibers to other premotor cortical areas and to subcortical areas including those that might be involved in the early steps of motor program planning. In addition to disrupting the execution steps of the motor program for those muscles directly affected by stimulation, it is also possible that motivation and/or aspects of the internal motor program for the whole limb movement might have become disrupted. In this case it would have affected movements at joints beyond those whose muscles were directly affected by stimulation. However, our results show that this was not the case. The monkey retained voluntary control of muscles that were not directly affected by RL-ICMS, even muscles acting at joints adjacent to those where muscle activity was completely stimulus-driven (Griffin, et al., 2011).

Stable spatial end-points generated by stimulation of adjacent M1 cortical sites tended to be spatially contiguous in the monkey's work space. This yielded a global cortical map of end-point positions in which the monkey's three-dimensional workspace was represented in a relatively orderly fashion across the two-dimensional surface of the M1 cortex. This can be observed by the color coding of adjacent cortical sites in Figures 4.5A and 4.5B. The distance between spatial end-points in the work space corresponding to all combinations of adjacent cortical sites was 170.0 ± 95 mm for monkey A and 107.5 ± 57 mm for monkey X. The maximum distance covered between two spatial end-points in the work space was 520.5 mm for monkey A and 399.3 mm for monkey X. For

reference, the mean length each monkey's hand, from the dorsal tubercle of the radius to the tip of the third digit, was 106.3 mm.

While there were distinct cortical topographical differences in end-point representations between monkeys, there were also clear similarities such as hand-to-mouth postures elicited from cortical loci neighboring the M1 face representation in both monkeys. One example of neighboring cortical sites between monkeys yielding similar end-point postures is from cortical site 140 in monkey A and cortical site 91 in monkey X. Both cortical sites are near the face representation in M1, and both yielded end-point postures with the monkey's hand at the mouth. Figure 4.6 illustrates the spatial end-point resulting from stimulation at both sites, as well as the associated EMG activity for 23 forelimb muscles recorded during stimulation. Although not precisely identical, the pattern of EMG activity that yielded similar end-point postures is quite similar across monkeys. Of particular note is the co-activation pattern of proximal antagonist muscles in both monkeys that drove the arm to this posture, and the difference between this pattern compared to the voluntary EMG activity over a very similar movement trajectory.

Extent of work space represented by RL-ICMS-evoked movements

The results reveal RL-ICMS-evoked forelimb spatial end-points that encompass a considerable range of locations throughout the forelimb work space at or below head level. Figures 4.7A and 4.7B represent two-dimensional medio-lateral views of the monkeys performing the reach and prehension task, with superimposed successful spatial end-points elicited from each cortical site in M1 for each monkey. A similar spectrum of

spatial end-points were elicited from stimulation of M1 in each monkey. It should be emphasized that these maps of cortically mediated end-point positions present the full extent of end-points that could be elicited by stimulation of single cortical loci since we systematically mapped all of M1 at 0.5-1 mm resolution. It is clear in both monkeys that the stimulus evoked end-points encompass a large part of the monkeys available work space. The similarity between the monkeys' end-point distributions broken into mediolateral spatial planes can be observed particularly well in Figure 4.4B. In this figure, numbered spatial end-points correspond to numbered cortical sites (Figure 4.5A and 4.5B). These results reveal an extensive movement reportoire that can be elicited by applying RL-ICMS to M1.

The majority of the end-points reside on the limb's ipsilateral side of the midsagittal plane and below the level of the monkey's head, probably reflecting the fact that RL-ICMS activates muscle synergies encompassing both flexors and extensors at each joint. The resulting movement equilibrium point is then most likely to end at locations other than the most peripheral points in the work space. It should be noted that some movements were blocked from continuing to completion due to physical barriers present. One such barrier was a protective face shield surrounding the monkey's head. Additionally, a homeplate lever and protective waistplate prevented movement below waist level.

DISCUSSION

Orderly representation of the work space across primary motor cortex

Topographical muscle and functional representation in the motor cortex has been mapped comprehensively using many techniques including RS-ICMS, RL-ICMS, SpTA, StTA and immunohistochemical (Leyton and Sherrington, 1917, Penfield and Boldrey, 1937, Woolsey et al., 1952, Asanuma and Rosen, 1972, Cheney and Fetz, 1980, Park et al., 2001, Graziano et al., 2002, Eisner-Janowicz et al., 2008, Rathelot and Strick, 2009). Each subsequent and increasingly high resolution study using these investigative techniques have largely corroborated and built upon each other, with the consensus suggesting a hierarchical system of voluntary movement encoding that involves primary and secondary motor areas. However the results from a recent experiment in which RL-ICMS was applied to primary and secondary areas of the motor cortex has raised questions regarding the interpretation of these studies (Graziano et al., 2002). The results suggest that, rather than the motor cortex being comprised of discrete hierarchical structures and areas of muscle representation, the motor cortex is comprised of large underlying functional circuits that encode a limited set of ethologically relevant movements (Graziano et al., 2002). Evidence from this and other studies suggest that movement representation in both the cortex and the spinal cord are limited to movement modules (primitives) that combine to produce more complex voluntary movements (Bizzi et al., 1995, Graziano et al., 2002, Ethier et al., 2006).

The present findings expand upon these RL-ICMS studies by providing a high resolution comprehensive map of stimulus-evoked forelimb end-points using stimulus parameters determined previously in our lab to be optimal for evoking stable forelimb movements to spatial end-points (Chapter III). Our data suggest that stimulation of areas throughout the forelimb representation area in M1 activates a large repertoire of forelimb movements that span the spectrum of the monkey's available movement space. The present data suggest a general topographical arrangement of movements elicited in three-dimensional space that is represented in a relatively orderly fashion across the unfolded two-dimensional M1 cortex. While our findings do not support the presence of discrete areas of M1 that yield a limited number of prototypical movements, there do appear to be spatial end-points that tend to be relatively spatially contiguous with respect to adjacent cortical sites. In comparing possible topographical representations between monkeys the similarities are subtle, however some were striking. For example, spatial end-point postures of the forelimb elicited from cortical sites near the face representation area tended to drive the monkey's hand to the mouth. However not all hand-to-mouth evoked movements combined flexion of the elbow with supination of the wrist, as one would expect with voluntary feeding behavior. We observed instances where flexion of the elbow was combined with pronation of the wrist, leading to a seemingly unnatural posture.

Representation of specific purposeful movements in primary motor cortex

A previous RL-ICMS study produced an RL-ICMS-evoked hand-centered topographical map of the motor cortex, and suggested that applying stimulation to these circuits for durations matching those of voluntary movements results in overt and natural movements (Graziano et al., 2002). These results were obtained, at least in part, from stimulation of cortical sites in which other mapping studies revealed specific muscle representations or functionality. For example, Park et. al. (2001) mapped the forelimb muscle representation in M1 cortex using StTA. This method applies very low stimulus parameters to correlate neural connectivity of cells within M1 with downstream target muscles (Cheney and Fetz, 1985). While extensive overlap of individual muscle representations was present, there was a clear central core of distal muscle representation in the rostral bank of the central sulcus, a large “horseshoe”-shaped region representing proximal muscles primarily on the dorsal bank of the central sulcus, and a region separating these two that represented proximal-distal muscle co-facilitation. However in the RL-ICMS study by Graziano et. al. (2002), isolated movements of the distal or proximal muscle groups were not reported from stimulation of M1 nor were forelimb movements other than those ending in the central space in front of the monkey or extending below the chest (Graziano and Aflalo, 2007a). In addition, apparent defensive postures and feeding movements were found when the medial and ventral premotor areas were stimulated, areas thought to be associated with motor planning.

Our data reveal that, while many evoked movements end in the monkey's central work space, a large movement repertoire can be elicited from the entirety of M1 with a spectrum of movements encompassing much of the monkey's available work space. In addition, we observed examples of stimulation activating exclusively distal or proximal

muscle groups, primarily in their respective StTA-derived muscle representation areas, allowing the monkey to voluntarily modulate activity of unaffected muscles and associated joint throughout the duration of stimulation.

Mechanism of RL-ICMS evoked movements

A previous hypothesis proposed that cortical stimulation can lead to target muscle activity switching from facilitation to suppression with opposing limb starting positions, as a result of stimulation activating natural underlying circuits which have specific limb end-points (Graziano et al., 2004). Were this the case, muscle EMG activity recorded during stimulated movements should closely resemble the EMG activity of the same muscles during voluntary movements over the same trajectories. An alternative hypothesis is that stimulation activates neural elements within the physical and physiological current spread surrounding the stimulating electrode. The stimulation-evoked movement might therefore mimic a natural movement through tonic activation of target muscles, and the forelimb's end-point would then be a product of the summed length-tension relationships of the muscles. In this case the EMG activity during voluntary movements would not be expected to match that of stimulated movements over the same trajectories.

Data from our laboratory supports the latter hypothesis. Prior work in our laboratory suggests that switching of muscle activity from facilitation to suppression upon opposing limb starting positions rarely occurs (Griffin et al., 2011). Additionally, it is apparent that the stimulus-evoked EMG activity, corresponding to movements over

trajectories similar to voluntary movements, shows co-activation of antagonist muscles in a manner inconsistent with voluntary movement. For example, voluntary movement of the forelimb from elevated elbow extension and wrist pronation (hand at the feeder) to elbow flexion and wrist supination (hand at the mouth) produces EMG activity that follows a logical pattern of proximal flexor activation and extensor inactivation, while stimulated activity over the same trajectory produces synchronous co-activation of proximal flexors and extensors (Figure 4.6). The pattern of stimulus-evoked EMG activation suggests that stimulus-evoked movements and end-points are the product of sustained activation of muscles that lead to a physical equilibrium. The observation that many evoked movement end-points in this study reside in a central part of the work space (Figure 4.4B) is consistent with the fact that stimulation of the cortex tends to activate co-localized flexor- and extensor-specific corticospinal elements, often resulting in activation of muscle ensembles that include antagonist muscles which drive the arm to an intermediate equilibrium position. Indeed, this may help explain why movements of the arm elevated above head level were not found in this study, even though such movements can easily be made under voluntary control.

While one possible explanation for not observing movements of the hand elevated above head level is that the force of gravity asserts a downward force on the stimulus-evoked movement of the arm, resulting in movements that tend to move inferiorly rather than superiorly, gravity cannot be the sole reason for the absence of such elevated movements in this study. We routinely evoked converging forelimb end-point postures from initial positions above and below the final end-point supporting previous findings that suggest final end-point posture is consistent regardless of starting position of the

limb (Graziano et al., 2005), provided that stimulation produced a sufficiently forceful activation of the muscle synergy represented at a particular cortical site. If gravity can be overcome through stimulus-evoked forelimb elevation from an inferior starting position to a position at or below head level, elevation above head level should be equally achievable were gravity the sole impediment.

Another possible explanation for the absence of forelimb movements above head level is that such elevation of the arm would require activation of a relatively select group of muscles with concurrent inactivation or inhibition of antagonist muscles. For this to occur, stimulation would need to activate a sufficiently large population of corticospinal cells targeting this select group of muscles while concurrently avoiding activation of descending output to the antagonist muscles. Our results suggest that RL-ICMS rarely activates descending output in such a specific manner. This conclusion is supported by the fact that the majority of the spatial end-points we observed tended to be toward the central work space of the monkey and therefore were likely the product of flexor and extensor co-activation.

Our findings suggest that M1 neural encoding of movement capitalizes on strong corticospinal output with concomitant horizontal collateral connections to associated corticospinal outputs, both of which are activated with RL-ICMS provided sufficient stimulation parameters are applied. Stimulation thereby produces activation of motoneuron pools and subsequently muscle synergies that result from cortical neuronal activation through both physical and physiological spread of stimulation.

Summary and Conclusions

Results from the present study reveal RL-ICMS-evoked forelimb spatial end-points that encompass a considerable range of locations throughout the available forelimb work space at or below head level. Cortical sites yielding successful RL-ICMS-evoked forelimb translocation with subsequent stabilization at an end-point tended to be located around cortical output zones that produced StTA-derived facilitation of both proximal and distal muscles, suggesting that co-activation of proximal and distal muscle ensembles were required to stabilize the forelimb at a spatial end-point. This supports our observation that stimulation affecting exclusively proximal or distal muscles allows the monkey to voluntarily activate the unaffected muscles and associated joint throughout the duration of stimulation. Additionally, our findings support the view that stimulus-evoked movements and associated end-points represent equilibrium points in the length-tension relationships of the activated muscles, as opposed to activation of underlying natural circuits. Finally, stable end-points generated by stimulation of adjacent M1 cortical sites tended to be spatially contiguous in the monkey's work space. This yielded a global cortical map of end-point positions in which the monkey's three-dimensional workspace was represented in a relatively orderly fashion across the two-dimensional surface of M1 cortex. These results reveal an extensive movement reportoire that can be elicited by applying RL-ICMS to M1, and add to our understanding of cortical encoding of motor output.

Figure 4.1. Red arrows represent the movement sequence required to perform the task: Monkey holds homeplate lever (A) until a food reward drops and he retrieves a pellet from the food dispenser (B) and feeds himself (C). In this illustration, RL-ICMS is applied when the monkey's hand arrived at the food dispenser (B), subsequently driving his right forelimb to a spatial end point. Vicon motion capture reflective spheres (multi-colored spheres on the forelimb) of the lower forelimb were used to calculate the 3D coordinates of the dorsal tubercle of the radius (large green sphere, one for each movement cycle represented). Illustrated are RL-ICMS-evoked example trajectories (solid green lines) and example voluntary movement trajectories following stimulation end (dashed green lines). These trajectories do not represent actual data, rather are used for illustrative purposes.

Monkey performing reach and prehension task

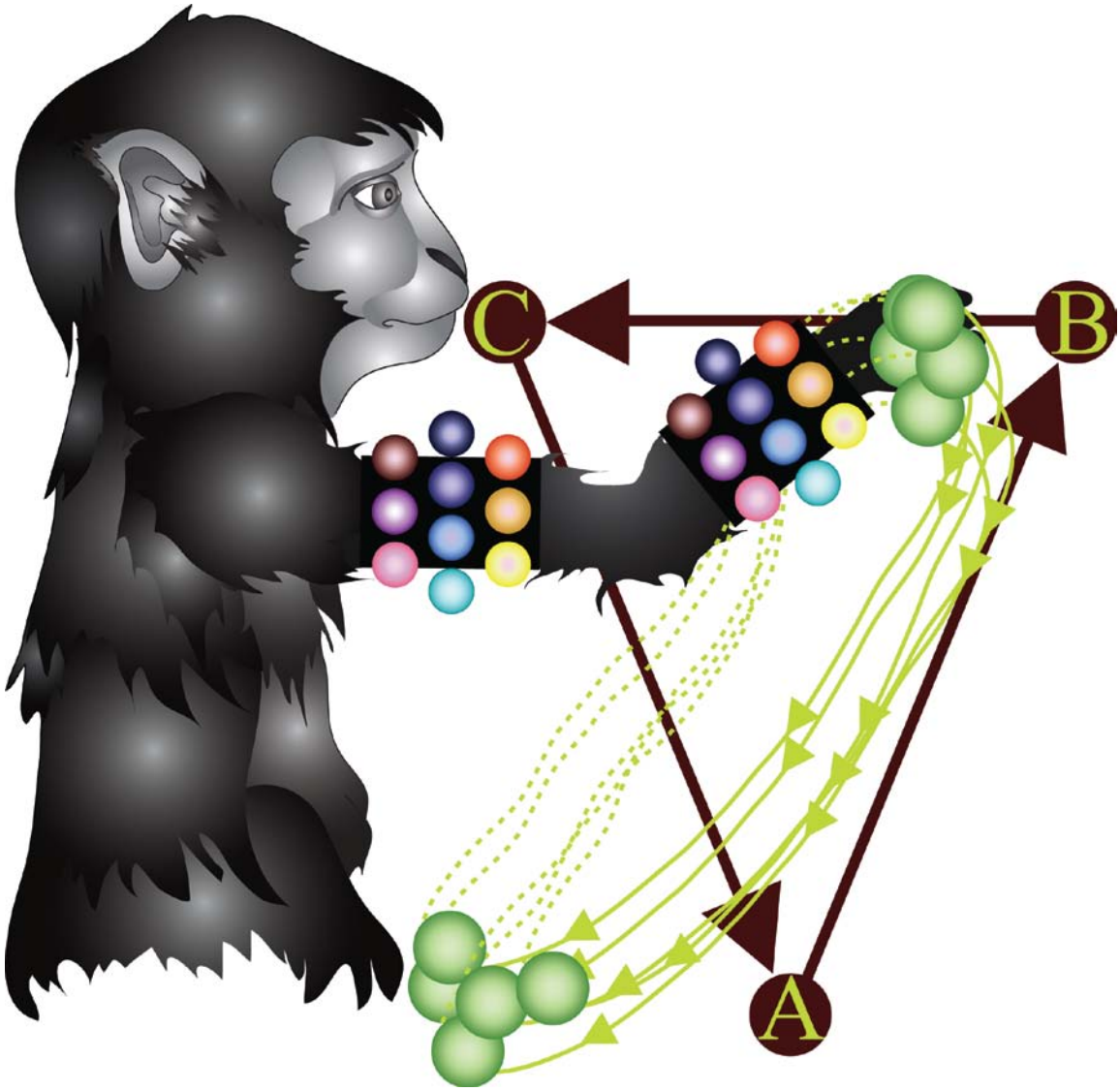

Figure 4.2. Modifiable chair developed for behavioral task.

Custom primate chair

Figure 4.3A. StTA-derived muscle representation map includes a view of the dorsal surface of the precentral gyrus and the rostral wall of the central sulcus. Anterior, posterior, medial and lateral are indicated by the compass rose. Sites of RL-ICMS are indicated by the orange dots, and are numbered in logical order for presentation purposes rather than chronological order. Areas producing facilitation in StTAs of distal forelimb muscles (blue), proximal forelimb muscles (red) and both proximal and distal muscles (purple) are indicated.

.

Monkey A's M1 forelimb representation including RL-ICMS-mapped sites

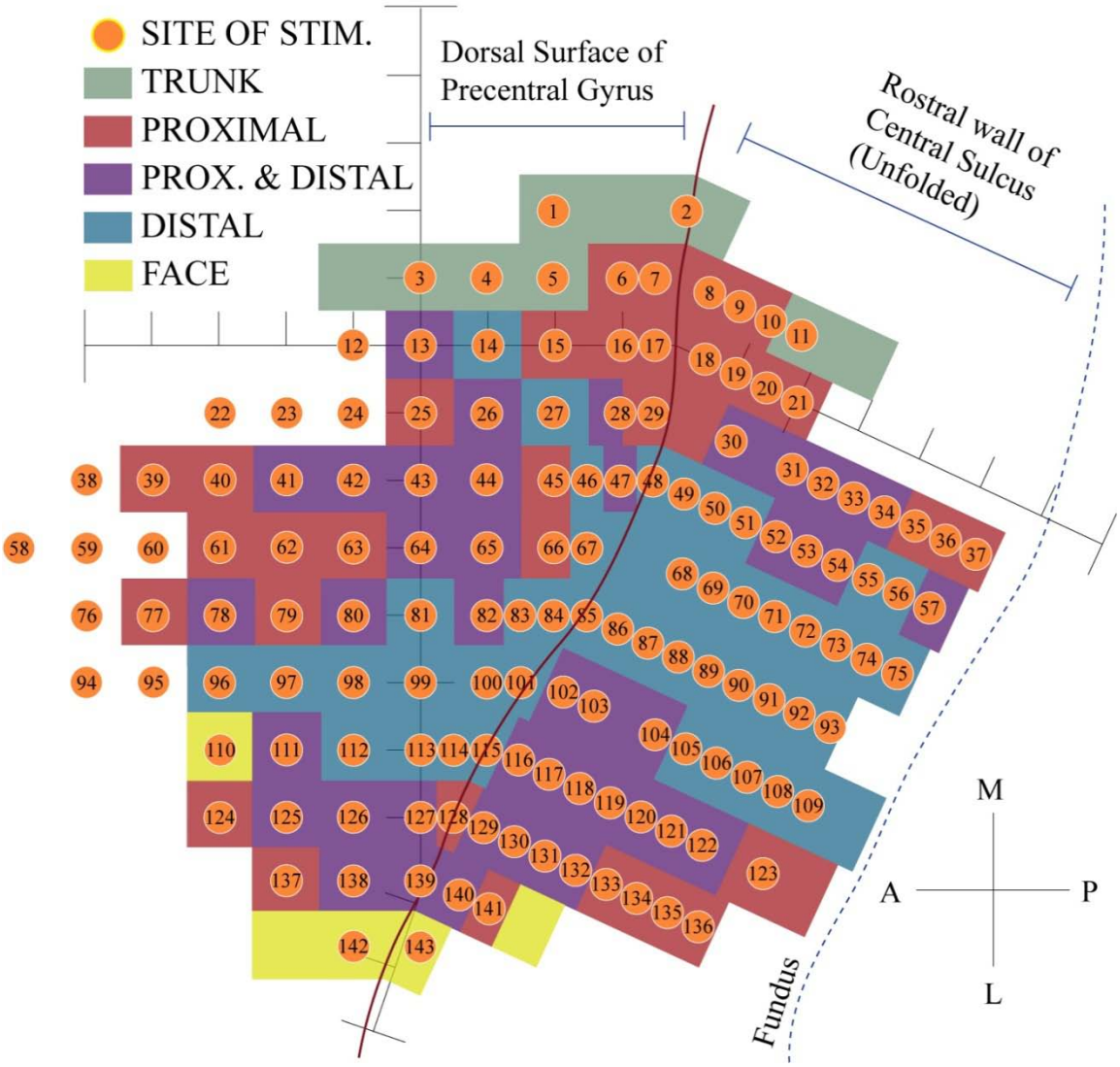

Figure 4.3B. Unfolded StTA-derived muscle representation map includes a view of the dorsal surface of the precentral gyrus and the rostral wall of the central sulcus. Anterior, posterior, medial and lateral are indicated by the compass rose. Sites of RL-ICMS are indicated by the orange dots, and are numbered in logical order for presentation purposes rather than chronological order. Areas producing facilitation in StTAs of distal forelimb muscles (blue), proximal forelimb muscles (red) and both proximal and distal muscles (purple) are indicated.

Monkey X's M1 forelimb representation including RL-ICMS-mapped sites

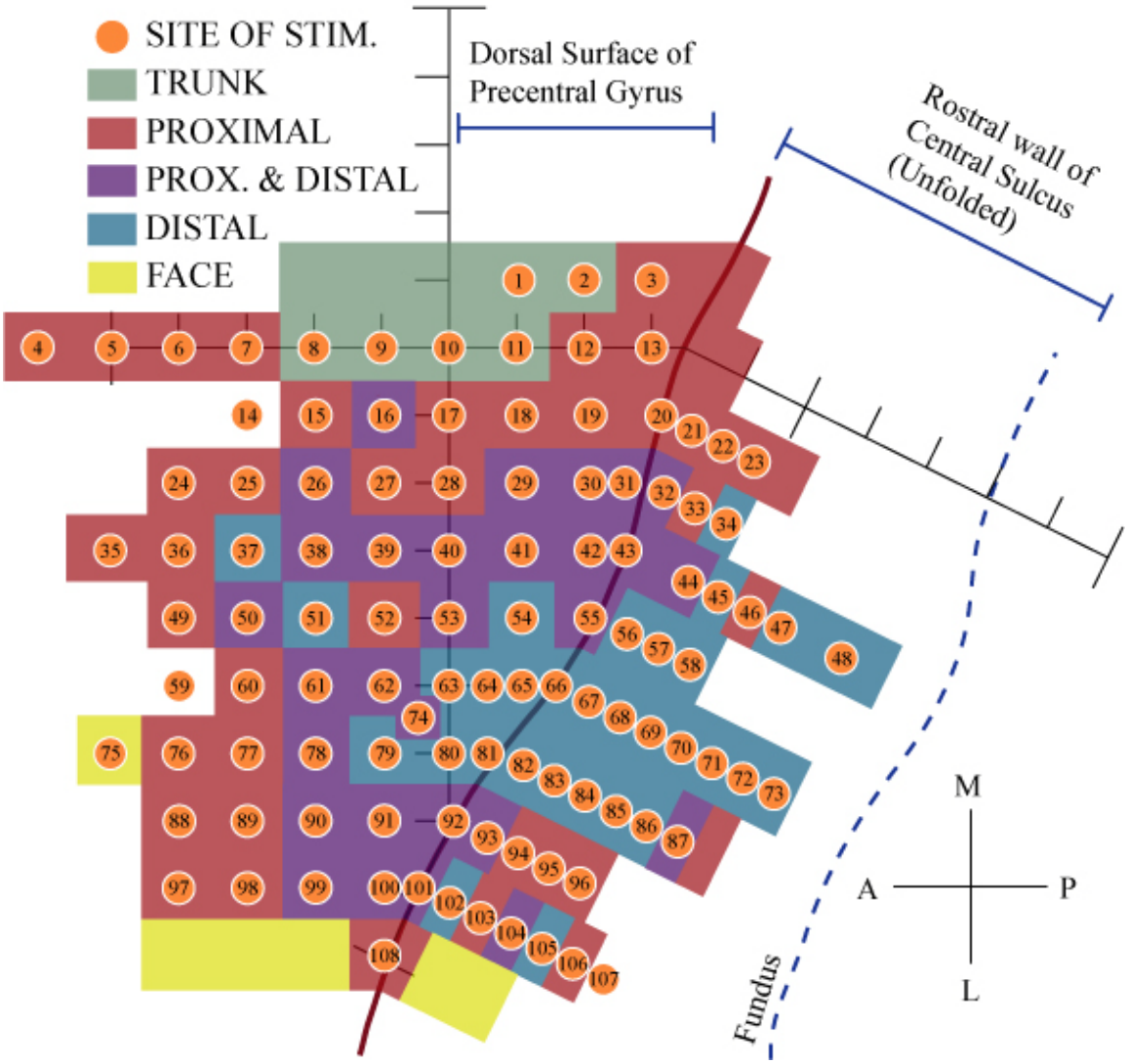

Figure 4.4. Color-coded voxels representing monkey's work space and monkey forelimb end-points illustrated on parasagittal planes. *A*: Illustration of color-coded voxels covering the monkey's work space. The monkeys were situated with midsagittal plane at approximately mediolateral coordinate 0 mm, and mid-coronal plane at approximately anterior-posterior 100 mm. Voxel size is 154.2 mm in the anterior-posterior direction, 126.1 mm medial-lateral, and 98.7 mm superior-inferior. *B*: RL-ICMS-evoked end-points for each cortical site represented by numbers for monkey A and X corresponding to cortical site numbers in figures 4.3A and 4.3B, respectively. Spatial planes are divided into medial, central and lateral planes.

Spatial representation key with end-points illustrated on parasagittal planes

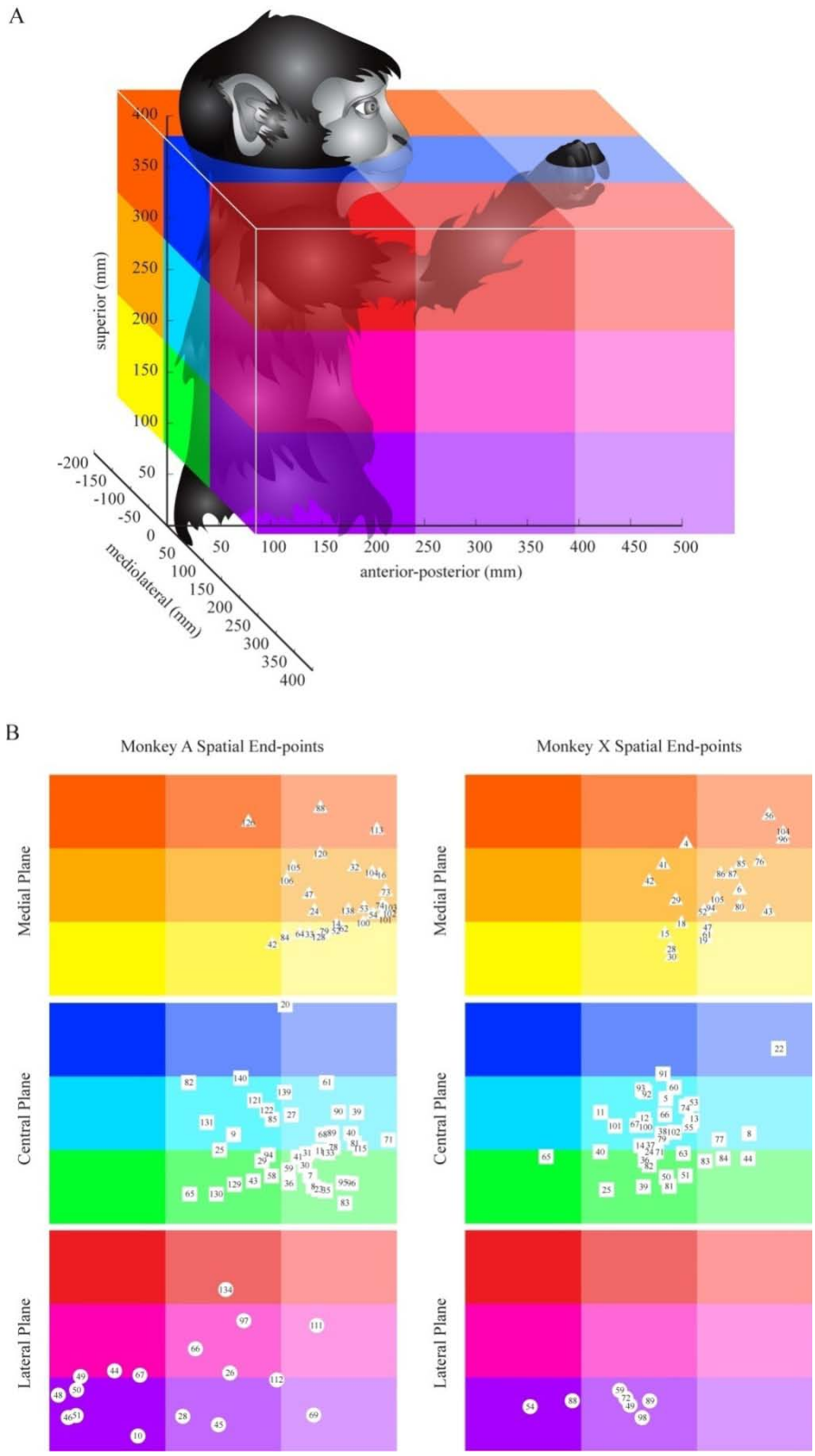

Figure 4.5A. Color-coded spatial end-points on a cortical representation map of A's M1. Cortical sites where RL-ICMS was applied are numbered. Colored sites are those that yielded successful spatial end-points of the forelimb upon repetitive stimulation, whereas gray sites are those that did not. Colors correspond to voxels within the monkey's work space using the same color coding as illustrated in Figure 4.4.

Monkey A's M1 cortical representation of spatial end-points

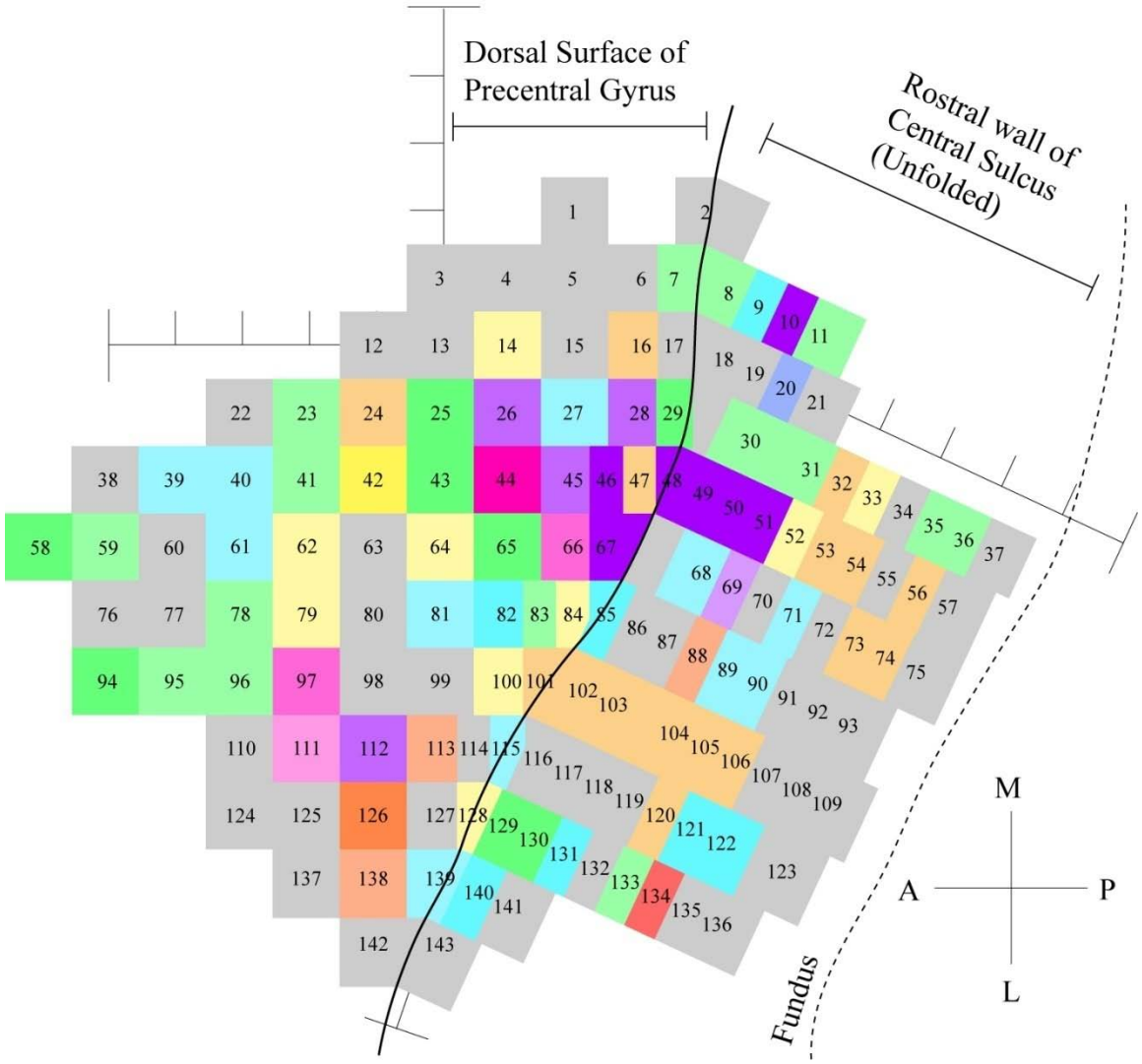

Figure 4.5B. Color-coded spatial end-points on a cortical representation map of X's M1. Cortical sites where RL-ICMS was applied are numbered. Colored sites are those that yielded successful spatial end-points of the forelimb upon repetitive stimulation, whereas gray sites are those that did not. Colors correspond to voxels within the monkey's work space using the same color coding as illustrated in Figure 4.4.

Monkey X's M1 cortical representation of spatial end-points

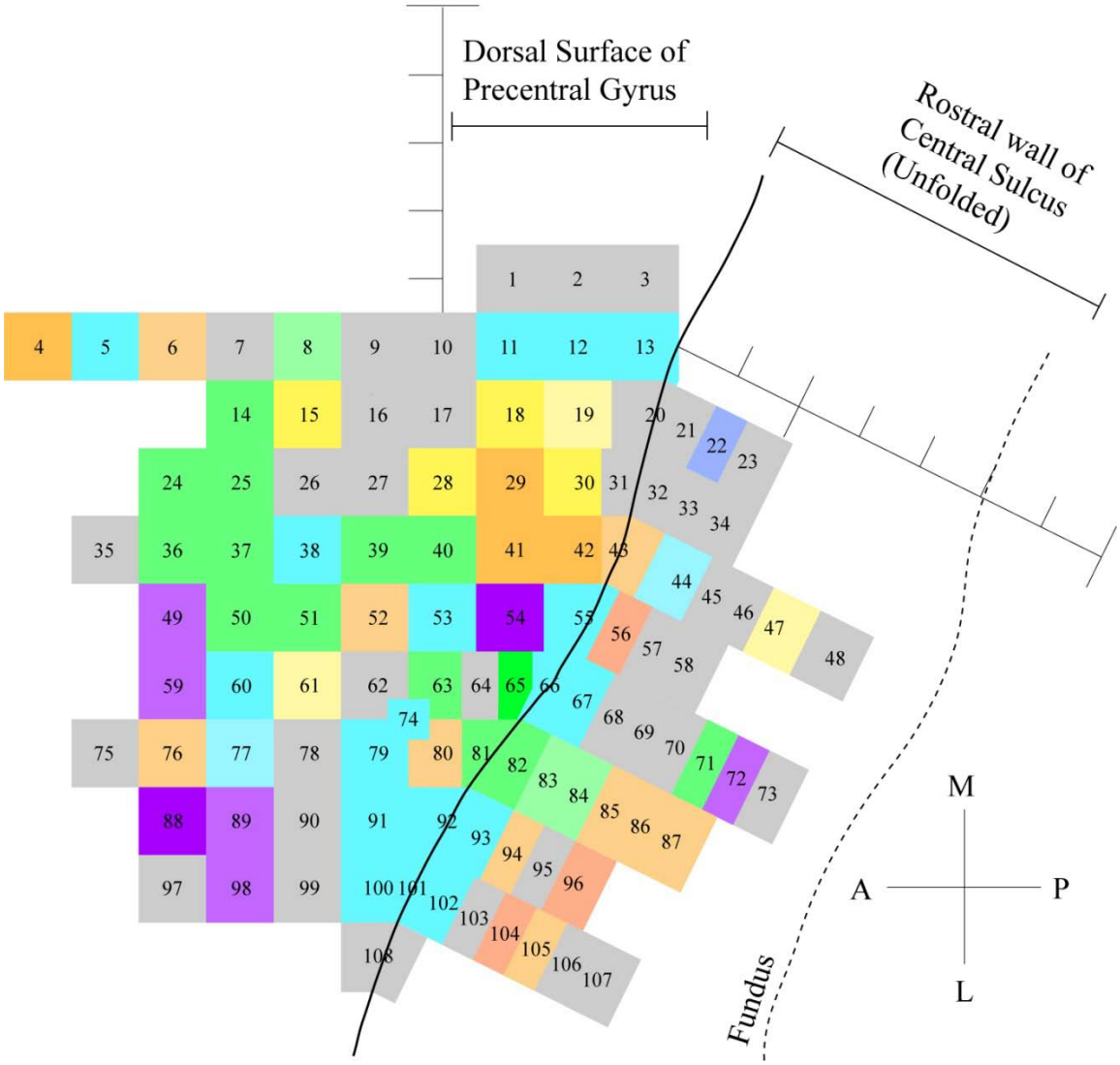

Figure 4.6. Comparison of EMG activity and spatial end-point recorded during stimulation of neighboring M1 sites between monkeys. Mediolateral view of monkey with evoked spatial end-points of monkey A and monkey X represented by a red and blue square respectively. The spatial end-point coordinates are 22.1x, 256.2y, 274.8z and 29.7x, 264.8y, 280.0z for monkey A and X, respectively. EMG tracings for all forelimb muscles are superimposed; red and blue EMG tracings are stimulus-evoked activity in monkey A and monkey X, respectively; black EMG tracings are voluntary activity in monkey A over same movement trajectory elicited with stimulation. Each EMG tracing is averaged and smoothed over 5 trials. Stimulation epoch is defined by purple bars, and is 1000 ms in duration. Examples represent stimulation applied to site 140 in monkey A and site 91 in monkey X, as well as voluntary activity recorded in monkey A directly following stimulation at site 140. Green sphere represents dorsal tubercle of radius. See methods for muscle abbreviations.

EMG activity and end-points from neighboring M1 sites between monkeys

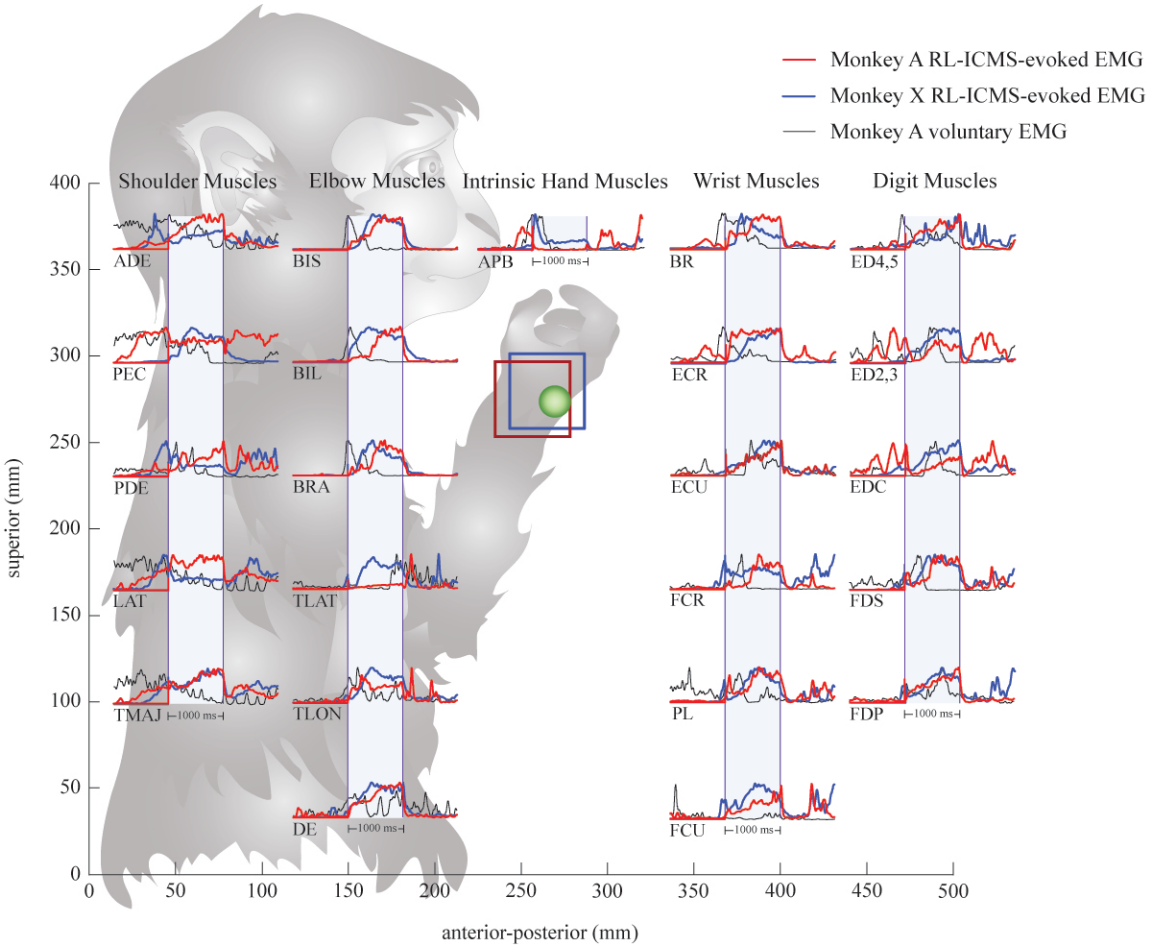

Figure 4.7A. Two-dimensional representation of monkey A's work space including all RL-ICMS-evoked spatial end-points superimposed. Mediolateral view of monkey A performing reach and prehension task, with evoked spatial end-points represented by colored shapes (assigned in key legend). Lateral plane lies between the mediolateral coordinates of 116.1 and 142.2 mm; central plane -10 to 116.1 mm; medial plane -136.1 to -10 mm. The monkey's midsagittal plane is situated at approximately mediolateral coordinate 0 mm. Green sphere represents dorsal tubercle of radius.

Spatial end-point representation in monkey A's work space

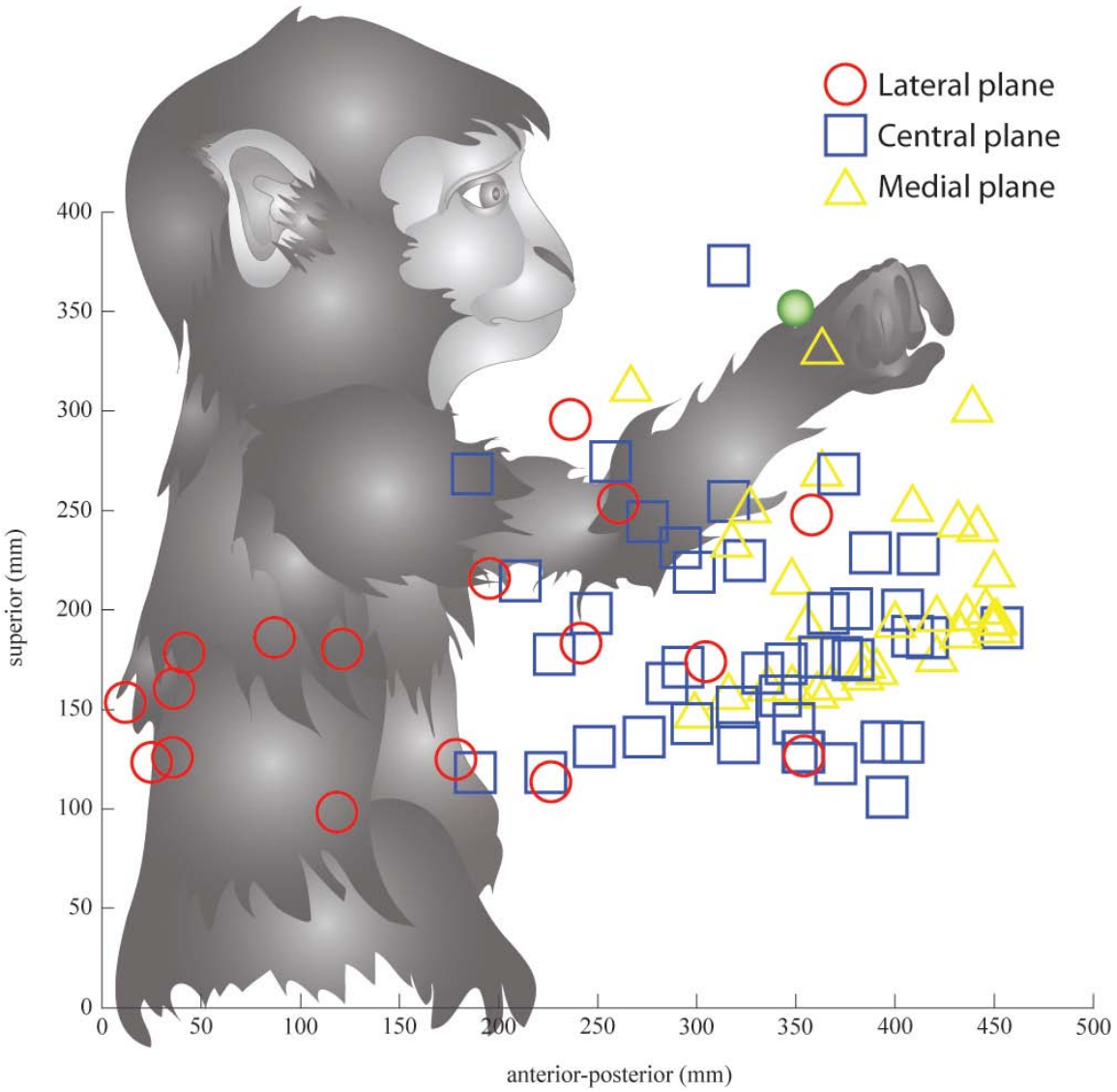

Figure 4.7B. Two-dimensional representation of monkey X's work space including all RL-ICMS-evoked spatial end-points superimposed. Mediolateral view of monkey X performing reach and prehension task, with evoked spatial end-points represented by colored shapes (assigned in key legend). Lateral plane lies between the mediolateral coordinates of 116.1 and 142.2 mm; central plane -10 to 116.1 mm; medial plane -136.1 to -10 mm. The monkey's midsagittal plane is situated at approximately mediolateral coordinate 0 mm. Green sphere represents dorsal tubercle of radius.

Spatial end-point representation in monkey X's work space

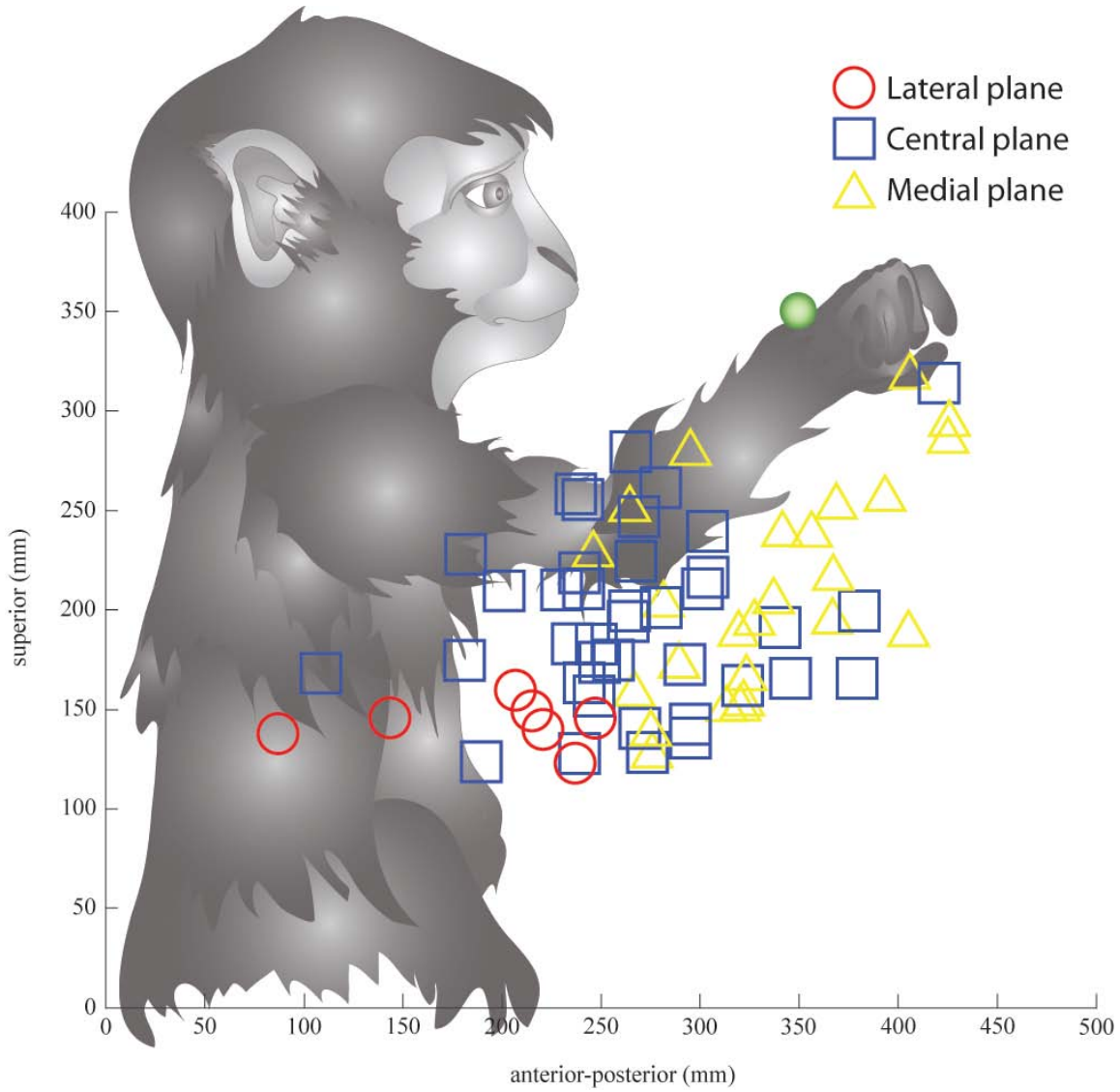

CHAPTER V:

CONCLUSION

Understanding cortical control of movement: the importance of basic science research

There exists a delicate interplay between two dichotomous forces in science: the desire to explore and to gain knowledge of a system, and the desire to apply existing knowledge in a functional manner. The contemporary inertia of the latter force, in part acted upon by a dearth of basic science funding, has increased in many biomedical research fields even when we still have much to learn of the basic systems from which we are utilizing information. The present study is an example of what has recently become common in basic science research, to some degree in order to compete for funding and therefore survive in the current scientific environment: to present any and all research in a light that suggests at the very least an ever-so-subtle bridging of basic science and clinical science.

Our principal goal in the present set of experiments was to more fully explore the brain's encoding of voluntary movement. However, while we defend that this information is invaluable from a basic science perspective, our research is also important for the development of effective therapies for patients with neuromuscular disorders. We will discuss how the present findings, while basic in nature, may indeed help advance treatment of motor disorders in the near-future clinical setting. Firstly, however, let us begin by revisiting the basic principles elicited in the present body of work from a basic science approach.

Present aims in relation to basic science

Specific aim 1: to assess the timing of cortico-muscle transmission during active movement

Previous studies report disparities in the delays between cortical cell activity and the onset of voluntary movement or EMG activity (Humphrey and Corrie, 1978, Cheney and Fetz, 1980, 1985, Lemon et al., 1986, Baker and Lemon, 1998, McKiernan et al., 1998, Park et al., 2004). In order to clarify the mechanisms of cortico-muscle transmission, it is essential that we obtain an accurate measurement of the transmission latency when muscles are fully active. In the present study we evoked time-varying modulations of corticospinal output to motoneurons by applying frequency-modulated stimulus trains to individual M1 cortical sites. This procedure yielded corresponding modulations of EMG activity whose latencies were measured directly relative to the applied stimulus train modulations. These latencies then allowed us to determine the timing of cortico-muscle transmission.

Although the time delay between peaks in the frequency-modulated cortical stimulus train and corresponding EMG modulation varied somewhat with the stimulus parameters, the overall mean latency of excitatory modulation across all parameters determined via cross-correlation analysis (11.5 ± 5.6 ms) was only 1.9 ms longer than the conduction time through the cortex-to-muscle pathway derived from StTAs computed at the same sites (9.6 ± 2.1 ms). These results demonstrate that, during active movement, cortical output can modulate muscle activity at latencies approaching the minimum

conduction time through the cortico-muscle pathway. The results support the hypothesis that the longer time delays reported for the timing between cortical cell activation and muscle activation are due largely to the time required to bring motoneurons to firing threshold from a hyperpolarized state.

It should be noted that our method of stimulation differs from natural muscle activation by cortical cells in two important respects. Firstly, stimulation activates a population of cells simultaneously whereas natural activation involves the recruitment of cells at varying times relative to movement or EMG onset. Secondly, with stimulation the discharge of cells is synchronous with each stimulus, at least at the cortical level, whereas the natural activity of cells is overtly asynchronous. Yet another difference is that stimulation may co-activate unnatural combinations of cells compared to those that would occur during natural movement.

To more closely simulate natural activation of motor units by cortical stimulation, a logical extension of our study would be to modulate the intensity of the stimuli in the stimulus train while concurrently, as was done in the present study, modulating frequency. Modulating intensity would provide a mechanism to simulate the range of cortical cell recruitment times relative to movement/EMG onset evident in studies of cortical cell activity during natural movements.

Specific Aim 2: to determine the optimal stimulus parameters for M1 RL-ICMS-evoked translocation with subsequent stabilization of the forelimb

The rationale of identifying the optimal stimulus parameters that translocate and subsequently stabilize the forelimb at a new end-point in space is two-fold. Firstly, the parameters used in previous studies applying RL-ICMS to evoke movements are highly variable from one study to another as well as within individual studies; therefore, determining optimal parameters could aid in creating a standard for future RL-ICMS studies. Secondly, our results provide an objective basis for selection of the parameters that were utilized in the third aim of our study. To identify optimal parameters we applied stimulation to M1 as combinations of frequency (30 - 400 Hz), intensity (30 - 200 µA) and duration (0.5 - 2 s) while concurrently recording the EMG output to 24 forelimb muscles as well as the stimulus-evoked limb kinematics using a Vicon motion capture system. Our results suggest a relatively narrow range of stimulus parameters applied to M1 that are both safe and effective for evoking translocation with subsequent stabilization of the stimulated forelimb at a spatial end-point: 70 - 130 Hz, 70 - 130 µA and 1000 ms. The mean successful frequency, normalized for all trials recorded in the study, was 115.2 ± 22.3 Hz while the mean successful intensity was 108.8 ± 23.7 µA. Additionally, the median successful frequency for all trials was 110 Hz and the median successful intensity was 110 µA. The mean spatial end-point time from the onset of stimulation was 469 ± 156 ms. Attenuated parameters resulted in inconsistent, truncated or undetectable movements, while intensified parameters increased the potential for large-scale physiological spread and adverse focal motor effects. Establishing cortical stimulation parameters that yielded consistent stimulus-evoked end-points formed the basis for a systematic and complete mapping of movement space and associated muscle synergies in primary motor cortex.

It is important to note that, while we found optimal stimulus parameters for evoking forelimb movement from the forelimb representation in macaque primary motor cortex, there likely exists some variability between studies due to various cortical locations, animal species, stimulating electrodes and possible anesthetizing agents used. However, the parameters obtained in this study correspond well with the proposed mechanism of RL-ICMS-evoked movement (Griffin et al., 2011), and are similar to stimulus parameters used in the DBS treatment of neurological disorders which is thought to act therapeutically via a similar mechanism (Garcia et al., 2005).

Specific Aim 3: to obtain a comprehensive spatial end-point map of the M1 cortical forelimb representation using RL-ICMS

The importance of this third and final goal was to further investigate previous studies that applied RL-ICMS to primary and secondary motor areas, in which hypotheses were proposed concerning cortical encoding of motor control that conflicted with previous understanding of the system (Graziano and Aflalo, 2007b). In the present study, we constructed a systematic and comprehensive RL-ICMS-evoked spatial end-point map of M1 utilizing a subset of stimulus parameters, typically 100-120 Hz, 100-120 μA and one second duration, determined previously as part of this dissertation (Chapter III) to be optimal for eliciting stable spatial end-points of the forelimb. The results revealed RL-ICMS-evoked forelimb spatial end-points that encompass a considerable range of locations throughout the available forelimb work space at or below head level. Cortical sites yielding successful RL-ICMS-evoked forelimb translocation with

subsequent stabilization at an end-point tended to be located around cortical output zones that produced StTA-derived facilitation of both proximal and distal muscles, suggesting that co-activation of proximal and distal muscle ensembles were required to drive the forelimb to a spatial end-point. This is consistent with the observation that stimulation affecting exclusively proximal or distal muscles allows the monkey to voluntarily activate the unaffected muscle group throughout the duration of stimulation. Although such residual voluntary movement capability interfered with establishing stable stimulation-evoked end-points, it was instructive in demonstrating that RL-ICMS seizes only the output apparatus of the brain-motor control system while leaving intact earlier, upstream aspects of the internal motor program such as motivation and planning. If these functions were disrupted by stimulation, possibly through antidromic and orthodromic activation of fibers in the cortex, we would have expected that voluntary movements would have been affected on a more global level rather than affecting only the muscles directly targeted by stimulation. Additionally, as opposed to stimulation activating underlying natural circuits as proposed by others (Graziano and Aflalo, 2007b), our evidence suggests that stimulus-evoked movements and associated end-points represent equilibrium points in the length-tension relationships of the activated agonist and antagonist muscles. Finally, stable end-points generated by stimulation of adjacent M1 cortical sites tended to be spatially contiguous in the monkey's work space. This yielded a global cortical map of end-point positions in which the monkey's three-dimensional workspace was represented in a relatively orderly fashion across the two-dimensional surface of M1 cortex. This finding is at odds with the presence of discrete prototypical movements encoded at the level of M1 reported in previous studies (Graziano et al.,

2002). Applying RL-ICMS to M1 cortex yielded a surprisingly extensive movement repertoire representing a substantial volume of the monkey’s work space. The results provide a complete map of cortical output in terms of movement end-points and add broadly to our understanding of cortical encoding of motor output.

The present study utilized reflective spheres attached to the monkey's forelimb with which we were able to quantify forelimb kinematics and spatial end-points using a Vicon motion capture system. These reflective spheres were easy targets for the monkey to remove with either his teeth, contralateral hand or feet. Therefore it was necessary to install physical barriers that prevented the removal of spheres. While the barriers worked well, they did somewhat limit the available work space of the forelimb in some dimensions. These physical barriers affected the final spatial end-point of some evoked movements, particularly inferior movements that were blocked due to the waist plate. In future studies requiring tracking forelimb spatial coordinates, one possible method to avoid the use of physical barriers could employ an implanted telemetric system that relays forelimb spatial coordinates, in particular one which utilized implanted telemetric EMG electrodes.

This study focused on the elicited spatial end-point of a single point on the wrist, the dorsal tuberosity of the radius, in order to characterize evoked movements and subsequent stabilization of the limb. Therefore many interesting elements of the evoked movements, such as hand postures and joint angles, were not quantified in the current study. However during each recording session we attached a proximal arm band of Vicon reflective spheres to the monkey that, when analyzed together with the distal markers, could be used to determine the evoked elbow joint posture at each cortical site. In

addition, analyzing these markers together with the monkey's standard torso location and posture also yielded shoulder joint postures. This line of investigation is currently being pursued in our laboratory, the results of which will add to the comprehensive mapping of stimulus-evoked end-point postures.

Present aims in relation to future clinical advancements

The results obtained from the research conducted in this body of work will help further advance therapeutic treatments for some forms of motor disorders, ranging from Parkinson's Disease to locked-in syndrome. In Chapter II we discovered that, during active movement, the transmission time between M1 corticospinal activity and target muscle activity closely approaches the conduction time through the cortico-muscle pathway. We also know that information encoded at the level of the primary motor cortex is the primary final cortical stop of voluntary movement planning prior to acting upon motoneurons and subsequent target muscles. Because M1 is the final step in the execution of planned voluntary movement, it is likely a good candidate with which to incorporate volitional activity into applied neuroprosthetic devices. Knowledge of the timing between voluntary corticospinal activity and muscle activity is important for multiple forms of treatment for patients who have lost functionality of their limbs. Many neuroprosthetic devices can incorporate this timing to improve directly the imposed timing used in algorithms that communicate M1 cortical cell activity with external devices or muscles of an affected limb (Moritz et al., 2007, Moritz et al., 2008, Chadwick et al., 2011). Additionally, timing is key when attempting, using Hebbian theory, to

utilize synaptic plasticity in order to create connections between disparate locations within the central nervous system, a therapeutic approach currently being investigated that may be used to treat both stroke and paralysis.

In Chapter III we revealed the optimal stimulus parameters for evoking stable forelimb spatial end-points upon stimulation of M1. The hypothetical mechanism underlying these findings incorporates basic knowledge of neuronal activation in response to stimulation, and the results can be integrated into therapies involving closed-loop neuroprosthetic devices. In addition, current deep brain stimulation for Parkinson's Disease and intractable cases of obsessive compulsive disorder and depression (Howland et al., 2011), as well as future DBS treatments applied to various areas of the brain, can benefit from the threshold of effective stimulus parameters uncovered in this study. DBS treatment currently uses stimulus parameters determined empirically to be effective (Garcia et al., 2005), and are similar to the optimal parameters revealed in the present study.

Finally, in Chapter IV, we mapped the forelimb spatial end-points that can be evoked throughout the entirety of M1 cortex. The results suggest that recording from select sites throughout M1 may translate well into optimizing a large repertoire of coordinated movements with brain signal-controlled prosthetic limbs.

In addition to each of the possible therapeutic applications mentioned, there is the potential for unforeseen applications down the road. Many past discoveries that provided leaps in the basic understanding of a particular system led to contemporary advancements in medicine only after decades of further insight. This fact highlights the importance of basic science remaining an integral aspect of our scientific approach.

REFERENCES

Andriacchi TP, Alexander EJ, Toney MK, Dyrby C, Sum J (1998) A point cluster method for in vivo motion analysis: applied to a study of knee kinematics. J Biomech Eng 120:743-749.

Asanuma H, Arnold A, Zarzecki P (1976) Further study on the excitation of pyramidal tract cells by intracortical microstimulation. Exp Brain Res 26:443-461.

Asanuma H, Rosen I (1972) Topographical organization of cortical efferent zones projecting to distal forelimb muscles in the monkey. Exp Brain Res 14:243-256.

Asanuma H, Sakata H (1967) Functional organization of a cortical efferent system examined with focal depth stimulation in cats. J Neurophysiol 30:35-54.

Baker SN, Lemon RN (1998) Computer simulation of post-spike facilitation in spike-triggered averages of rectified EMG. J Neurophysiol 80:1391-1406.

Belhaj-Saif A, Karrer JH, Cheney PD (1998) Distribution and characteristics of poststimulus effects in proximal and distal forelimb muscles from red nucleus in the monkey. J Neurophysiol 79:1777-1789.

Binder MD, Heckman CJ, powers RK (2011) The physiological control of motoneuron activity. Handbook of Physiology Section 12:3-53.

Bizzi E, Giszter SF, Loeb E, Mussa-Ivaldi FA, Saltiel P (1995) Modular organization of motor behavior in the frog's spinal cord. Trends Neurosci 18:442-446.

Buys EJ, Lemon RN, Mantel GW, Muir RB (1986) Selective facilitation of different hand muscles by single corticospinal neurones in the conscious monkey. J Physiol 381:529-549.

Capaday C, van Vreeswijk C, Ethier C, J. F-B, Weber D (2011) Neural Mechanism of Activity Spread in the Cat Motor Cortex and its Relation to the Intrinsic Connectivity. J Neurophysiol.

Chadwick EK, Blana D, Simeral JD, Lambrecht J, Kim SP, Cornwell AS, Taylor DM, Hochberg LR, Donoghue JP, Kirsch RF (2011) Continuous neuronal ensemble control of simulated arm reaching by a human with tetraplegia. J Neural Eng 8:034003.

Cheney PD, Fetz EE (1980) Functional classes of primate corticomotoneuronal cells and their relation to active force. J Neurophysiol 44:773-791.

Cheney PD, Fetz EE (1985) Comparable patterns of muscle facilitation evoked by individual corticomotoneuronal (CM) cells and by single intracortical microstimuli in primates: evidence for functional groups of CM cells. J Neurophysiol 53:786-804.

Donoghue JP, Leibovic S, Sanes JN (1992) Organization of the forelimb area in squirrel monkey motor cortex: representation of digit, wrist, and elbow muscles. Exp Brain Res 89:1-19.

Eisner-Janowicz I, Barbay S, Hoover E, Stowe AM, Frost SB, Plautz EJ, Nudo RJ (2008) Early and late changes in the distal forelimb representation of the supplementary motor area after injury to frontal motor areas in the squirrel monkey. J Neurophysiol 100:1498-1512.

Ethier C, Brizzi L, Darling WG, Capaday C (2006) Linear summation of cat motor cortex outputs. J Neurosci 26:5574-5581.

Evarts EV (1964) Temporal Patterns of Discharge of Pyramidal Tract Neurons during Sleep and Waking in the Monkey. J Neurophysiol 27:152-171.

Evarts EV (1972) Contrasts between activity of precentral and postcentral neurons of cerebral cortex during movement in the monkey. Brain Res 40:25-31.

Ferrier D (1875) Experiments on the brain of monkeys. Proc R Soc Lond 23:409-430.

Fritsch G, Hitzig E (1870) Uber die elektrische Erregbarkeit des Grosshirns. Archs Anat Physiol Wiss Med 37:300-332.

Garcia L, D'Alessandro G, Bioulac B, Hammond C (2005) High-frequency stimulation in Parkinson's disease: more or less? Trends Neurosci 28:209-216.

Graziano MS, Aflalo TN (2007a) Mapping behavioral repertoire onto the cortex. Neuron 56:239-251.

Graziano MS, Aflalo TN (2007b) Rethinking cortical organization: moving away from discrete areas arranged in hierarchies. Neuroscientist 13:138-147.

Graziano MS, Aflalo TN, Cooke DF (2005) Arm movements evoked by electrical stimulation in the motor cortex of monkeys. J Neurophysiol 94:4209-4223.

Graziano MS, Patel KT, Taylor CS (2004) Mapping from motor cortex to biceps and triceps altered by elbow angle. J Neurophysiol 92:395-407.

Graziano MS, Taylor CS, Moore T (2002) Complex movements evoked by microstimulation of precentral cortex. Neuron 34:841-851.

Griffin DM, Hudson HM, Belhaj-Saif A, Cheney PD (2011) Hijacking Cortical Motor Output with Repetitive Microstimulation.

Houk JC, Dessem DA, Miller LE, Sybirska EH (1987) Correlation and spectral analysis of relations between single unit discharge and muscle activities. J Neurosci Methods 21:201-224.

Howland RH, Shutt LS, Berman SR, Spotts CR, Denko T (2011) The emerging use of technology for the treatment of depression and other neuropsychiatric disorders. Ann Clin Psychiatry 23:48-62.

Hubel D (1957) Tungsten microelectrode for recording from single units. Science 125:549-550.

Humphrey DR, Corrie WS (1978) Properties of pyramidal tract neuron system within a functionally defined subregion of primate motor cortex. J Neurophysiol 41:216-243.

Jackson A, Gee VJ, Baker SN, Lemon RN (2003) Synchrony between neurons with similar muscle fields in monkey motor cortex. Neuron 38:115-125.

Lemon RN, Mantel GW, Muir RB (1986) Corticospinal facilitation of hand muscles during voluntary movement in the conscious monkey. J Physiol 381:497-527.

Leyton SSF, Sherrington CS (1917) Observations on the excitable cortex of the chimpanzee, orangutan and gorilla. Q J Exp Physiol 11:135-222.

McKiernan BJ, Marcario JK, Karrer JH, Cheney PD (1998) Corticomotoneuronal postspike effects in shoulder, elbow, wrist, digit, and intrinsic hand muscles during a reach and prehension task. J Neurophysiol 80:1961-1980.

McKiernan BJ, Marcario JK, Karrer JH, Cheney PD (2000) Correlations between corticomotoneuronal (CM) cell postspike effects and cell-target muscle covariation. J Neurophysiol 83:99-115.

Moritz CT, Lucas TH, Perlmutter SI, Fetz EE (2007) Forelimb movements and muscle responses evoked by microstimulation of cervical spinal cord in sedated monkeys. J Neurophysiol 97:110-120.

Moritz CT, Perlmutter SI, Fetz EE (2008) Direct control of paralysed muscles by cortical neurons. Nature 456:639-642.

Morrow MM, Miller LE (2003) Prediction of muscle activity by populations of sequentially recorded primary motor cortex neurons. J Neurophysiol 89:2279-2288.

Park MC, Belhaj-Saif A, Cheney PD (2000) Chronic recording of EMG activity from large numbers of forelimb muscles in awake macaque monkeys. J Neurosci Methods 96:153-160.

Park MC, Belhaj-Saif A, Cheney PD (2004) Properties of primary motor cortex output to forelimb muscles in rhesus macaques. J Neurophysiol 92:2968-2984.

Park MC, Belhaj-Saif A, Gordon M, Cheney PD (2001) Consistent features in the forelimb representation of primary motor cortex in rhesus macaques. J Neurosci 21:2784-2792.

Penfield W, Boldrey E (1937) Somatic motor and sensory representation in the cerebral cortex of man as studied by electrical stimulation. Brain 60:389-443.

Penfield W, Jasper HH (1954) Epilepsy and the functional anatomy of the human brain. Churchill, London.

Porter R, Lemon RN (1993) Corticospinal function and voluntary movement. Oxford:Clarendon.

Rathelot JA, Strick PL (2006) Muscle representation in the macaque motor cortex: an anatomical perspective. Proc Natl Acad Sci U S A 103:8257-8262.

Rathelot JA, Strick PL (2009) Subdivisions of primary motor cortex based on cortico-motoneuronal cells. Proc Natl Acad Sci U S A 106:918-923.

Schieber MH, Rivlis G (2007) Partial reconstruction of muscle activity from a pruned network of diverse motor cortex neurons. J Neurophysiol 97:70-82.

Senesh M, Wolf A (2009) Motion estimation using point cluster method and Kalman filter. J Biomech Eng 131:051008.

Shapiro NP, Lee RH (2007) Synaptic amplification versus bistability in motoneuron dendritic processing: a top-down modeling approach. J Neurophysiol 97:3948-3960.

Smith WS, Fetz EE (2009) Synaptic linkages between corticomotoneuronal cells affecting forelimb muscles in behaving primates. J Neurophysiol 102:1040-1048.

Strick PL, Preston JB (1978) Multiple representation in the primate motor cortex. Brain Res 154:366-370.

Tehovnik EJ, Lee K (1993) The dorsomedial frontal cortex of the rhesus monkey: topographic representation of saccades evoked by electrical stimulation. Exp Brain Res 96:430-442.

Tehovnik EJ, Tolias AS, Sultan F, Slocum WM, Logothetis NK (2006) Direct and indirect activation of cortical neurons by electrical microstimulation. J Neurophysiol 96:512-521.

Thier P, Andersen RA (1998) Electrical microstimulation distinguishes distinct saccade-related areas in the posterior parietal cortex. J Neurophysiol 80:1713-1735.

Townsend BR, Paninski L, Lemon RN (2006) Linear encoding of muscle activity in primary motor cortex and cerebellum. J Neurophysiol 96:2578-2592.

Woolsey CN, Settlage PH, Meyer DR, Sencer W, Pinto Hamuy T, Travis AM (1952) Patterns of localization in precentral and "supplementary" motor areas and their relation to the concept of a premotor area. Res Publ Assoc Res Nerv Ment Dis 30:238-264.